Poly(glycerol adipate) – Indomethacin conjugates for modified drug release

Dissertation

zur Erlangung des

Doktorgrades der Naturwissenschaften (Dr. rer. nat.)

der

Naturwissenschaftlichen Fakultät I

Biowissenschaften

der Martin-Luther-Universität Halle-Wittenberg

vorgelegt von

Herrn Tom Wersig

geboren am 22.11.1989 in Görlitz

Gutachter:

1. Prof. Dr. Karsten Mäder

2. Prof. Dr. Jörg Kressler

3. Prof. Dr. Achim Göpferich

Datum der öffentlichen Verteidigung: Halle (Saale), 19.07.2019

Bildung ist das, was übrig bleibt, wenn man alles vergessen hat, was man gelernt hat.

Werner Heisenberg (1901-1976)

Dedicated to my family

TABLE OF CONTENTS

ABBREVIATIONS AND SYMBOLS

% (mol)	Percentage by molecular weight
% (v/v)	Percentage by volume
% (w/v)	Percentage by weight per volume
% (w/w)	Percentage by weight
^{1}H-NMR	Proton Nuclear Magnetic Resonance
2D	Two-dimensional
A549	Human Lung Carcinoma Cells
Ag	Argentum
Asp	Aspartic acid
ASTM	American Society for Testing and Materials
ATR	Attenuated Total Reflection
BB	Backbone
COOH	Carboxylic acid groups
CPS	Counts per second
D	Deuterium
DCC	*N,N´*-Dicyclohexalcarbodiimide
DDS	Drug Delivery System
DiR	1,1`-Dioctadecyl-3,3,3`,3`- (tetramethylindotricarbocyanine iodine)
D15PCU	3-Carboxamido-2,2,5,5,-tetramethyl-d$_{12}$-pyrroline-1-oxyl-1-^{15}N
DLS	Dynamic Light Scattering
DCM	Dichloromethane
DMEM	Dulbecco's Modified Eagle Medium
DPBS	Dulbecco's phosphate buffer saline
DSMZ	Leibniz Institute DSMZ-German Collection of Microorganisms and Cell Cultures
D-TL	D-Tempol (4-Hydroxy-TEMPO-d17)
DVA	Divinyl adipate
EDC-HCl	1-Ethyl-3- (3-dimethylaminopropyl) carbodiimide-hydrochlorid
EPR	Electron Paramagnetic Resonance
EPR-effect	Enhanced Permeability and Retention Effect
FBS	Fetal Bovine Serum
FT	Fourier Transformation

G'	Storage Modulus
G''	Loss Modulus
GHz	Gigahertz
GPC	Gel Permeation Chromatography
h	Hour
HCl	Hydrochloric acid
HD-PMI	2-Heptadecyl-2,3,4,5,5-penta-methylimidazolidine-1-oxyl
HeLa	Human Cervix Adenocarcinoma Epithelial Cells
HES	Hydroxyethyl starch
His	Histidine
HPMA	N-(2-hydroxypropyl)methacrylamide
IDMC	Indomethacin
IR	Infrared
JAP	Japanese Pharmacopeia
LAF	Laminar Air Flow
LLC-PK1	Pig Kidney Epithelial Cells
keV	Kiloelectronvolt
M	Molar
min	Minute
mT	Millitesla
M_n	Average molecular weight by number
MP	Microparticle
M_r	Relative molecular mass
M_w	Average molecular weight by weight
MWCO	Molecular weight cut off
NP	Nanoparticle
NTA	Nanoparticle Tracking Analysis
OH	Hydroxyl Group
PBS	Phosphate Buffered Saline
PCS	Photon Correlation Spectroscopy
PDI	Polydispersity Index
PEG	Poly(ethylene glycol)
PES	Polyethersulfone
PGA	Poly(glycerol adipate)
pH	Power of hydrogen

PH.Eur.	European Pharmacopeia
PK	Pharmakokinetic
PLA	Polylactic acid
PLGA	Poly(D,L-lactide-co-glycolide)
PVAc	Polyvinyl acetate
PVP	Polyvinyl pyrrolidone
PVP/AV	Polyvinyl pyrrolidone/ polyvinyl acetate co-polymer
ppb	Parts per billion
ppm	Parts per million
PTFE	Polytetraflourethylene
RBC	Red Blood Cells
RC	Regenerated Cellulose
rpm	Revolutions per minute
SDS	Sodium Dodecyl Sulfate
SEM	Scanning Electron Microscopy
SLS	Static Light Scattering
Ser	Serine
TCM	Trichlormethane (Chloroform)
TEM	Transmission electron microscopy
USP	United States Pharmacopeia
°C	Celsius degree
δ	Loss Angle or chemical shift
η	Dynamic Viscosity
η*	Complex Viscosity
τ_R	Rotational Correlation Time
T	Transmission
WAX	Wide Angle X-ray scattering

1 <u>INTRODUCTION</u>

1.1 POLYMER THERAPEUTICS

The term polymer therapeutics is a generic term used to represent polymeric drugs [1–3], polymer-drug conjugates [4,5], polymer-protein conjugates [6–8], polymeric micelles with covalently linked drugs [9–11] and multicomponent polyplexes [12–15]. Since the 1940s, synthetic polymers have been investigated for their therapeutic application. The first polymers, like poly(vinyl pyrrolidone) (PVP) or dextran were mainly used as plasma expanders. PVP-iodine was and is still used as wound dressing. At the beginning of the 1960s, the development of synthetic polymer-based drugs and polymer-protein conjugates emerged. Poly(ethylene glycol) was especially focused for protein conjugation. The early 1970s laid milestones in the research of polymer therapeutics. Lysosomotropic polymer-drug conjugates block copolymer micelles and PEG-protein conjugates have been developed by the pioneering work of De Deuve *et al.* [16], Ringsdorf *et. al* [17,18] and Davis *et al.* [19,20]. Based on these studies, the PEGylation of proteins [21,22] and aptamers is a common and established principle until this day. A bit later, the development of polymer-drug conjugates as anticancer agents due to the advantages in polymer chemistry [17] and cell biology [23] began. R. Duncan, H. Ringsdorf and J. Kopeček and their colleagues are outstanding in this field of research. Their work focused on synthetic (HPMA)-doxorubicin conjugates, which were the first synthetic polymer-drug conjugates that reached Phase I/II clinical trials (1994) [24–28]. At about the same time, Kataoka *et al.* [29] and Kabanov *et al.* developed first micelles based on block copolymers, which should be also used as anticancer agents. They also reached Phase I/II in clinical trials. In summary, Ruth Duncan finally coined the term polymer therapeutics for the described systems. She wanted to distinguish from the conventional DDS with creation of this concept. In conventional DDS, drugs are usually non-covalently entrapped. Polymer therapeutics must therefore be regarded as new chemical entities. Thus far, polymeric drugs [30,31] polymer sequestrants [32] and PEG-aptamer conjugates [33] have reached the market. An overview of market products is shown in the following Table 1. Surprisingly, after about 50 years of research no polymer-drug conjugates and no block copolymer micelle product has reached marked maturity anymore, but there are many in the pipeline (Table 2). This may be due to the complex characterization, including molecular weight, polydispersity, size and surface

properties and the difficult scale up. However, the search for alternative drug carriers continues relentlessly. In addition to HPMA, poly(glutaminic acid) is gaining more and more importance [34], and therefore the number of poly(glutaminic acid)-anticancer conjugates in clinical trials is therefore increasing. The big advantage over HPMA and PEG is its biodegradability. HPMA and PEG are non-biodegradable and show the risk of intracellular accumulation which must be considered within the dose management. Therefore, biodegradable polymers are favorable.

Table 1. *Examples of polymer therapeutics in the market.*

Class	Trade name	Composition	Indication
Polymeric drugs	Copaxone®	Glu, Ala, Tyr copolymer	Multiple sclerosis
Polymeric sequestrants	Renagel®	Phophate binding polymer	Hyperphosphataemia
Polymer-protein conjugates	Zinostatin Stimalamer (Japan)	Styrene maleic anhydride-neocarzinostatin	Antioneplastic agent
PEGylated proteins	Cimzia	PEG.anti TNF Fab	Crohn's disease, Rheumatoid arthritis
	Mircera	PEG-EPO	Treatment of anemia in dialysis patients
	Peg-Intron™	PEG-Interferon alpha 2b	Hepatitis C
	Peg-Asys®	PEG-Interferon alpha 2a	Hepatitis B, C
	Uricase-PEG 20	PEG-Uricase	Hyperuricemia Gout
PEGylated-aptamer	Macugen	PEG-aptamer (apatanib)	Age-related Macular Degeneration

Table 2. *Examples of polymer therapeutics in clinical development.*

Class	Example	Composition	Status	Indication
Polymeric drugs	Vivagel®	Lysine-based dendrimer	Completed Phase III	Bacterial vaginosis
Polymer-protein conjugates	SuliXen®	Polysialyted insulin	Phase I/II	Diabetes mellitus
PEGylated proteins	ADI-PEG 20	PEG-arginine deaminase	Completed Phase III	Hepatocellular Carcinoma
PEGylated-aptamer	Fovista® E10030	PEG-anti PDGF aptamer	Completed Phase III	AMD
Polymer-drug conjugate	CT-2103; Xyotax; Opaxio	Poly(glutaminic acid)-paclitaxel conjugate	Completed Phase III	Various cancer
	Prolindac	HPMA-copolymer-DACH platinate	Phase II	Various cancer
	PEG-SN38	Multiarm PEG-camptothecin derivative	Phase II	Various cancer
	XMT-1001	Polyacetal-camptothecin conjugate	Completed Phase I	Various cancer
	NKTR-118	PEG-naloxone	Completed Phase III	Opioid-induced bowel dysfunction
Block copolymer micelles	SP1049C	Doxorubicin block copolymer micelle	Phase I/II	Various cancer
	NK105	Paclitaxel block copolymer micelle	Completed Phase III	Various cancer
	NK-6004	Cisplatin block copolymer micelle	Completed Phase II	Various cancer
Self-assembled polymer conjugate NP	IT-101 CRLX101	Polymer conjugated cyclodextrin NP-camptothecin	Completed Phase II	Various cancer

1.2   POLYMER-DRUG CONJUGATES

In general, polymer-drug conjugates may be referred to as prodrugs. The drug is covalently bound via a cleavable linker and remains inactive during its delivery and is activated by specific conditions in the target site *in vivo*. Polymer-drug conjugates are therefore inactive precursors with altered physicochemical properties. Ideally, drug conjugation enhances drug solubility, bioavailability and plasma half-life. The drug should simultaneously be protected against enzymatic degradation or unspecific cellular uptake. Moreover, the conjugation should lead to reduction of antigenic activity and the possibility to prepare advanced drug delivery systems. So far, just a few polymer-conjugates [4] are in clinical trials until this day. A selection of important representatives is given in Table 2. Possible reasons for this small number of clinical trials could be the lack of suitable polymers, poor manufacturing reproducibility and the lack of validation opportunities. As already noted, most drug conjugates are based on the biopersistent carriers HPMA and PEG as well as on biodegradable poly(glutaminic acid). Due to the possible lysosomal storage disease syndrome the non-biodegradable polymers are limited for parenteral administration of high doses [35]. The biodegradability is therefore a key factor for the ongoing research for new polymers. Biodegradable polymers in preclinical use include polypeptides [34,36], polyacetals [37], dextrins [38] and hydroxyethyl starch (HES) [39]. Apart from biodegradability, well defined molecular weight is essential. High molecular weights are favorable in order to increase passive targeting provided by the EPR effect. Therefore, polymer architecture is an important field of research in order to guarantee well defined conformations, high homogeneity and high drug loading capacities. Examples of branched polymer architectures are presented in Figure 1.
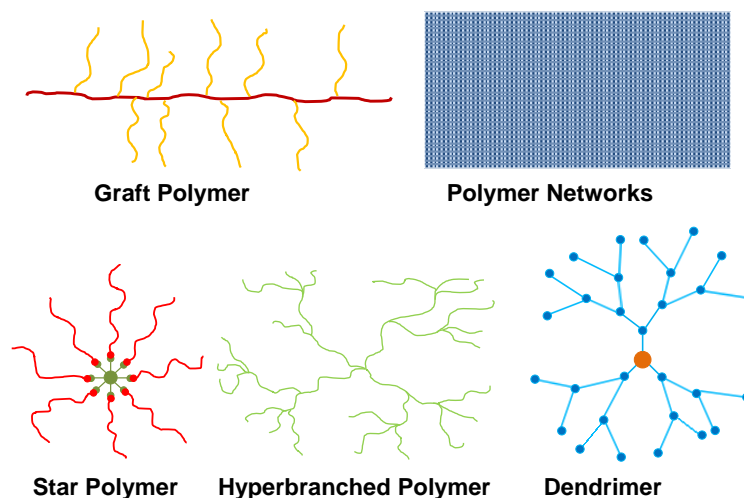
Figure 1. *Examples for various branched polymer-drug conjugate architectures.*

A **star polymer** consists of linear side chains attached to a central core. There are differentiated structured as so called symmetric stars (identical linear side chains) and asymmetric stars (varying linear side chains). These polymers are characterized by a globular shape, large surface and a high number of functional groups with respect to the molecular weight. Moreover, their unique rheological and mechanical behavior make star polymer-drug conjugates promising drug delivery platforms [40–42]. Most star like polymers are based on the previously mentioned HPMA with focus on treating various cancer disease using doxorubicin [43,44]. Also hybrid structures out of star structures and dendrimers which based on poly(L-lactic acid) and polyester dendrons of 2,2-bis(hydroxymethyl)propionic acid were investigated by Cao *et al.* [45].

Hyperbranched polymers are three dimensional polymers with a structure similar to the dendritic polymers; they have a highly branched architecture. Structurally, they represent the link between simple linear polymers and dendrimers. They are characterized by their simple synthesis. In contrast to star like polymers, the hyperbranched ones developed rapidly. Some hyperbranched polymers, such as Boltorn® and Hybrane® are already in the market. Hyperbranched polymer based drug carriers were developed for the treatment of various cancer diseases like the other mentioned polymers. Examples are hyperbranched polyphosphates loaded with chlorambucil [46] or hyperbranched polyglycerols with conjugated cisplatin [47] and hyperbranched polyglycerol-PEG copolymers with doxorubicin linked via pH-labile hydrazine bonds [48].

Graft polymers are linear polymeric backbones with attached polymeric or non-polymeric branches. As previously stated, graft polymers belong to the group of branched polymers with the difference, that the sidechains are usually different from the backbone structure (graft polymer). Depending on the degree of modification they are sometimes also called brush-polymers (high degree of grafting). The third sub-class are comb-like-polymers, where the side chains are of the same structure as the main chain. Since the 1990s, the interest in graft polymers as drug carriers increased. Hudecz *et al.* [49] worked on polypeptide-daunomycin conjugates, Etrych *et al.* [50] described graft copolymer-doxorubicin conjugates for passive tumor targeting based on multivalent HPMA and Bao *et al.* [51] proposed chitosan-graft-polyethyleneimine-candesartan conjugates as nanovectors.

Dendrimers are three-dimensional highly branched "tree-like" macromolecules. In contrast to star like or hyperbranched polymers the structure can be divided into core, interior and shell structures. The most important dendrimer structures are polyamidoamine (PAMAM) [52], poly(L-lysine) (PLL), polyamides [53], polyester (PGLSA-OH) [54], polypropylenimine (PPI) and poly(2,2-bis(hydroxymethyl)propionic acid (bis-MPA) [55]. The drug encapsulation is limited. Therefore, the covalent attachment for dendrimers is highly investigated. The focus on dendrimer-drug conjugate lies on PAMAM. So far, for example PEG5000 [56], doxorubicin [57], paclitaxel [58] and methotrexate [59] have been successfully bound to the PAMAM carrier.

Polymeric networks are structures usually obtained by cross-linking the structures described above.

1.3   POLYMER-DRUG CONJUGATES AND NON-CANCEROUS DISEASES

As mentioned earlier, almost all previously developed polymers have been created for the treatment of various cancer diseases but polymer-drug conjugates may also be used for the treatment of other diseases. For example, bone-targeting HPMA copolymer (prostaglandin E_1, PGE_1) have been developed for the treatment of osteoporosis and other musculoskeletal diseases [60–62]. D-aspartic acid and alendronate were used for mediating the biorecognition [60]. Moreover, polymer-drug conjugates possess high potential for the treatment of inflammatory diseases. The treatment of inflammatory tissues [63] and inflammatory arthritis [64] should be highlighted. NPC1161 (8-[(4-amino-1-methylbutyl)amino]-5-[3,4-dichlorophenoxy]-6-methoxy-4-methylquinolone [65] and amphotericin B [66] have been successfully applied in the HPMA conjugated form as anti-leishmanial agents.

1.4   POLY(GLYCEROL ADIPATE)

Poly(glycerol adipate) (Figure 2) is a linear polyester with free pendant hydroxyl groups. It can be synthesized via a one-step enzymatic polycondensation using divinyl adipate (DVA) and glycerol [67]. The reaction is catalyzed by Novozym 435, a triacyl glycerol lipase derived from *Candida antarctica* which is selective towards primary alcohols [68]. The enzymatic catalysis was reported as "green reaction" [69] working under mild conditions, especially low temperatures. This is important due to the increased possibility for chain branching at higher temperatures [70]. The molecular weights [M_w] of the resulting polyesters can be tuned in the range from about 3000 to 14000 Da. The pendant hydroxyl groups are 90-95 % secondary.
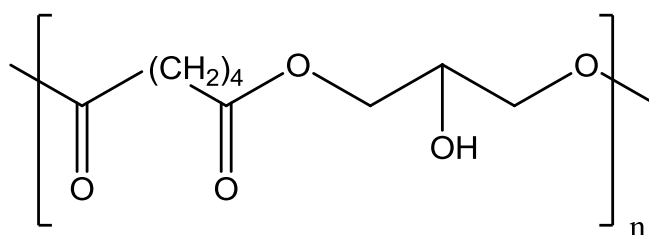
Figure 2.   *Chemical structure of poly(glycerol adipate) repeating unit.*

These free pendant hydroxyl groups are the major advantage over most other commercial polyesters such as PLGA. The free OH- groups allow further modification of the polymer backbone in order to create graft polymers with tailored physicochemical properties. Poly(glycerol adipate) is a hydrophilic, but not water soluble. Further glycerol based polymers are polyglycerols, where the secondary hydroxyl group was used for hyperbranching which leads to dendrimers [71]. These dendrimers are biocompatible but not biodegradable due to the ether bonds. In contrast, poly(glycerols) is based on ester bonds and therefore biodegradable [72].

The potential of PGA as DDS was first demonstrated in 2005 by Kallinteri *et al.* [72]. They used acyl- modified poly(glycerol adipate) for the preparation of biodegradable nanoparticle formulations with incorporated water soluble drugs [73]. Because poly(glycerol adipate) is biocompatible [72] and biodegradable it is well suited as promising platform for DDS, such as PGA-drug conjugates. Moreover, in the sense of economics, the scale up has already been published which underlines the high potential of PGA as platform for DDSs [74].

1.5   POLY(GLYCEROL ADIPATE) GRAFT POLYMERS

A well-studied possibility for the modification of the PGA backbone is the grafting with fatty acids. The group around Garnett was the first who grafted the PGA backbone with caprylic acid and stearic acid respectively (in the range of 20 to 100 mol% with respect to the pendant hydroxyl groups), through an acid chloride catalyzed esterification reaction in 2005 [72]. Moreover, they presented promising results for cell viability and release profiles for ^{125}I-deoxy-uridine. In 2008, the same group incorporated the hydrophilic drugs dexamethasone phosphate (DXMP) and cytosine arabinose (CYT-ARA) in C_8-PGA NP (20, 40 and 100 %) and showed varying drug release over 25 days depending on the degree of grafting [73]. At the same time, the physicochemical properties of caprylic acid modified PGA had been published [75]. At the beginning of the 2010s, the research groups around Karsten Mäder and Jörg Kressler, from Halle (Saale) extended research in cooperation in the field of fatty acid modified poly(glycerol adipate). Weiss *et al.* extended the spectrum of used fatty acids (lauric-, stearic- and behenic acid) and reported, that the texture of the polymers can be tuned from viscous to solid depending on the chain length of the fatty acids and the degree of grafting. Moreover, nanoparticles haven been produced successfully with interesting, partly cube like structures [76,77].

Promising results for these polymers *in vitro* were obtained [78]. In 2012, stearic acid modified PGA was used as NP platform with various NSAR's incorporated. The drug loading was very low (1-2 %) and a controlled release over two weeks was reached with a high initial burst release of about 20 % [79]. Later, the group working with Kressler focused on possibilities to tune the degree of crystallinity by varying the substituents such as poly(ethylene oxide) (PEO) or poly(ε-caprolactone) (PCL) or diblock copolymer sidechains of both [80,81]. Also first *in vivo trials* were carried out by Weiss *et al.* Stearic acid modified PGA nanoparticles were prepared containing non-covalently bound DiR, a lipophilic fluorescent dye. In a second experiment, PGAS NP's were coated with the forementioned HPMA attached with the fluorescent dye DY676. In this study the given nanoparticles were well accepted by mice. Interestingly, fluorescence signals were obtained in the bones for non-coated PGAS NP. Besides, NP accumulation in the ovaries and the adrenal glands could be confirmed [82,83]. Recently, the scientists from Halle (Saale) achieved a patent for poly(dicarboxylic acid multi-oil esters) based drug delivery systems [84].

1.6 INDOMETHACIN

Indomethacin is an indolic acid derivative and potent inhibitor of both cycloxygenase-1 (COX-1) and cyclooxygenase-2 (COX-2). Therefore, indomethacin has many applications. The most important areas are summarized in Table 3.

Table 3. *Important applications for indomethacin.*

Application area	Source
Acute gout	[85]
Persistent ductus arteriosus	[86]
Hemicrania continua	[87]
Pericarditis (CORP-2)	[88]
Dysmenorrhea	[89]
Juvenile idiopathic arthritis	[90]
Rheumatoid disease	[91,92]
Ocular inflammation	[93,94]
Glioblastoma*	[95,96]

* preclinical

1.7   RESEARCH OBJECTIVES

The search for new polymers, especially polymer drug conjugates, for advanced drug delivery continues all the time and it is not over yet. The large demand is reflected in the drastically increasing number of publications within the last 20 years (Figure 3).
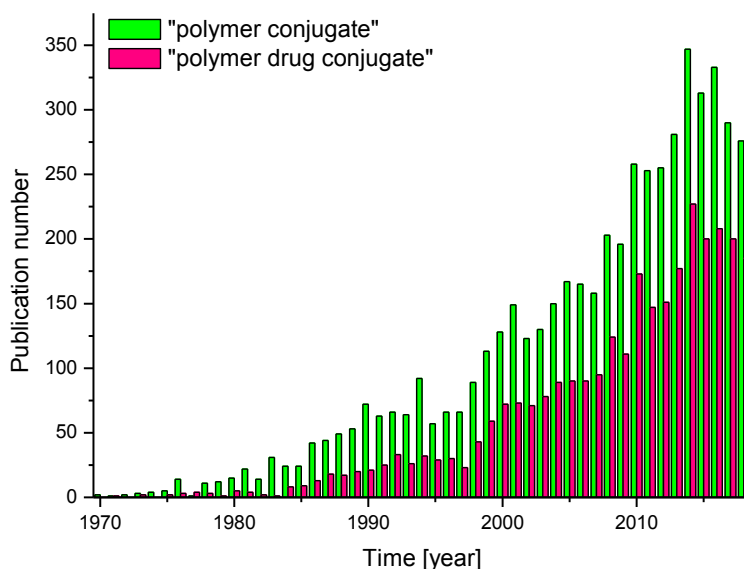
Figure 3.   *Comparative "pubmed" literature search for the terms "polymer conjugate" (green) and "polymer drug conjugate (pink) from 1970 to 2018.*

Aim of the present work was the development of various DDSs based on PGA-drug conjugates. The potent and versatile drug indomethacin (Table 2) was selected as a promising candidate for these trials. This work focused on the following aspects:

- **Synthesis** of poly(glycerol adipate)-indomethacin conjugates with different degrees of modification. In this regard, the chemical structure (determined via ^{1}H-NMR- and IR-spectroscopy), molecular weight distribution (GPC), drug loading (^{1}H-NMR and HPLC-UV) as well as the physiochemical properties are of particular interest.

- Based on the results mentioned under the previous point one, it should be estimated what possibilities are given for the **formulation of innovative DDS**.

- Production and examination of **preformed implants** *in vitro*. Especially the release behavior under various conditions (buffer pH 7.4, acidic and enzymatic

influence) and the behavior in water (EPR) should be addressed. The release should be compared with non-covalently incorporated indomethacin-PGA mixtures.

- Development of **nanoscale DDS** based on the synthesized polymers. Therefore, detailed size measurements have to be carried out by dynamic light scattering, nano tracking analysis and electron microscopy. For these formulations, a release profile (*in vitro*) should be created, depending on the degree of modification. Therefore, a special and innovative release cell is to be developed, which is universally valid for nanoscale DDS.

- Preparation of PGA-IDMC based **microparticles** with subsequent characterization of the particle size using static light scattering, electron microscopy and light microscopy. Additionally the release behavior in vitro should be inspected.

- Selecting **promising formulations** for *in vivo* experiments

- *In vitro* **cytoxicity and hemolytic assay**, in comparison to free indomethacin, of the selected formulations to determine biocompatibility in preparation for the *in vivo* trials.

- Selection of **suitable fluorescent dyes** for multispectral fluorescence imaging, covalently and non-covalently labeled. Final **bio distribution** study *in vivo*.

A schematic illustration of the presented dissertation is shown in Figure 4.
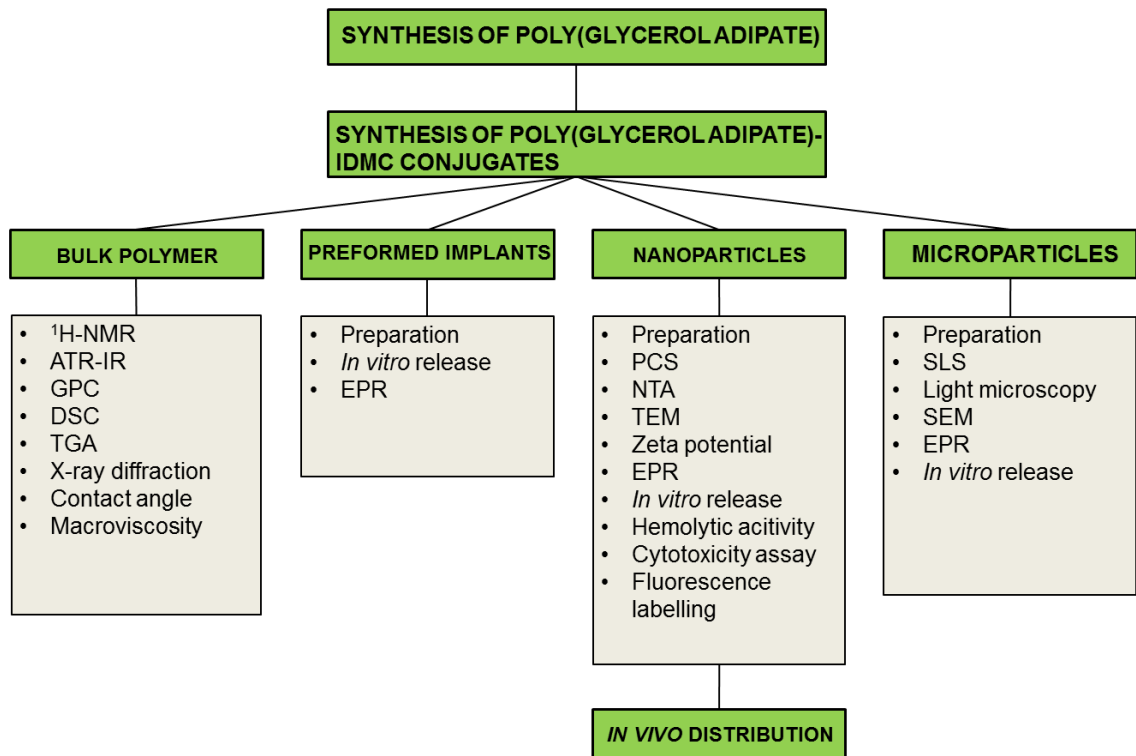
Figure 4. *Structure of experimetal work of this thesis.*

2   MATERIALS

2.1   INDOMETHACIN

Indomethacin (Figure 5) is a white or yellow crystalline powder. Indomethacin belongs to the group of no-steroidal anti-inflammatory drugs of the aryl acetic acid type. Further representatives of this group are acemetacin as well as diclofenac potassium and diclofenac sodium. The substance is described in the Ph.Eur., USP and JAP: Indomethacin is mainly present in two crystalline modifications with melting points of 155 °C and 162 °C [97]. Indomethacin is nearly insoluble in water (767.5 µg/ml at pH 7.2) [98]. One part of the substance dissolves in 50 parts of ethanol, 40 parts of diethyl ether or 30 parts of trichloromethane. In neutral or weakly acidic medium, indomethacin (pka = 4.5) is stable, in alkaline media it degrades to *p*-chlorobenzoyl [99]. Indomethacin (purity 100.2 %, Batch 1205002-01) was purchased from Euro OTC Pharma GmbH (Bönen, Germany).
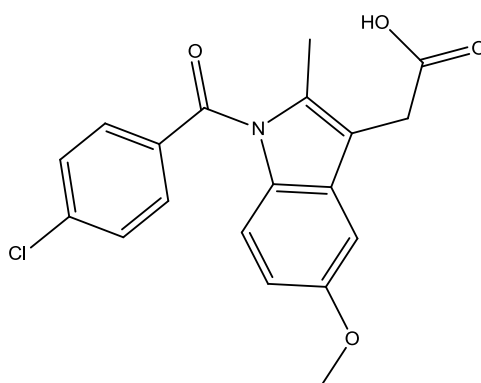
Figure 5.   *Chemical structure of indomethacin.*

2.2 FLUORESCENT DYES

The near-infrared fluorescent dye DY-782 (carboxylic acid derivate) was purchased from Dyomics (Dyomics GmbH, Jena, Germany) and was used for the covalent labelling of PGA-IDMC 50 %. Moreover, the lipophilic carbocyanine dye $DiOC_{18}(7)$ (DiR) (ThermoFisher Scientific, Waltham, USA) was used for non-covalent labelling of PGA-IDMC 100 % NP. The chemical stuctures and some important properties of the mentioned dyes are shown below in Figure 6.

	DY-782		**DiR**
M_W:	879.0 g/mol	M_W:	1013.41 g/mol
Ex:	783 nm	Ex:	750 nm
Em:	800 nm	Em:	780 nm
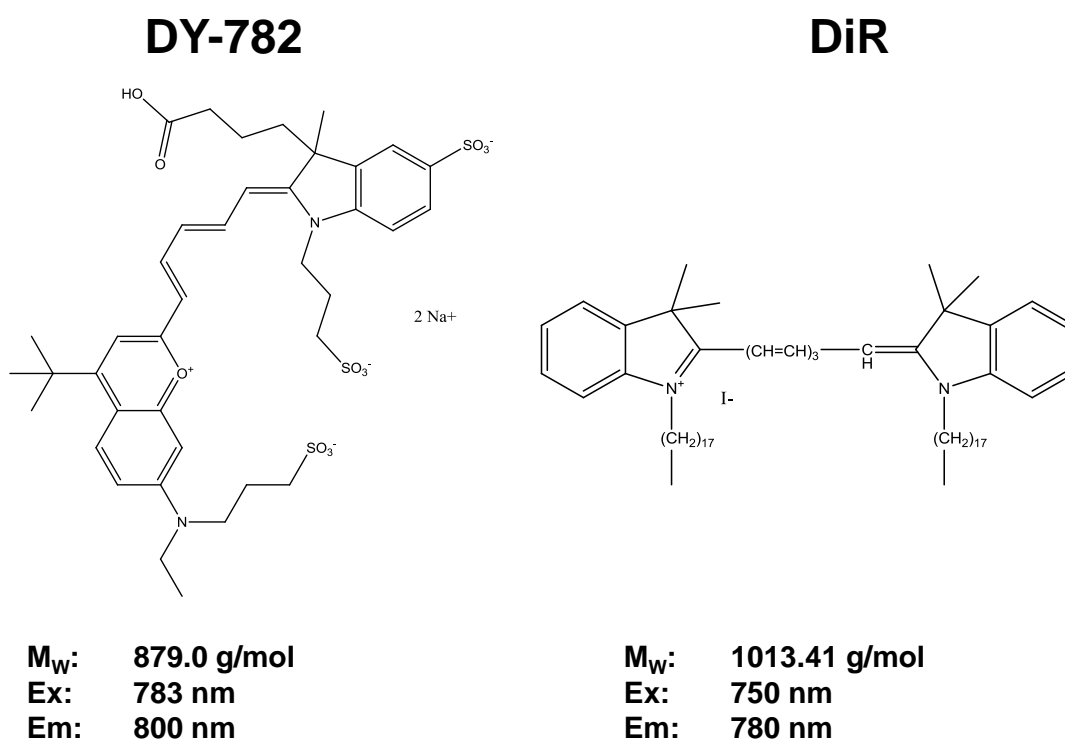
Figure 6. *Chemical structures and relevant properties of the used fluorescent dyes. The excitation and emission maxima are displayed for measurements in ethanol.*

2.3 SYNTHESIS MATERIALS

Table 4. *Organic solvents, reagents and further materials used for the syntheses of the polymer backbone and the drug conjugates.*

Substance	Source	Purity/ Remark
Aqua bidest.	Institute of Pharmacy, Martin-Luther-University, Halle-Wittenberg, Germany	Produced by double distillation
Brown Glass Vial	Infochroma AG, Switzerland	For the release experiments
Dichloromethane (DCM)	Carl Roth, Germany	≥ 99.9 %
Calcium hydride	Sigma-Aldrich, Germany	95 %
Diethyl ether	Carl Roth, Germany	≥ 99.5 %
4-(Dimethylamino)pyridine	Carl Roth, Germany	≥ 99 %
Divinyl adipate (DVA)	TCI Chemicals, Japan	≥ 99 %
Glycerol	Grüssing GmbH, Germany	DAB, waterfree
Hydrochloric acid	Carl Roth, Germany	37 %
Lipase B from *Candida Antarctica* (Novozyme 435)	Sigma-Aldrich, Germany	> 5000 U/g
Methanol	VWR Chemicals	HPLC grade
N-(3-dimethylaminopropyl)-*N'*-ethylcarbodiimide hydrochloride (EDC-HCl)	Carl Roth, Germany	≥ 99 %
Phosphorus pentoxide	Carl Roth, Germany	≥ 99 %
Sodium hydrogen carbonate	Carl Roth, Germany	≥ 99 %
Tetrahydrofuran (THF)	Carl Roth, Germany	≥ 99.9 %

2.4 FURTHER EXCIPIENTS AND MATERIALS

Table 5. *Further excipients and materials and their origin and application area (table continues on the next pages).*

Substance	Source	Purity/ Remark
A549 (Human lung carcinoma cells)	DSMZ, Germany	For cytotoxicity assay

Acetic acid	Carl Roth, Germany	100 %
Acetonitrile	VWR Chemicals	HPLC grade
AlamarBlue[®]	Invitrogen GmbH, Germany	Used for cytotoxicity assay
Aqua ad *injectabilia*	B. Braun, Germany	For cytotoxicity and hemolytic and *in vivo* tests
Biomaterial Hemolytic Assay Kit	Haemoscan, Netherlands	LOT #: 170831 For the hemolytic assay
DiR	ThermoFisher Scientific, USA	Lipophilic fluorescent dye for multispectral fluorescence imaging
D15PCU (3-Carboxamido-2,2,5,5,-tetramethyl-d$_{12}$-pyrroline-1-oxyl-1-^{15}N)	Sigma-Aldrich, Germany	99 % Spin probe, used for nanoparticle EPR measurements M_r 395.7 g/mol
Dimethylsulfoxide D6	Carl Roth, Germany	M_r 184.24 g/mol 99.8 Atom %D ^{1}H-NMR solvent
Disodium hydrogen phosphate	Carl Roth, Germany	> 98 % HPLC eluent buffer
Dulbecco's modified eagle medium (DMEM)	Sigma-Aldrich, Germany	Cell culture
Dulbecco's phosphate buffered saline (DPBS) 10x	Sigma-Aldrich, Germany	Used 10-fold diluted
Fetal Bovine Serum (FBS)	Sigma-Aldrich, Germany	Cell culture
FlexiPor[®] **membrane**	SmartMembranes, Gemany	Material: aluminum oxide Pore size: 20 nm Diameter: 20 mm
Forene[®] **100 % (v/v)**	AbbVie, USA	Anesthesia of the mice during the *in vivo* experiments
Gastight[®] **syringes**	Hamilton Germany GmbH, Germany	1; 2.5; 10 ml
HD-PMI	Institute of Chemical Kinetics and Combustion, Russia	Spin probe, used for microparticle EPR measurements
HeLa cells (Human cervix adenocarcinoma epithelial cells)	DSMZ, Germany	Used for *in vitro* cytotoxicity experiments

Hematocrit sealant set	Brand GmbH, Germany	To close the micropipettes during the EPR (L-band) measurements
Isopropyl alcohol	Sigma-Aldrich, Germany	> 99.5 %
Kolliphor P 188 (Poloxamer 188)	BASF SE, Germany	LOT #: WPCI522B
Lipase from *Pseudomonas* sp.	Sigma-Aldrich, Germany	LOT #: SLBM5366V ≥ 15 units/mg For enzymatic release studies
LLC-PK1 cells (Pig kidney epithelial cells)	DSMZ, Germany	Used for *in vitro* cytotoxicity experiments
Micropipettes 50 µl	Brand GmbH, Germany	For the EPR measurements (X-band)
Omnican® F	B. Braun, Germany	Injection syringes (needle 30Gx1/2``) used for the *in vivo* distribution/elimination experiments
Osmofundin® 15 % N	B. Braun, Germany	Carrier solution used for the *in vivo* distribution/elimination experiments
Parafilm® M PM-922	Pechiney Plastic Packaging Inc., United States of America	Sealing
Poly(vinyl alcohol)	Sigma-Aldrich, Germany	LOT #: 28F-0159 Average molecular weight 10000 g/mol
Sodium acetate	Carl Roth, Germany	> 99 %
Sodium azide	Merck, Germany	Synthesis grade
Sodium chloride	Grüssing, Germany	99.5%
Sodium dihydrogen phosphate dihydrate	Carl Roth, Germany	> 99 % HPLC eluent buffer
Sodium dodecyl sulfate	Sigma-Aldrich, Germany	98 %
Spectra/Por® 7 Dialysis Tubing	Spectrum, Inc; United States of America	MWCO 1kDa For polymer purification
Sterican cannulas	B. Braun, Germany	23G x 3 1/8"
Sterile filter	VWR, Germany	Material: PES, RC
D-Tempol (4-Hydroxy-TEMPO-d17)	Sigma-Aldrich, Germany	M_r 189.35 g/mol Spin probe, used for preformed implant EPR measurements

Tetramethylsilane	Sigma-Aldrich, Germany	> 99 % ^{1}H-NMR standard
Trichlormethane D1	Carl Roth, Germany	99.8 Atom %D, stab. with Ag ^{1}H-NMR solvent
Well plate	Greiner BioOne GmbH, Germany	96 wells

2.5   MISCELLANEOUS LABORATORY EQUIPMENT

Table 6.   *Overview of used laboratory equipment*

Equipment	Manufacturer	Remark/ Use
Christ Alpha 2-4	Martin Christ, Germany	Lyophilization
Centrifuge 5810 R	Eppendorf, Germany	Centrifugation
Centrifuge Minispin	Eppendorf, Germany	Centrifugation
CryoMill	Retsch Technology; Germany	Cryogenic grinding
HERAsafe™ Clean Bench	Heraeus Instruments, Germany	Hemolytic activity assay
Epoch 2 Microplate Spectrophotometer	BioTek Instruments Inc., United States of America	Cytotoxicity Assay
IKA C-MAG HS 7 Magnetic stirrer	IKA Werke, Germany	Dissolution, Preparation of nano- and microparticles
Portamess® 911 pH Electrode	Knick, Germany	pH measurements
Thermomixer compact	Eppendorf, Germany	Sample preparation, heating
MS2 Minishaker	IKA Werke, Germany	Dissolution, sample preparation
Syringe Pump 11 Elite	Harvard Apparatus, United States of America	Preparation of nano- and microparticles
Vacuum oven VD 53	Binder, Germany	Storing of polymer samples
Water bath shaker	GFL, Germany	Heating of samples

3 **METHODS**

3.1.1 SYNTHESIS OF POLY(GLYCEROL ADIPATE)

Poly(glycerol adipate) was synthesized as described by Kallinteri *et al.* [72] from glycerol and DVA (Figure 7). Glycerol (11.5 g, 0.12 mol) and DVA (23.8 g, 0.12 mol) were placed into an oven dried and nitrogen-purged two-necked 250 ml round bottom flask. Subsequently, 15 ml of anhydrous THF were added. A 150 ml Soxhlet extractor (105 g molecular sieve 5 Å, 100 ml anhydrous THF) with an attached condenser was positioned on top of the flask. The mixture was stirred by vigorous magnetic stirring and slowly heated up to 50 °C. Finally, the enzyme (0.71 g, 2 % (m/m)) was added. The pressure was reduced gradually to 300 mbar in order to induce the evaporation process. The reaction conditions were maintained for 10 hours. After the reaction, the mixture was diluted with 35 ml THF and the enzyme removed by filtration. The solvent was removed by rotary evaporation under reduced pressure at 60 °C. In order to deactivate remaining enzymes the residue was finally heated up to 95 °C for 1 h [100]. Finally the polymer was precipitated three times in cold diethyl ether and used for the next step without further purification. Residual solvents were removed by storing the polymers in a vacuum drying oven (Binder VD E2.1, Fa. Binder GmbH, Tuttlingen, Germany) for seven days.
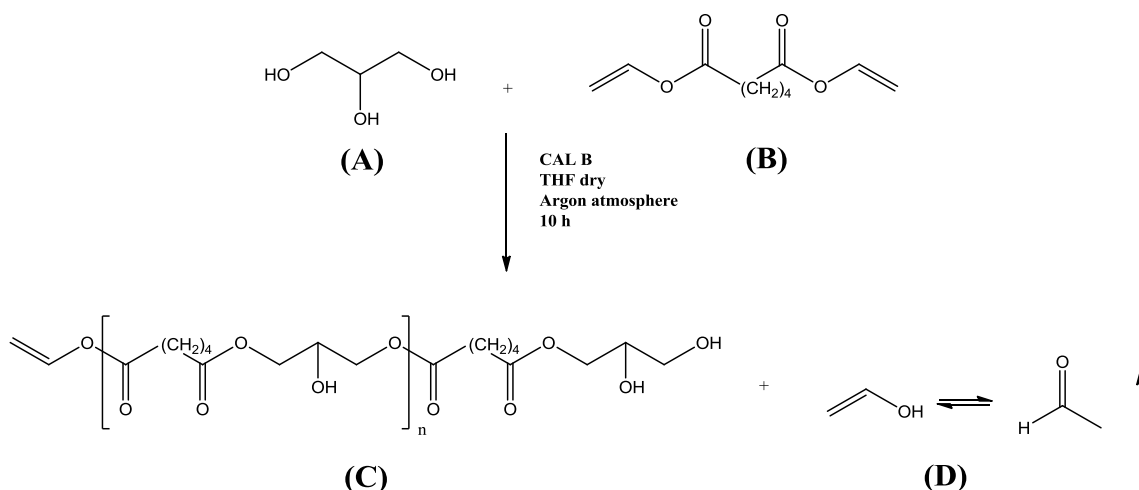
Figure 7. *Synthesis of the poly(glycerol adipate) backbone (C) by using glycerol (A) and divinyl adipate (B). The ethenol by-product disappears as a gas after convertion into acetaldehyde (D).*

3.1.2 CONJUGATION CHEMISTRY

The conjugation (Figure 8) was carried out via modified Steglich esterification [101] as follows:

Indomethacin (for 100 mol% conjugation 1.78 g, [5 mmol]; for 50 mol% conjugation 0.89 g, [2.5 mmol]; for 25 mol% conjugation 0.445 g, [1.25 mmol]), EDC-HCl (for 100 mol% conjugation 1.43 g, [7.5 mmol], for 50 mol% conjugation 0.72 g, [3.75 mmol]; for 25 mol% conjugation 0.36 g, [1.88 mmol]) and DMAP as catalyst (for 100 mol% conjugation 60 mg, [0.5 mmol]; for 50 mol% conjugation 30 mg, [0.25 mmol]; for 25 mol% conjugation 15 mg, [0.125 mmol]) were placed into an oven dried and nitrogen-purged two-necked round bottom 50 ml flask. 15 ml of anhydrous DCM were added under stirring with the magnetic stirrer. The preparation was cooled down to 0 °C with an ice bath. Afterwards a solution of PGA (1.0 g, 5 mmol with respect to the OH groups) in 10 ml anhydrous DCM was added dropwise over 30 mins. The solution was stirred at 0 °C for additional 30 min. The ice bath was removed and the mixture kept being stirred at room temperature for 24 h. The reaction took place in a fume hood with cloud windows to protect the light-sensitive indomethacin. The preparation was diluted with 25 ml DCM and extracted three times with diluted hydrochloric acid (10 %), saturated sodium hydrocarbonate solution and demineralized water in order to remove the remaining DMAP, EDC-HCl, indomethacin and urea - byproducts. The organic layers were collected and dried over anhydrous sodium sulfate under vigorous stirring. The solvent was removed by rotary evaporation under reduced pressure at 40 °C. The polymeric residues were precipitated in cold methanol. Finally, the polymer was collected in 5 ml anhydrous DCM and dialyzed (Spectra/Por® 7, 1 kD) over 3 days with frequent solvent exchange yielding a yellowish viscous/solid (depending on the degree of grafting) polymer.
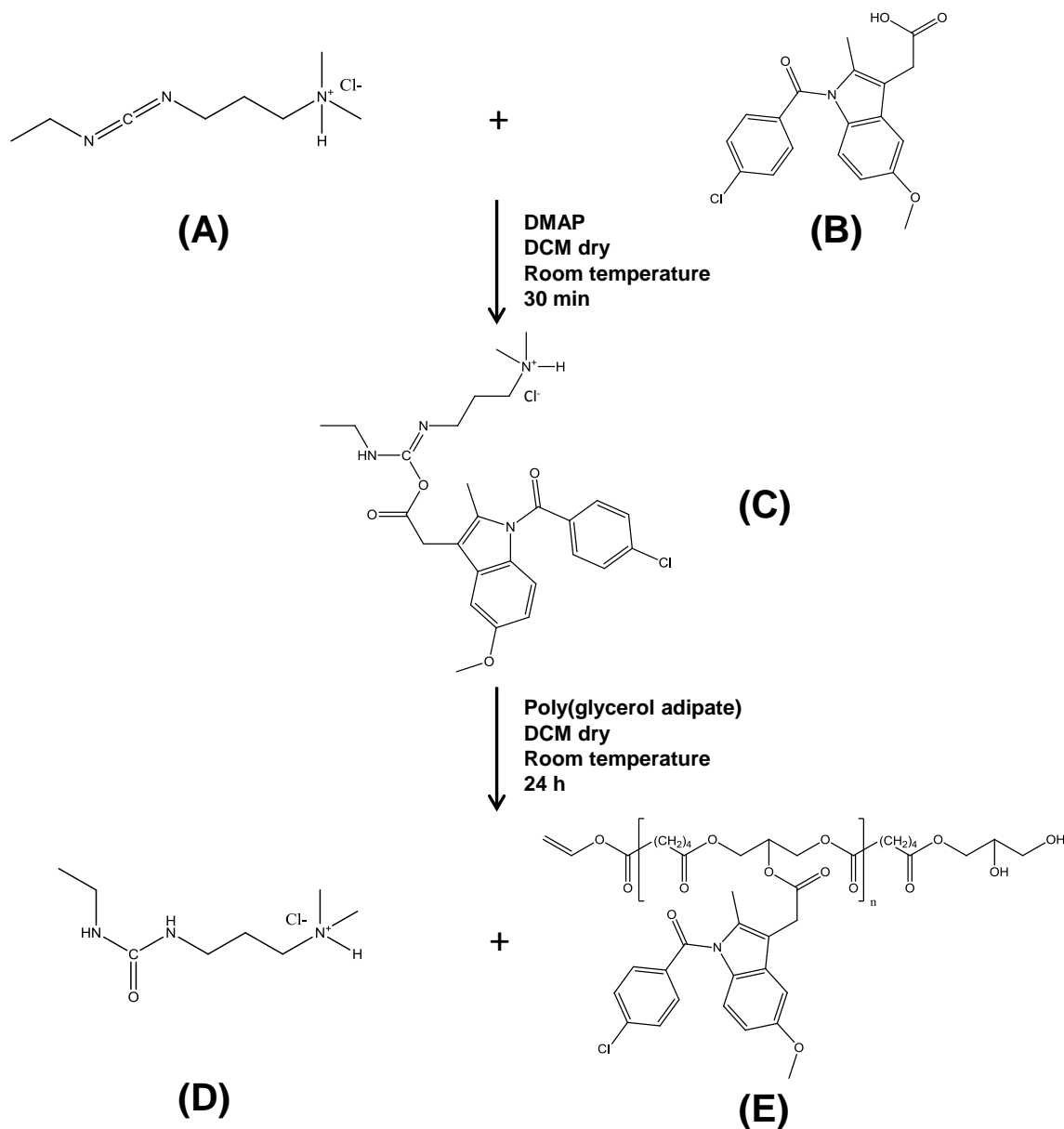
Figure 8. *Synthesis of poly(glycerol adipate)-indomethacin conjugates via Steglich esterification. (A) EDC-HCl; (B) indomethacin; (C) reactive o-acylisourea intermediate; (D) water soluble isourea by-product; (E) poly(glycerol adipate)-indomethacin conjugate.*

The fluorescent dye DY-782 (Figure 6) was covalently bond as follows (Figure 9):

100 mg [0.25 mmol with respect to the OH-groups] of PGA-IDMC 100 % were placed in an argon purged oven-dried 25 ml round bottom flask. Dry DMF, one crystal of DMAP and 0.2 mg EDC-HCl [0.001 mmol] were added. The mixture was cooled down to 0 °C with the help of an ice bath. Finally, 0.2 mg DY-782-NHS-ester [0.21 µmol] were dissolved in 1 ml dry DMF and added to the mixture dropwise over 1 h. The reaction was carried out at room temperature over 24 h. After the reaction, DMF was removed by

vacuum evaporation. Finally, the polymer was collected in 5 ml anhydrous DCM and dialyzed (Spectra/Por® 7, 1 kD) over 3 d with frequent solvent exchange yielding a greenish viscous polymer.
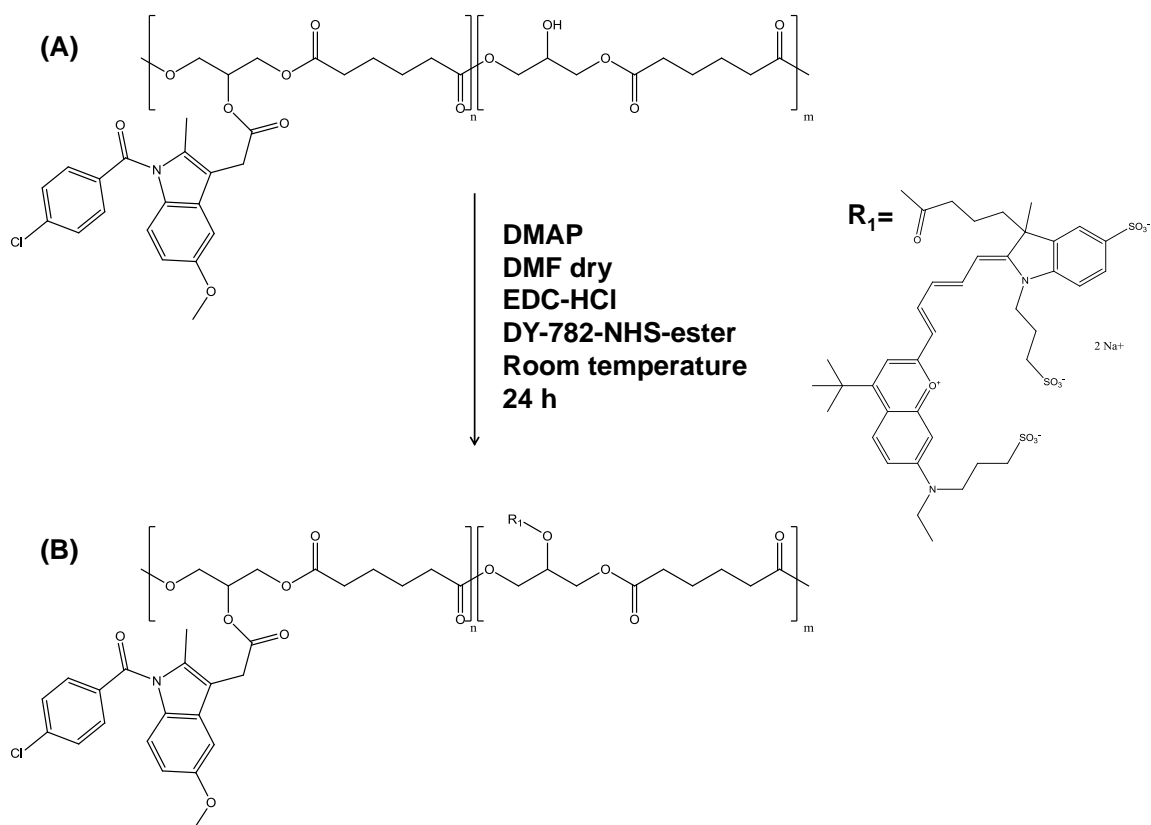
Figure 9. *Synthesis of poly(glycerol adipate)-indomethacin 100 %-DY-782 conjugates via Steglich esterification. (A) PGA-IDMC 50 %; (B) PGA-IDMC 100 %-DY-782; R₁ represents the fluorescent dye DY-782.*

3.2   METHODS FOR PHYSICOCHEMICAL CHARACTERIZATION OF BULK POLYMERS

3.2.1   [1]H-NUCLEAR MAGNETIC RESONANCE

Successful conjugation reactions of poly(glycerol adipate) with different amounts of indomethacin amounts were proven by nuclear magnetic resonance. ^{1}H NMR spectra were acquired using a Gemini 2000 spectrometer (Varian, Palo Alto, USA) operating at 400 MHz. All bulk polymers (20 mg/ml) were measured in deuterated chloroform $CDCl_3$ (stabilized with silver). Tetramethylsilane was used for internal calibration with complete proton decoupling. The NMR spectra were interpreted using the MestReC v.4.9.9.6 program (Mestrelab Research, Santiago de Compostela, Spain). With the same software the solvent as well as tetramethylsilane peaks were removed. The esterification degree of OH groups in PGA was calculated from the ^{1}H NMR spectra integrals of the peaks b and d in Figure 19 according to the following Equation (1) for 100 mol% grafting, comparable to Bilal *et al.* [102].

$$\frac{d}{b} = \frac{1}{4} \qquad \text{(Equation 1)}$$

3.2.2   DETERMINATION OF THE DRUG CONTENT

In addition to the calculations using the ^{1}H-NMR spectra (Section 3.2.1), the indomethacin content of the PGA-indomethacin conjugates were analyzed by UV/VIS spectroscopy. Measurements were carried out on an Agilent 1100 series HPLC system (Agilent Technologies, Santa Clara, USA) with an HP UV Detector (Hewlett-Packard Company, Palo Alto, USA) attached to prevent evaporation of DCM. The system was used without column and the the polymeric solution (0.1 mg/ml in DCM) was directly analyzed. The absorption was measured four times at λ_{max} = 318 nm. The calibration was carried out in the following steps: 1, 5, 10, 15, 20, 25, 30, 35, 40, 45 and 50 mg/ml. The drug content was calculated using the calibration curve.

3.2.3   GEL PERMEATION CHROMATOGRAPHY

Poly(glycerol adipate) and its synthesized PGA-IDMC conjugates were characterized by GPC. The measurements were performed on a ViscotekGPCmax VE 2002 using HHRH Guard-17360 and GMHHR-N-18055 columns and a refractive detector (VE 3580 RI detector, Viscotek). THF was used as eluent. The concentration of each sample was 3 mg/ml. The flow rate was 1 ml/min. Polystyrene was used as calibration standard. All samples were filtered prior to the measurement through a 0.22 μm PES filter.

3.2.4   STATIC CONTACT ANGLE

Contact angle values were measured at 25 °C using a Krüss G10 apparatus (Krüss GmbH, Hamburg, Germany) with a zoom lens (Jenoptik, Jena, Germany) attached, operating at 1:6.5 magnification (Figure 10). Samples were prepared by coating microscopy glass slides. A thin polymer layer was prepared through solvent evaporation from 7.5 % (w/w) solutions of polymers in dichloromethane. The measurements were carried out as follows: The coated glass slides were placed on the object table and a small drop of water (8 μl) was placed onto the polymer film with a syringe attached with a flat needle. Measurements were performed in triplicate immediately after spotting a drop of water and after an equilibration time of 2 min.
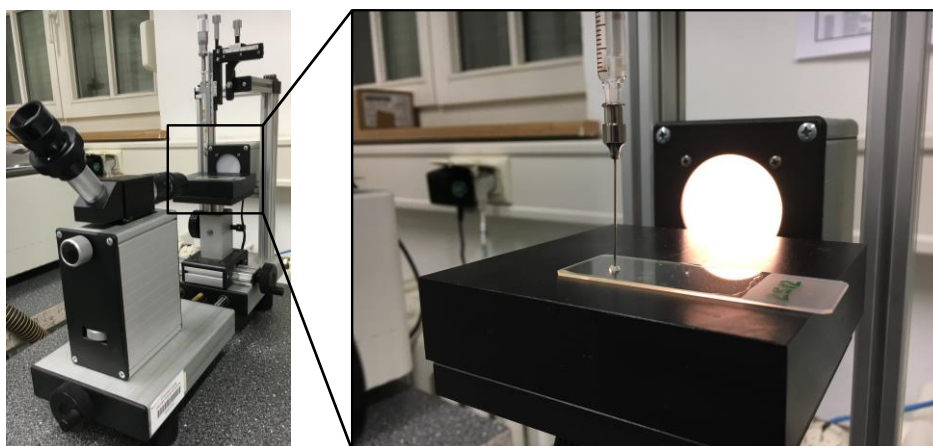
Figure 10. *Setup of the static contact angle measurements using the Krüss G10 (left). On the right, glass slide covered with a thin polymer film of PGA-IDMC 25 %. Measurements were carried out at room temperature in triplicate.*

3.2.5 DIFFERENTIAL SCANNING CALORIMETRY

The DSC measurements for PGA and the PGA-IDMC conjugates were recorded on a Differential Scanning Calorimeter 200 (Netzsch, Selb, Germany). If not stated otherwise, closed aluminum standard pans (pierced lid) were used. An empty aluminum pan was used as reference. Every sample was cooled down to -25 °C and kept at this temperature for 20 mins. The sample was then heated up to 100 °C with a rate of 5 K/min, kept at this temperature for 20 min and cooled down to -25 °C afterwards with a rate of -5 K/min. During all measurements a constant inert gas (nitrogen) flow of 10 l/min was upheld.

3.2.6 X-RAY DIFFRACTION

Wide angle X-ray scattering was performed on a STOE STADI MP (STOE & Cie GmbH, Darmstadt, Germany) powder diffractometer, equipped with a cobalt anode (40 kV and 30 mA) and a Ge (111) monochromator to select the Co K_α radiation at 0.1788965 nm. Data of the rotating samples were collected in the transmission mode from $2\theta = 4\text{-}45°$ in 0.5° steps for 60 s each. Prior to the X-ray analysis, the samples were powdered using a CryoMill (Retsch GmbH, Haan, Germany).

3.2.7 ATTENUATED TOTAL REFLECTION INFRARED SPECTROSCOPY

Infrared spectra were recorded on a Bruker IFS 28 equipped with a Sensir ATR unit (Bruker, Billerica, United States) attached with MIR – DTGS detector operating from 4000-400 cm^{-1}. The spectral resolution was 0.5 cm^{-1}. Software OPUS 4.2 was used to analyze the data. All samples were measured at room temperature.

3.2.8 OSCILLATORY RHEOLOGY

Viscosity measurements of visco-elastic materials were frequently performed using oscillatory rheometry. The rheological behavior of the described polymers was analyzed by oscillatory rheology using a Physica MCR 301 oscillating rheometer (Anton Paar GmbH, Graz, Austria) equipped with a cone-plate geometry (Figure 11). The plate diameter was 24.982 mm. The cone angle was 1.003°, gap size 0.048 mm. Resulting from the gap, the sample volume was about 200 µl and placed directly on the plate. When the gap was closed to measurement position, excess polymer was removed. The

measurements were carried out at 37 °C in order to simulate the polymer behavior at physiological temperature. The following samples were investigated: PGA, PGA-IDMC 25 %, 50 % and 100 %. First of all a deformation test was carried out at a radial frequency of 1 Hz (equals 6.28 rad/s) with a strain range from 0.01 % to 100 %, in order to determine the linear visco-elastic range (LVR). In the range the polymer structure remained intact. The results indicated that a deformation over the entire amplitude range was within the linear viscoelastic range. The following parameters were used for the subsequent frequency sweep tests: strain (γ): 1 %, frequency range: 0.1 – 10 Hz (equals 0.628 to 628 rad/s). The data were analyzed using the Rheoplus software (Anton Paar, Austria).
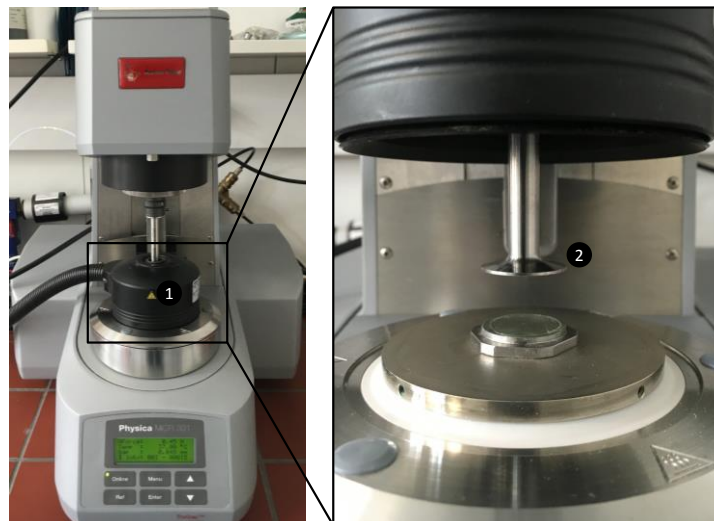
Figure 11. *Setup of the oscillating rheometer, attached with temperature chamber (1) adjusted to 37 °C. On the right, cone plate geometry with polymer film (2).*

3.2.9 PREPARATION OF PREFORMED IMPLANTS

Polymeric implants were prepared using a custom-made heating press (Figure 12). The heating press was developed and manufactured by fine mechanics factory (Institute of Chemistry, Martin-Luther-University, Halle/Saale). 50 mg of each polymer were placed in the cylindrical channel (diameter 5.5 mm). The temperature was adjusted to 25 °C. The probes were tempered with an equilibration time of 10 mins. Afterwards, the polymers were compressed using a cylindrical stamp (diameter 5.5 mm, polytetrafluorethylene). The Teflon stamp was loaded with 2 kg. Compression time was 2 mins to obtain yellowish, cylindrical implants with 5.5 mm diameter and 2.8 mm edge thickness. The implants were stored under light protection at 4 °C in the fridge until they were used.
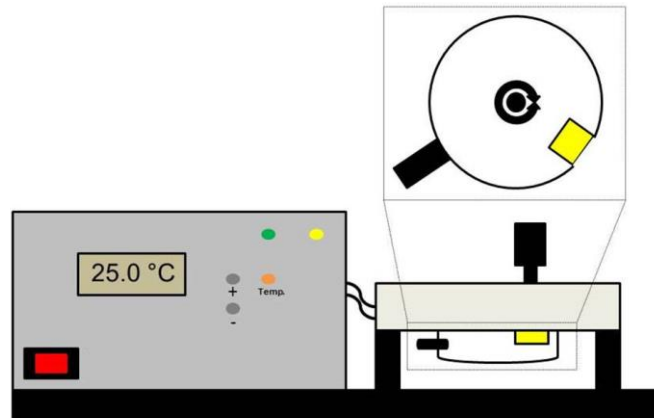
Figure 12. *Schematic illustration of the used heating press.*

3.2.10 ELECTRON PARAMAGNETIC RESONANCE OF PREFORMED IMPLANTS

Electron paramagnetic resonance is a powerful non-invasive tool to get further information about the insights of PGA-IDMC NP during release and storage in buffer. This method, also known as electron spin resonance, enables the investigation of the behavior of incorporated spin probes.

Electron paramagnetic resonance was carried out to get more information about the microviscosity and the kinetics of the penetration of release medium *in vitro*. Therefore, 100 mg of PGA-IDMC 25, 50 and 100 % were dissolved in dichloromethane (DCM). The spin probe D-Tempol (4-Hydroxy-TEMPO-d17) was added to the polymer solutions as a stock solution. The mixtures were poured into PFTE coated petri dishes and DCM was removed under vacuum conditions using a vacuum oven dryer (VG 53, Binder GmbH, Germany) attached with a NZ 2C NT vacuum pump (Vacuubrand, Germany). The drying time was 24 h. Subsequently, 50 mg of each polymer conjugate was used for the preparation of preformed implants according to the procedure described above (Section 3.2.9). Finally, the preformed implants contained 0.25 mmol/kg D-Tempol relating to the polymer mass. 2 ml Eppendorf Tubes® (Eppendorf GmbH, Germany) were perforated with 20 small holes (diameter 2 mm) to guarantee optimal wetting of the samples. The preformed implants were placed into the modified Eppendorf Tubes®, both were inserted into 20 ml brown glass vials (Infochroma Ag, Zug, Switzerland). At last, 10 ml of PBS pH 7.4, acetate buffer pH 4.75 and 0.9 % (w/v) aqueous NaCl solution containing lipase from *Pseudomonas* sp. was added in each vial respectively. The implants, as well as the release medium were measured in regular intervals.

For the measurements, the implants were withdrawn from the Eppendorf tubes and dried carefully from the outside using a paper towel. The samples were placed in a custom-made sample holder.

A PTFE sample holder was used to guarantee reproducibility of the sample position (Figure 13). Measurements were carried out using an L-band spectrometer (Magnettech GmbH, Berlin, Germany) operating at a microwave frequency of 1.1-1.3 GHz equipped with a reentrant resonator. Measurement parameters were set as follows: field center 49.5 mT, scan range 10 mT, scan time 600 s, modulation amplitude 0.0625 mT. The peak amplitudes of the obtained spectra were analyzed with the MultiPlot 2.0 software (MagnetTech, Berlin, Germany).
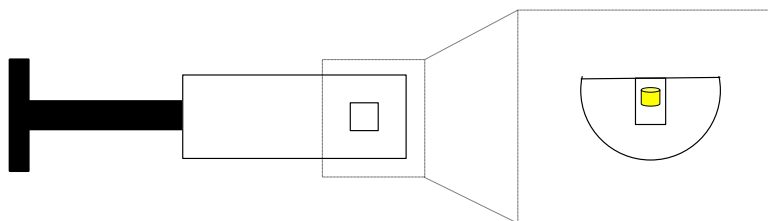
Figure 13. *Schematic illustration of the PTFE sample holder used during the EPR measurements (L-band) of preformed implants. Top view (left) and cross view at the sample position with schematic preformed implant (right).*

3.2.11 *IN VITRO* RELEASE

The preformed implants were produced according to the previousl described procedure (Section 3.2.9). The samples were placed in Spectra/Por® 7 dialysis tubes (Spectrum, Inc; United States of America) with a MWCO of 1kD, and were exposed to 70 ml of pH 7.4 phosphate buffer, pH 4.75 acetate buffer and enzyme solution respectively and distressed in a shaker with light protection (Memmert GmbH + Co. KG, Schwabach, Germany) at 37 °C. For enzymatic release studies lipase from *Pseudomonas* sp. was dissolved in sterile 0.9 % (w/v) sodium chloride solution to a concentration of 4 mg/cm^3 and stored at -20 °C. This stock solution was diluted to an enzyme concentration of 0.17 mg/ml for the release tests. During the enzymatic release studies the pH value was kept at 7.0 with 0.01 M sodium hydroxide solution to ensure adequate enzyme activity. For monitoring purposes, PGA was blended with unbound indomethacin using a CryoMill (Retsch GmbH, Haan, Germany) corresponding to the covalently bound drug contents described in Table 7. Samples were taken at regular time intervals, filtered through Rotilabo® PES sterile syringe filter 0.22 µm (Carl Roth, Karlsruhe, Germany) and

analyzed according to the described HPLC method (Section 3.5). Appropriate volumes of phosphate buffer were replaced after taking samples and the dialysis tubes were changed during each sampling. At the same time as the release studies, the stability of indomethacin in the used release media (PBS, acidic conditions, enzyme) was investigated. This should prevent any falsification of the obtained results. Therefore, saturated indomethacin solutions in pH 7.4 phosphate buffer, pH 4.75 acetate buffers and enzyme solution were prepared and the recovery was determined in additions to the release studies by means of HPLC (Section 3.5).

3.3 NANOPARTICLES

3.3.1 PREPARATION OF NANOPARTICLES

Nanoparticles were prepared according to an optimized interfacial deposition method [72,103,104] (Figure 14). 10 mg of each polymer were dissolved in 1 ml of THF which was then dropped into the aqueous phase using a syringe pump (Pump 11 Elite, Harvard Apparatus, Holliston, Massachusetts, United States of America) into 15 ml of double distilled water, using a 1.0 ml GASTIGHT® syringe (Hamilton Germany GmbH, Planegg - Martinsried, Germany). The syringe was equipped with a Sterican® 23G x 3 1/8" needle (B. Braun Melsungen AG, Melsungen, Germany). The injection flow was adjusted to 0.01 ml/min (total injection time 100 mins). The aqueous phase contained between 0.1 and 0.5 % (w/w) of Poloxamer 188 or PVA as stabilzers and was filtered through a 0.2 μm polythersulfone filter (VWR International GmbH, Darmstadt, Germany) prior. The polymer solutions were injected under continuous stirring with 800 rpm using a magnetic stirrer (20 mm x 7 mm) at room temperature. Remaining THF was removed by rotary evaporation (water bath T = 30 °C, 600 mbar, t = 24 h) to obtain 1 % (m/v) dispersion. The dispersions were stored at 8 °C and protected from light.
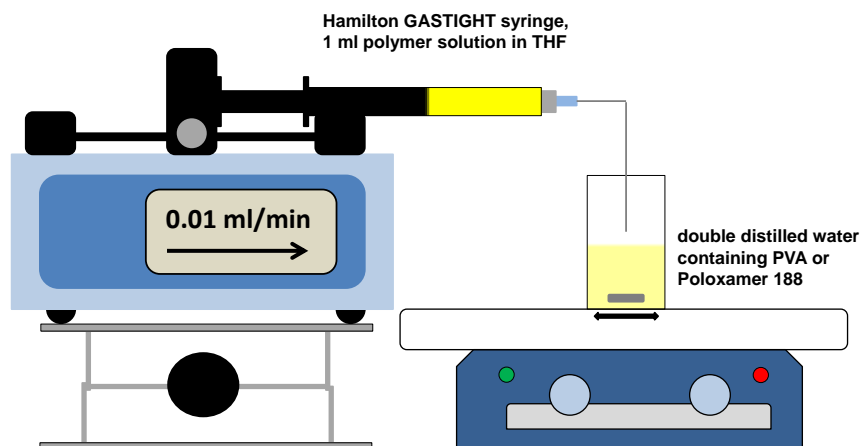
Figure 14. *Schematic illustration of the nanoparticle preparation process.*

3.3.2 METHODS FOR PHYSICOCHEMICAL AND SIZE CHARACTERIZATION

3.3.2.1 PHOTON CORRELATION SPECTROSCOPY

Particle size measurements by PCS were carried out using a Zetasizer Nano ZS (Malvern Instruments, Malvern, United Kingdom). All nanoparticle dispersions were diluted with 0.2 µm (PES, VWR International GmbH, Darmstadt, Germany) filtered double distilled water to a polymer concentration of 0.1 mg/ml. The measurements were performed in the backscattering mode at 173° to prevent multiple scattering events. Each sample was measured 5 times in the automatic mode with 12-17 runs each and 180 s were given to equilibrate at 25 °C. Z-average diameters and polydispersity indices (PDI) were calculated by the Zetasizer software 6.30.

3.3.2.2 NANO TRACKING ANALYSIS

Nano tracking analysis is a unique and innovative technique for sizing particles from 10 to 1000 nm (depending on the refractive index of the particles). This method was first commercialized in 2006 [105]. NTA combines the properties of light scattering and Brownian motion to obtain particle size distributions of nanoparticle dispersions and is especially suitable where the resolution of bright field microscopes are limited due to the Abbe limit. A laser beam, available in different wavelengths, passes through a flat glass and impacts on the suspended nanoparticles in the sample chamber. The particles scatter the light which can be visualized through a microscope. Additionally, the microscope can be equipped with a charged coupled device (CCD), electron multiplied charged coupled device (EMCCD) or high-sensitivity complementary metal-oxide-

semiconductor (CMOS) camera, which captures a video sequence of the moving particles. Therefore, the particle movement caused by the Brownian motion can be visulised either via microscope oculars or through the camera. Subsequently, the image analysis software determines the distance traveled (in two dimensions) by every single particle regarding to the particle center (Figure 15). From this, the hydrodynamic particle diameter can be calculated using the Stokes-Einstein equation (Equation 2). Brownian motion is three-dimensional, the visualization of the particle movement just two-dimensional. Therefore, a modified Stokes-Einstein Equation (Equation 3) is used [106].

$$D = \frac{\kappa_B T}{6\pi\eta r_h}$$

(Equation 2)

$$\overline{(x,y)^2} = \frac{2\kappa_B T}{3 r_h \pi \eta}$$

(Equation 3)

D	Diffusion constant
κ_B	Boltzmann constant
$\overline{(x,y)^2}$	Mean-squared speed of a particle
T	Temperature
η	Dynamic viscosity of the dispersion medium
r_h	Hydrodynamic radius of the particle

In contrast to the dynamic light scattering the size of every single particle is calculated, that makes the NTA superior especially for samples with broad or multimodal particle size distributions [106]. However, the small number of measured particles (40-70) is the greatest disadvantage of the NTA in contrast to DLS due to its statistical power.

The particle size measurements were carried in 0.2 µm filtered double distilled water. The particle concentration was adjusted to 60 particles within the field of vision (100 µm x 80 µm x 10 µm), which equates a dilution of 1 to 100000 in comparison to the samples used during the PCS measurements. Five different positions of each sample were measured for 30 s at 25 °C. A NanoSight NS300 (Malvern Instruments, Malvern, United Kingdom) equipped with a red laser beam (642 nm) was used for the described measurements. Particle movements were visualized by a sCMOS camera. The resulting hydrodynamic diameters were calculated with the corresponding software NTA 3.1.
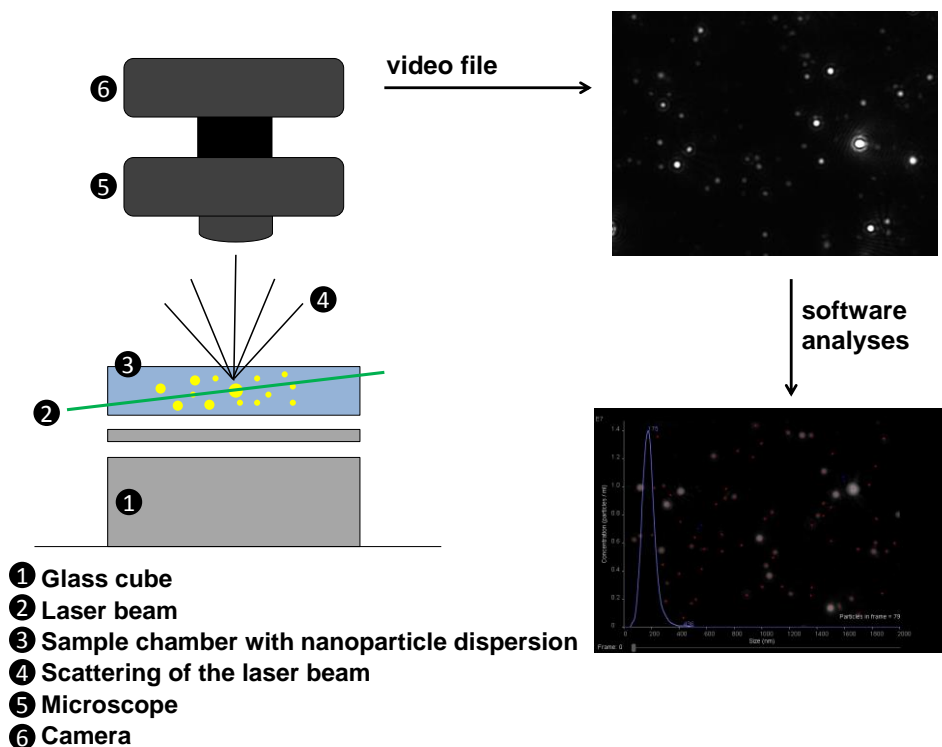
Figure 15. *Schematic illustration of the nano tracking analysis (NTA) measurements using the NanoSight NS 300.*

3.3.2.3 TRANSMISSION ELECTRON MICROSCOPY

The negative stains were prepared by placing 3 µl of the dispersion, diluted to 10 mg/ml, onto a Cu grid coated with a Formvar® film. Excess liquid was blotted off with blotting paper and the grids were washed with double distilled water. Subsequently, the samples were stained with one drop of 1 % (w/v) aqueous uranyl acetate solution. The residual liquid was drained after 1 minute and the samples were air dried. The dried samples were investigated with a Zeiss EM 900 transmission electron microscope (Carl Zeiss SMT, Oberkochen, Germany), operating at an acceleration voltage of 80 kV equipped with a slow scan camera (Variospeed SSCCD camera SM-1k-120, TRS, Moorenweis, Germany).

3.3.2.4 ZETA POTENTIAL MEASUREMENTS

Zeta potential measurements were carried out on a Zetasizer Nano-ZS (Malvern Instruments, Malvern, United Kingdom) using a laser Doppler anemometry. All nanoparticle dispersions were diluted with sodium chloride (5 mM and 10 mM), sodium citrate (5 mM and 10 mM), 1:10 Sörensen's phosphate buffer (pH 4.9 and 6.8) to 0.1 % (w/v) polymeric content. All sample dispersions were incubated at 25 °C in the appropriate buffer for 4 h to ensure charge equilibration. The measurements were carried

out with three runs each at 25 °C, with 18 – 24 runs on average. The equilibration time before each measurement was 180 s. The zeta potential was calculated from the electrophoretic mobility using the Helmholtz-Smoluchowski Equation (4) [107].

$$\zeta = E \left(\frac{4\pi\eta}{\varepsilon}\right)$$

(Equation 4)

ζ   zeta potential

η   dynamic viscosity of the dispersion medium

ε   dielectric constants of the dispersion medium

E   electrophoretic mobility

3.3.3   HEMOLYTIC ACTIVITY

Hemolytic activity was assessed using a Biomaterial Hemolytic Assay Kit (Haemoscan, Groningen, Netherlands). 6 ml of RBCs concentrate were defrosted; 5 ml wash buffer was added and gently mixed by end-over-end tumbling in a centrifuge tube. Afterwards, the mixture was centrifuged at 400xg (Centrifuge 5810 R, Eppendorf Ag, Hamburg, Germany) for 10 mins. The supernatant was withdrawn. This procedure was repeated once more. Then, 2 ml of dilution buffer were added, mixed and centrifuged at 400xg and the supernatant was withdrawn again. This step was repeated twice with 5 ml dilution buffer. Finally, the pellet was re-suspended with 5 ml dilution buffer. Nanoparticle samples (10 mg/ml) as well as 60 µM aqueous indomethacin solutions were prepared resulting in an isotonic dispersion by adding sucrose 10 % (w/v). Isotonic sucrose solution was used as zero value and 2 % (w/v) of aqueous sodium dodecyl sulfate solution as total hemolysis. The samples were prepared by mixing 0.5 ml sample with 0.5 ml RBC suspension and incubated at 37°C in a water bath (GFL® Labortechnik GmbH, Burgwedel, Germany) for 60 minutes. Residual RBCs were removed by centrifugation at 4000xg (Minispin, Eppendorf AG, Hamburg, Germany). 20 µl of the supernatant were finally mixed with 180 µl assay buffer in a well of a microtiter plate. The hemoglobin absorption was measured at 380 nm using an Epoch 2 Microplate Spectrophotometer (BioTek Instruments Inc., Winooski, Vermont, United States of America). The calibration was carried out using a 10 mg/ml hemoglobin stock solution. The percentage of hemolysis was calculated according to Equation (5) below [108].

$$\text{Hemolysis (\%)} = \frac{(\text{Absorption}_{\text{sample}} - \text{Blank}_{\text{sample}}) - (\text{Absorption}_{\text{negative control}} - \text{Blank}_{\text{negative control}})}{\text{Absorption}_{\text{positive control}} - \text{Blank}_{\text{positive control}}} \times 100\%$$

(Equation 5)

3.3.4 CYTOTOXICITY

A549 (human lung carcinoma), HeLa cells (human cervix adenocarcinoma epithelial cells) and LLC-PK1 cells (pig kidney epithelial cells) were cultured in 75 cm^2 tissue culture flasks in Dulbecco's modified eagle medium (DMEM) adjusted to contain 4.5 mg·ml^{-1} glucose, 10 % (m/v) FBS at 37 °C and 5 % (v/v) CO$_2$. The cells were grown ~90 % confluent and were split regularly three times a week. For the experiments, cells in the range of passages 10-20 were used.

A549, HeLa and LLC-PK1 cells were seeded into 96-well plates (Cellstar, Greiner BioOne GmbH, Frickenhausen, Germany) at a density of 1·10^4-1.1·10^4 cells/well 24 h before incubation with the nanoparticles. The cells were washed once with PBS. Then the nanoparticles were added to the cells (0.5 – 40 µg per well). For the cytotoxicity assay, the same plates were used and 100 µL of a 2 % (m/v) alamarBlue$^®$/PBS solution (Invitrogen GmbH, Darmstadt, Germany) were added to every well. The plates were incubated for 1 h at 37 °C and 5 % (v/v) CO$_2$. The fluorescence signal was measured using a BMG 10 filter (λ_{ex} = 544 nm, λ_{em} = 590 nm) with a fixed gain. Viabilities above 100 % were set to 100 %. All measurements were performed six times (n = 6).

3.3.5 *IN VITRO* RELEASE

Release studies were performed with a self developed apparatus, illustrated schematically in Figure 16. The apparatus consists of a custom made vacuum-tight Erlenmeyer flask. Via a rubber seal a 5 ml luer-lock glass syringe, containing the nanoparticle dispersion (5 ml; 1 mg/ml) stabilized with 0.5 % (w/v) Poloxamer 188, can be directly attached to the system. Core unit is the FlexiPor$^®$ aluminum oxide membrane with an average pore diameter of 20 nm, which separates the released indomethacin (solubility 800 µg/ml at pH 7.4) from the remaining nanospheres. The release system was gently stirred using a magnetic stirrer. Samples (1 ml) were taken periodically under reduced pressure (300 mbar) directly into a HPLC auto sampler brown glass vial. Afterwards, the sample volume was substituted. Prior to the release experiments the recovery rate of indomethacin was determined to judge the impact of undesired

adsorption processes. The quantification of released indomethacin was carried out according to the subsequent described HPLC method (Section 3.5).

1 Vacuum-tight Erlenmeyer flask

2 5 ml Fortuna® Optima glass syringe (Luer lock) with nanoparticle dispersion and magnetic stirrer

3 Rubber seal

4 Polycarbonate syringe filter holder attached with FlexiPor® aluminium oxide membrane

5 1 ml autosampler vial

6 Vacuum adapter

7 Agitator
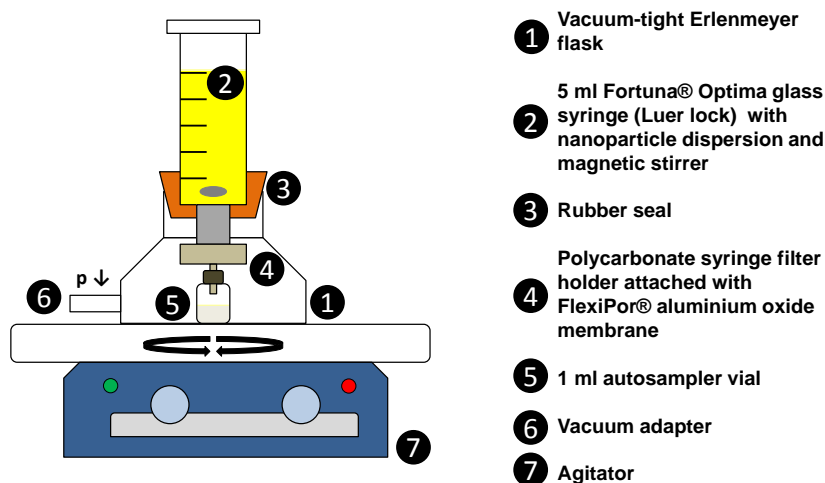
Figure 16. *Schematic illustration of the release apparatus.*

3.4   MICROPARTICLES

3.4.1   PREPARATION OF MICROPARTICLES

The microparticles were prepared using a modified oil-in-water (O/W) solvent evaporation technique [109]. The setup ist schematically illustrated in Figure 17. 100 mg of each polymer were dissolved in 2.5 ml dichloromethane. The polymeric solution was injected into 100 ml of 5.0 % (w/v) aqueous Poloxamer 188 solution. The aqueous phase was vigorously stirred with 500 rpm using a RW 20 agitator (Janke & Kunkel, IKA® Labortechnik, Staufen im Breisgau, Germany) equipped with a blade stirrer (40 mm x 6 mm). The injection was carried out using a syringe pump (Pump 11 Elite, Harvard Apparatus, Holliston, Massachusetts, United States of America) equipped with a 2.5 ml GASTIGHT® syringe (Hamilton Germany GmbH, Planegg - Martinsried, Germany). The syringe was equipped with a Sterican® 23G x 3 1/8" needle (B. Braun Melsungen AG, Melsungen, Germany). The injection flow was adjusted to 0.01 ml/min (total injection time 100 minutes). The total injection time was 250 minutes. Afterward, the dispersion was stirred for additional 120 min. After sedimentation the supernatant was withdrawn and the microparticles were transferred into a 15 ml centrifuge tube (VWR International GmbH, Darmstadt, Germany), double distilled water was added, and gently centrifuged (Labofuge 300, Heraeus GmbH, Hanau, Germany) with 400 rpm for 2 mins, the supernatant was withdrawn repeatedly. This process was repeated twice.

Finally, the microparticles were frozen in liquid nitrogen and residual water or solvents were removed by lyophilization (Christ Alpha 2-4, Martin Christ, Germany) (Section 3.7.2).
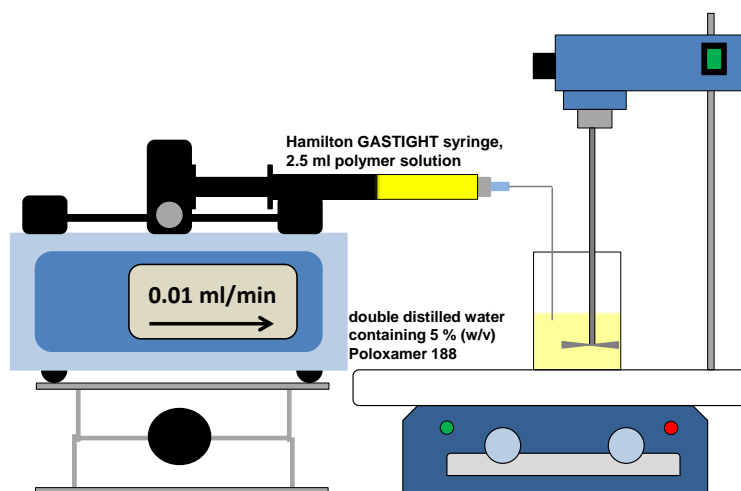
Figure 17. *Schematic illustration of the microparticle preparation process.*

3.4.2 METHODS FOR PHYSICOCHEMICAL AND SIZE CHARACTERIZATION

3.4.2.1 STATIC LIGHT SCATTERING

Measurements of the particle size distribution were carried out by laser diffractometry using a Mastersizer 2000 (Malvern Instruments, Malvern, United Kingdom) equipped with a Hydro 2000 S dispersion unit. The samples were measured with an average laser obscuration of 2.0 % in double distilled water. For each sample 5 runs were measured and the data were evaluated by the Mastersizer 2000 software (version 5.60). The Mie theory was the basis for the calculation of the particle size assuming spherical [110].

3.4.2.2 MICROSCOPY

For the visualization of the prepared microparticles two different microscopes were used. An Olympus SZX 9 reflected-light microscope (Olympus Europa Holding GmbH, Hamburg, Germany) was used to get an overview of the particles. For detailed pictures and single size measurements an Axiolab transmitted-light microscope (Carl Zeiss MicroImaging GmbH, Göttingen, Germany) was used.

3.4.2.3 SCANNING ELECTRON MICROSCOPY

Size and shape of the prepared microparticles were investigated using scanning electron microscopy (SEM). Prior to the measurements the microparticles were coated with a 15 nm chromium layer via ion beam sputter. This is a common method to improve the imaging of electrically non-conducting sample materials in the SEM. The measurements were carried out on a XL30 ESEM FEG (FEI, Hillsboro, United States of America). The images were taken at low acceleration voltage of 1 keV or 2 keV using the secondary electron signal (SE image).

3.4.3 *IN VITRO* RELEASE

The in vitro release of indomethacin from PGA-indomethacin microparticles was carried out as follows: 10 mg of microparticles made out of PGA-indomethacin 50 and 100 % were placed in a 10 ml brown glass vial (Infochroma AG, Zug, Switzerland). Afterwards, 5 ml of PBS pH 7.4, acetate buffer pH 4.75 and lipase from *Pseudomonas* sp. (stock solution in 0.9 % (w/v)) was added respectively. The samples were stored at 37 °C under light protection and were shaken in a water bath under light protection (Memmert GmbH & Co. KG, Schwabach, Germany). Samples were taken using a Hamilton Gastight® syringe (Hamilton GmbH, Höchst, Germany) attached with a PES sterile filter to prevent removal of small particles. Half of the release medium was exchanged at pre determined timepoints. The released indomethacin was quantified every three days during the first month, once a week thereafter. The quantification was carried out using the HPLC method described below (Section 3.5). 50 µl were injected into the column.

3.5   HIGH PERFORMANCE LIQUID CHROMATOGRAPHY

A modified United States Pharmacopeia (USP29) method was used to quantify the released indomethacin.

A high-performance liquid chromatography (HPLC) system, equipped with a Merck Hitachi L-6200A Intelligent Pump, D-6000 Interface, AS-4000 Intelligent Auto Sampler, L-4200 UV/VIS Detector (all Merck Hitachi, Tokyo, Japan) was used. Separations were carried out using a LiCrospher® 100 RP-18 5 µm column (Merck Millipore, Billerica, Massachusetts, USA) and a mobile phase of 70 % (v/v) phosphate buffer (0.01 M

sodium hydrogen phosphate / 0.01 M disodium hydrogen phosphate) / 30 % (v/v) acetonitrile. Runs were carried out at 1 ml/min over 10 mins and the absorption at 318 nm was recorded. Injection volume was 50 µl. The retention time of indomethacin was 4.6 min.

3.6   *IN VIVO* CHARACTERIZATION

3.6.1   ANIMAL CARE

All *in vivo* experiments complied with the regional regulations and guidelines and were approved (Approval No. 505.6.3-42502-2-1456 MLU) by the Animal Ethics Committee of the state Saxony-Anhalt (Germany) and the commissary of animal protection of the Martin-Luther-University Halle (Germany). Male as well as female immunocompetent and euthymic SKH1-Hr^{hr} were used because hair would have disturbed the multispectral fluorescence measurements. The mice were kept under controlled conditions (12 h light/dark cycle, 24 °C and 65 % relative humidity). Feed and water were provided *ad libitum*. They were kept in groups of two or three mice per cage. Initially, they had an average age of 6 months.

3.6.2   INJECTIONS AND ANESTHESIA

Formulations were injected using a mouse restrainer. 100 µl of each formulation was injected slowly into the *vena caudalis mediana*. Afterward mice were anesthetized initially with 2.5 % (v/v) of isoflurane (Forene®, AbbVie, North Chicago, USA) in oxygen (flow 3 l/min). The mixture was generated by a VIP 3000® Veterinary Vaporizer (Midmark, Dayton, USA). During the multispectral fluorescence imaging the mice were kept in anesthesia (2.5 % (v/v), flow 2.0 ml/min) and were imaged in groups of five mice. Group (A) consisted of 5 mice (3 female and 2 male), group (B) consisted of 4 mice (2 female and 2 male). Group (A) was treated with 100 µl of PGA-IDMC 100 % NP dispersion containing DiR (0.25 % (w/w)). One male and one female mouse of group (B) were treated with 100 µl fluorescence labelled PGA-IDMC-DY782 NP dispersion. The two others remained untreated as control group.

3.6.3 SAMPLE PREPERATION

Based on the biological characterization *in vitro* PGA-IDMC 100 % based NP have been chosen for the biodistribution and elimination study in vivo. The nanoparticles have been prepared as follows:

10 mg of PGA-IDMC 100 % were dissolved in 875 µl of dry THF and 125 µl of a DiR THF solution (2 mg/ml) were added, the solutions were mixed carefully using a MS2 Minishaker (IKA Werke, Staufen im Breisgau, Germany). Finally the nanoparticles were prepared according to the procedure previously described (Section 3.3.1). Aqueous mannitol solution 5 % (m/v) was used as dispersant.

Anymore, 900 µl of a PGA-IDMC 100 % solution in THF (10 mg/ml) were mixed with 100 µl of a PGA-IDMC 50 %-DY-782 conjugate solution (10 mg/ml). The solutions were carefully mixed as described above. Lastly, the nanoparticles were prepared according to procedure outlined above (Section 3.3.1). Aqueous mannitol solution 5 % (m/v) was used as dispersant.

3.6.4 MULTICPECTRAL FLUORESCENCE IMAGING

Biodistribution and elimination studies of the PGA-IDMC 100 % based NP were performed on an IVIS® Spectrum *In Vivo* Imaging System (Perkin Elmer, Waltham, USA) equipped with a small animal gas anesthesia system (XGI-8, Caliper LifeSciences, Waltham, USA). The biodistribution and elimination was studied based on fluorescence [82]. The near infrared tracer DiR was incorporated into the polymers and DY-782 was covalently bound. The imaging system contained a xenon lamp as light source. The suitable wavelength (745 nm) was filtered by a narrow band excitation filter (30 nm bandwidth). The emission light was selected by narrow band emission filter (800 nm) with a bandwidth of 20 nm. The filtered fluorescence light was detected by a precooled (-90 °C) CCD camera (13.5 micron pixels, 2048 x 2048). Data analysis was carried out using the corresponding software Living Image® (version 4.5.2.).

3.7   MISCELLANEOUS LABORATORY EQUIPMENT

3.7.1 CRYOMILLING

Cryomilling was conducted by using a CryoMill (Retsch GmbH, Haan; Germany).

1 g of each sample was placed in a 5 ml stainless steel grinding jar and two steel balls with 2 mm diameter were added. The samples were precooled to -197 °C using liquid nitrogen for 2 mins. Afterward, milling was performed for 1.5 mins at 15 CPS. This cycle was repeated four times. Finally, the milled samples were removed after room temperature was reached.

3.7.2 LYOPHILISATION

Freeze-drying was carried out on a Christ Alpha 2-4 freeze dryer (Martin Christ Gefriertrocknungsanlagen GmbH, Osteroder am Harz, Germany) equipped with a Vaccubrand RC 6 vacuum pump (Vaccubrand GmbH, Wertheim, Germany). Prior to freeze-drying the samples were rapidly frozen with liquid nitrogen at -196°C. The drying period was chosen to be 24 h. The chamber was evacuated to 0.05 mbar, corresponding to -48 °C on the sublimation curve of ice [111].

3.7.3 MICROSCOPY

Size and swelling behavior of preformed implants and microparticles were studied using an Olympus SZX9 reflected light microscope or an Axiolab (Carl Zeiss MicroImaging GmbH, Göttingen, Germany) transmitted light microscope equipped with a UC30 camera (Olympus Optical Co., Hamburg, Germany).

Pictures were analyzed with OLYMPUS stream motion (Olympus Optical Co., Hamburg, Germany).

3.8   SOFTWARE

This thesis was written in Microsoft Word 2010 (Microsoft Corporation, Redmond, USA). Literature was managed in Citavi 5 (Swiss Academic Software GmbH, Wädenswil, Suisse). If not stated otherwise, graphs were generated in OriginPro 8G (OriginLab Corporation, Northampton, USA). Chemical formulas were drawn in ChemBioDraw Ultra 12.0 (PerkinElmer, Corporation, Waltham, USA). Graphics and images were created, set or edited in Microsoft PowerPoint 2010 (Microsoft Corporation, Redmond, USA).

4   RESULTS AND DISCUSSION

4.1   SYNTHESES AND CHARACTERIZATION OF THE BULK POLYMERS

Lipases (triacylglycerol lipase; EC 3.1.1.3) are enzymes and generally known for their hydrolytic activity. *In vivo,* they catalyze the hydrolysis of fatty acid glycerol esters. Also, the opposite direction of this reaction can be catalyzed by enzymes leading to polyesters. Condensations are based on four basic reactions (dehydration, alcoholysis, acidolysis and intermolecular esterification), which all lead to esters. The three latterly mentioned reactions can be summarized as transesterification. Lipase catalyzed ester synthesis using polycondensation can catalyze all four reactions. Therefore, enzymes are promising and efficient catalysts for the *in vitro* syntheses of polyesters [112–118]. CALB (*Candida antarctica*) is an efficient catalyst for dehydration catalyzed esterification. When the lipase is immobilized on an acrylic resin it is easier to remove after the synthesis. Commercially it is called for example Novozym 435. The structure of CALB was first determined in 1993 and a year later by Uppenberg *et al.* [68]. CALB is composed out of 317 amino acids. The active center consists of Ser-His-Asp catalytic triad in its active site. The mechanism of the catalytic effect was summarized by Shiro Kabayashi in 2010 [69]. For the synthesis of poly(glycerol adipate) the mechanism of the reaction is as follows. In brief, divinyl adipate is interacting with the active site of the enzyme leading to an enzyme substrate complex followed by acylation and splitting of vinyl alcohol. In the last step (deacetylation) the new ester is formed. Therefore, this reaction is called transesterification. Like any other condensation, this polycondesation is reversible and the removal of byproducts affects the yield of the products positively. The vinyl alcohol converts directly into acetaldehyde by tautomerization during the reaction and disappears instantly. Therefore, the yield of the reaction is very high. There have also been reports of successful scale up experiments with yields of 200 kg polymer using this reaction [119]. The most important fact for the aim of this thesis is that the reaction proceeds regioselectively with preference for primary alcohols of the glycerol. This yields to linear polyesters with free pendant hydroxyl groups at its backbone which enables further derivatization at the secondary hydroxyl group with indomethacin in order to create poly(glycerol adipate)-indomethacin conjugates.

The coupling of indomethacin to the linear poly(glycerol adipate) BB was carried out using EDC-HCl and the Steglich catalyst DMAP [120]. In contrast to other carbodiimides, EDC-HCl as well as the urea by product are water-soluble and can be easily removed after the reaction. Reactions carried out with other carbodiimides such as DCC headed in remaining urea by-products which was difficult to remove completely.

4.1.1 CHEMICAL STRUCTURE

^{1}H-NMR spectroscopy is a common method for fast structure analysis of dissolved organic compounds, pharmaceutical ingredients, polymers and proteins [121]. The location and splitting of the individual signals is crucial for the structure elucidation of organic molecules [122]. Moreover, ^{1}H-NMR spectroscopy is a powerful tool for the calculation of the degree of grafting [102].

^{1}H-NMR spectra were recorded of PGA, PGA-IDMC 25, 50 and 100 % (mol) as well as of free indomethacin in CDCl$_3$ and shown in Figure 19.
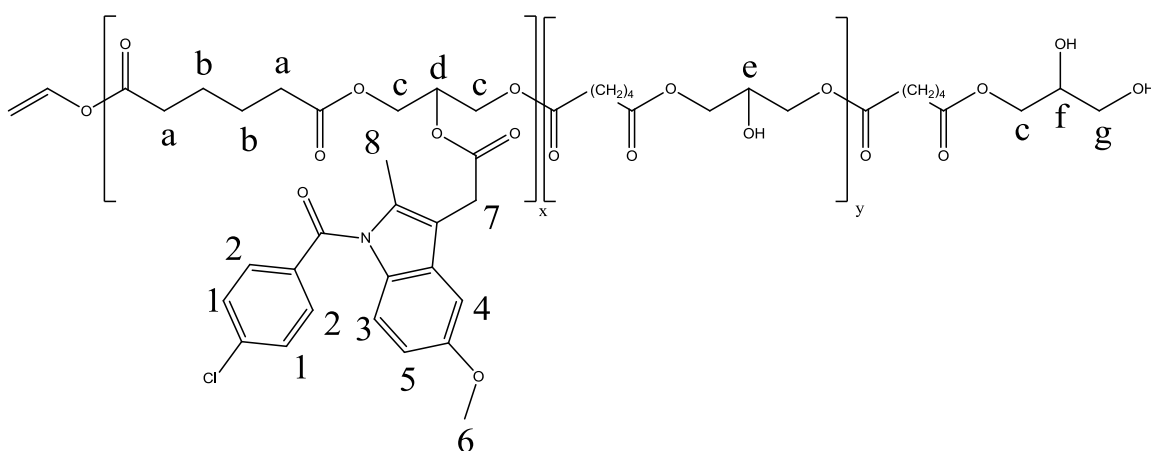
Figure 18. *Chemical structure of the PGA-IDMC conjugate. The corresponding structural features of the backbone were denoted by letters, those of indomethacin by numbers and were used in the following descriptions.*
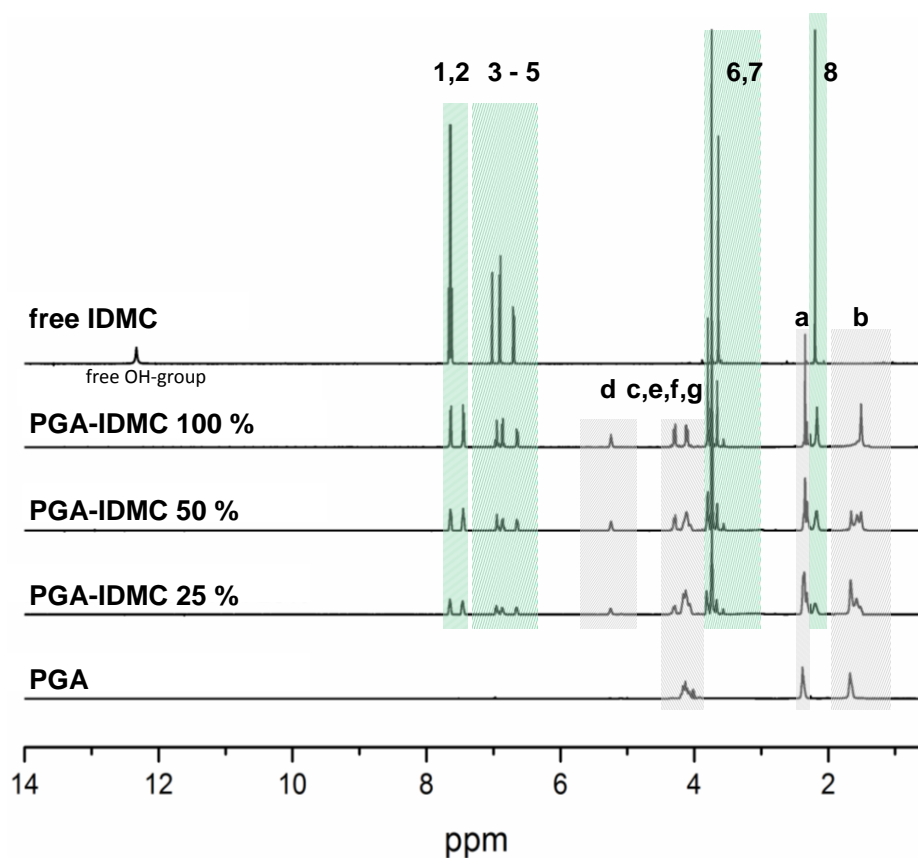
Figure 19. ^{1}H-NMR spectra of PGA, different PGA-IDMC conjugates bulk polymers and free indomethacin measured at room temperature in $CDCl_3$[*]. The magnetic resonance signals are signed corresponding to the positions of the protons in the chemical formula of Figure 18 above. For better clarity, the peaks belonging to the indomethacin were highlighted in green and those of the backbone in gray. ([*]solvent peaks are not shown)

The protons around a chemical shift of 4 ppm (Figure 19; c,e,f,g) belong to the glyceride repeating units of the polymer backbone [70]. The peak region from 5.0 – 6.0 ppm (Figure 19, d) is important to assess the presence or absence of secondary ester moieties. The absence of this peak indicates that the PGA backbone is linear and has no branches due to esters of secondary alcohol groups. With increasing grafting the mentioned secondary ester moiety peak at a chemical shift of 5.25 ppm (Figure 19, d) and the integral increases as well. The peaks in the high field of the spectrum at 2.3 and 1.5 ppm (Figure 19, a and b) represent the methylene groups of adipic acid repeating units. Upon closer examination of the peak complex "-c,e,f,g-" it is noticeable that with increasing degrees of substitution the peaks become more separated (c from e, f and g) and, when almost completely modified with indomethacin, a double multiplet consisting of only "c" remains. Furthermore, the hydroxyl group peak of free indomethacin in the low field is missing for the grafted polymers. It was confirmed that there was no free indomethacin incorporated in the polymer samples. The remaining peaks, labelled with

"1-8" are representatives of indomethacin protons. As already mentioned, the degree of grafting can be determined using ^{1}H-NMR spectroscopy. Therefore, the integrals of the methine groups of triple esterified glycerol (Figure 19, d, δ=5.25 ppm) were compared with the ones of the methylene peak (Figure 19, b, δ=1.5 ppm) [123]. The ratio of the integrals is 1 to 4 for 100 % (mol) of grafting according to the Equation 6 below.

$$\frac{d}{b} = \frac{1}{4} \qquad\qquad \text{(Equation 6)}$$

Using the previously described syntheses, PGA-indomethacin conjugates with grafting between 23 and 92 mol% could be synthesized (Table 7). As an additional method, the content of indomethacin was determined by UV/VIS spectroscopy (Section 3.2.2). Prior to the quantitative measurements, it was examined whether the absorption maxima of bond and free indomethacin showed any shift (Figure 20). Comparing the values for PGA-indomethacin 25 mol% it is noticeable that the real content of active substance is higher than the theoretically expected one. There is the possibility of unbound, dispersed indomethacin. For PGA-indomethacin 50 mol% conjugation theoretically and real drug content were nearly equal, merely the ^{1}H NMR calculated value was slightly lower. As expected the theoretical value for PGA-indomethacin 100 mol% could not be reached, because of the sterically hindrance of the conjugation with increasing grafting. Furthermore, chain branching due to reaction of secondary hydroxyl groups during the PGA synthesis cannot be excluded completely [124].
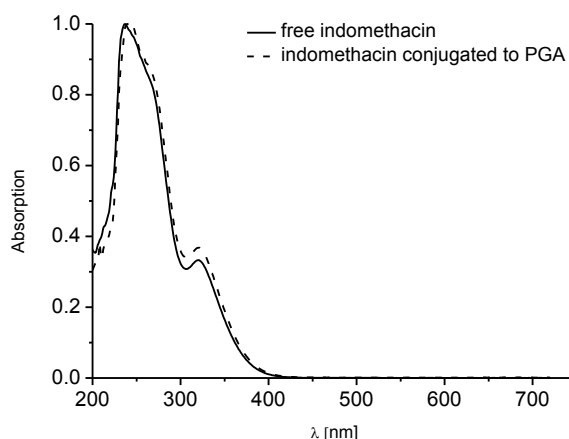
Figure 20. *Comparison of UV/VIS absorption spectra (200-750 nm) of free (black line) and covalently bond indomethacin (PGA-IDMC 100 %) (dashed line) recorded in dry DCM at room temperature.*

Thus not all theoretically available OH groups could be derivatized. To summarize, UV/VIS and NMR spectroscopy are suitable to quantify the drug loading and the

conjugation degree, respectively. UV/VIS spectroscopy is the prefered method, because it is fast, cheap and easy to perform. Furthermore the ^{1}H NMR method is more susceptible to inferences by the various options setting the integration limits. Since the syntheses were almost quantitative with the molecular ratios used, the three different polymers, for the sake of simplicity, are referred to below as PGA-IDMC 25, 50 and 100 % or low, medium and high modified. The indication of the mass share of indomethacin is more relevant for practice; the degree of derivatization was therefore converted into % (w/w) (Table 7).

Table 7. *Content of indomethacin in percent (w/w) of grafted PGA determined via ^{1}H-NMR and UV/VIS spectroscopy in comparison to theoretically calculated values, assuming ideal reactions.*

Polymer	Theory % (w/w)	^{1}H-NMR % (w/w)	UV/VIS % (w/w)
PGA-IDMC 25 %	30.7	28.3	35.6
PGA-IDMC 50 %	47.0	42.3	46.9
PGA-IDMC 100 %	63.9	58.8	54.1

In order to gain further insights into to the structure of the synthesized conjugates, the polymers and indomethacin were investigated using ATR FT-IR spectroscopy. IR spectroscopy is based on the following principles: By absorbing radiation from the infrared spectral range, the atoms in molecules are excited to mechanical vibrations. There are essentially two different vibrations. On the one hand the vibrations along the bond axis (valence or stretching vibrations) and on the other hand vibrations with deformation of the bond angle (deformation vibration). The molecular vibrations of certain groups of atoms are particularly characteristic and can be used for structural analysis. Therefore, infrared spectroscopy is particularly suitable for the identification of functional groups. In addition, there are so-called fingerprint regions of a spectrum which are characteristic for the entire molecule. Moreover, vibration spectroscopy is still a common method for the characterization of polymorphs as well as the investigation of crystalline states [125,126,127]. It is known that indomethacin has two monotropic polymorphic states, the stable γ form as well as the metastable α form. Furthermore, the amorphous state exists [128,129]. Infrared spectra were recorded for all polymers, to find out which form of indomethacin is present and to understand structural changes during conjugation. The spectra, with highlighted characteristic peaks, are shown in Figure 21.
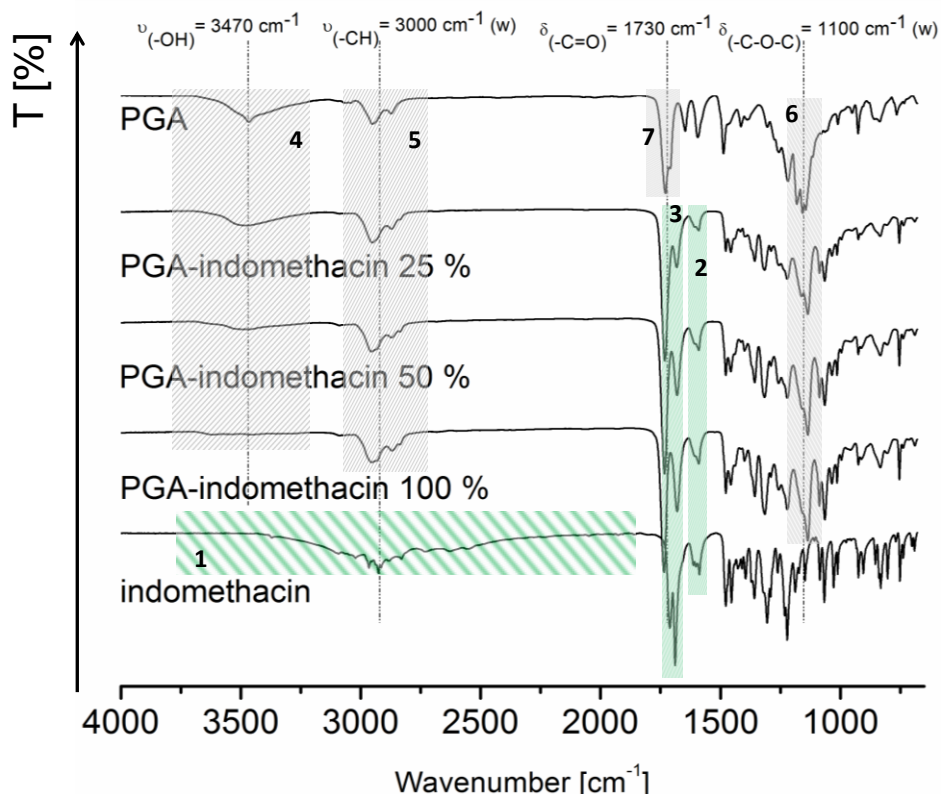
Figure 21. *ATR FT-IR spectra of poly(glycerol adipate), indomethacin and different conjugates measured at 25 °C between 650 and 400 cm^{-1}. For better clarity, the peaks belonging to the indomethacin were highlighted in green and those of the backbone in gray.*

Indomethacin has three different important structural features, which are illustrated in Figure 21 and in Table 8 with "1-3". Particularly noteworthy is the broad band of a hydrogen bonded hydroxyl group. The shape of this wide band is different for α, γ and amorphous indomethacin. Accordingly, the used indomethacin is the stable γ-indomethacin [125]. The peaks marked 2 and 3 can be attributed to the two carbonyl functions of indomethacin (benzoyl and acid/ester). It is striking that the amid peak (Table 8, number "2") remains unchanged. In contrast, the asymmetric peak of the free carboxylic acid (Table 8, number "3") in the course of the co-conjugation changes its shape; a successful esterification can be derived from this. The most important change occurs in the range of secondary hydroxyl groups (Figure 21, number "4"). With increasing degree of esterification, this broad peak disappears as well as the broad hydroxyl peak of the free indomethacin acid (Figure 21, number "1"). Considering the measuring accuracy, the results of the ^{1}H-NMR can be confirmed and the esterifications were successful. Furthermore, it can be stated that no unbound indomethacin is dispersed in the polymer.

Table 8. *Wavenumbers and assignments of the various functional groups mentioned in Figure 21. Highlighted in grey are the important peaks and regions caused by structures of the poly(glycerol adipate) backbone.*

Area	Wavenumber [cm^{-1}]	Assignment
1	2500 – 3400	Broad hydroxyl stretching region of the carboxylic acid group of indomethacin
2	1630 – 1695	Benzoyl stretch of indomethacin
3	1717 – 1730	Asymmetric carbonyl stretch of indomethacin
4	3250 – 3750	Stretching area of free secondary hydroxyl goups
5	2800 – 3000	Symmetric and asymmetric stretching of carbon-hydrogen bonds
6	1100	Stretching of carbon-oxygen-carbon bonds of the esters bonds
7	1730	Carbonyl stretch of the ester bond

4.1.2 MOLECULAR WEIGHT

The molecular weights as well as the PDIs of the synthesized polymers were investigated by GPC (gel permeation chromatography). GPC is also referred to as size exclusion chromatography (SEC). This type of chromatography differs from other liquid chromatographic methods, because the sample molecules do not interact (adsorption, distribution) with the column material. The separating material which is used is a porous gel with defined pore sizes. The separation is based on the different intrusion possibility of sample molecules of different sizes in the pores. Molecules that are too large are excluded (size exclusion) and exit from the column as first [130]. In general, with increasing degree of conjugation, M_n, M_w and the PDI are increasing (Table 9). Between two and three polydispersity indices are typical for branched polymers [131]. The esterification using EDC-HCl follows a random pattern. Hydrolytic degradation due to residual water and lipase, reactions between monomers and oligomers may cause the ascending polydispersity indices as well as the smaller M_n of PGA-IDMC 25 % in comparison to the poly(glycerol adipate) backbone. As expected, the retention volume slightly decreased with increasing molecular weight (Figure 22). Thus, large molecules are excluded first from the column.

Table 9. *Results of the molecular weight (M_n and M_w) analysis by GPC. Sample concentration was 3 mg/ml and the calibration was carried out using polystyrene.*

Polymer	M_n [Da]	Mw [D_a]	PDI	Retention volume [ml]
PGA	3838	8575	2.2	8.1
PGA-IDMC 25 %	3304	9586	2.9	8.07
PGA-IDMC 50 %	5678	14518	2.6	7.82
PGA-IDMC 100 %	6153	19603	3.2	7.78
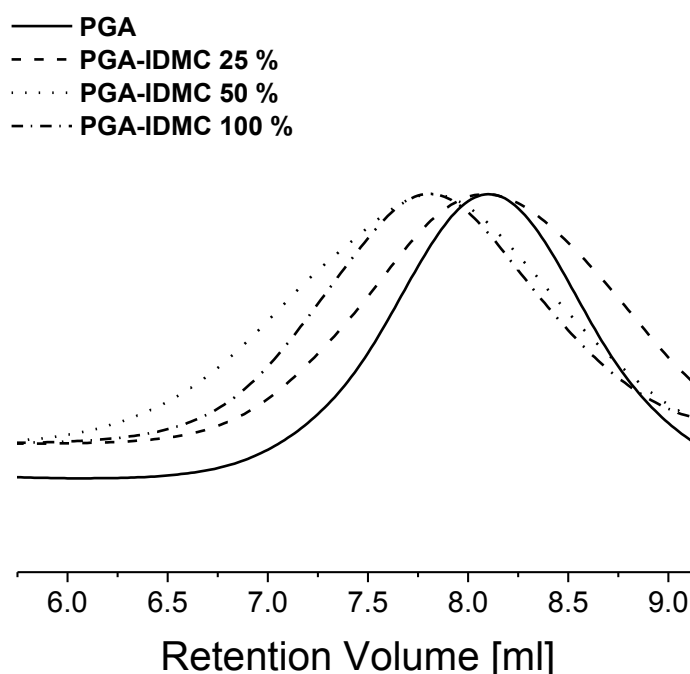
Figure 22. *GPC traces of grafted and non-grafted PGA. THF was used as eluent. Column material was poly(styrene-co-divinylbenzene).*

4.1.3   DIFFERENTIAL SCANNING CALORIMETRY

At the DSC, heat effects from the sample due to heat conduction from the oven to the sample are expressed by thermal resistances in the temperature differences between sample and reference. Furthermore, the heat flow can be determined quantitatively. The DSC measures the difference between the heat flows to the sample crucible and a reference crucible. The heat flow difference between sample and reference is proportional to the temperature difference. DSC allows the investigation of exothermic and endothermic processes; therefore it is used for the identification, purity testing and

characterization of substances, for example to determine the glass transition, the proportion of crystalline components or the melting curves of polymers [132]. The analysis of polymorphic or pseudo-polymorphic drugs is also a common field of application.

Aim of the DSC measurements was the investigation of the change in thermal behavior of the polymer backbone in comparison to grafted poly(glycerol adipate). Furthermore, physical mixtures of PGA and indomethacin were examined. Poly(glycerol adipate) is an amorphous polymer and the glass transition temperature was found to be -23.7 °C which is comparable to previously published research [80]. Indomethacin is polymorphic and the γ modification was used. It can be noted that indomethacin has a glass transition temperature around 46 °C and the melting point was about 163 °C (Figure 22). The tendency of crystallization of drug melts can be separated into three different classes [133]. It could be confirmed that the γ indomethacin form belongs to class (III), and therefore shows no crystallization from the melt.
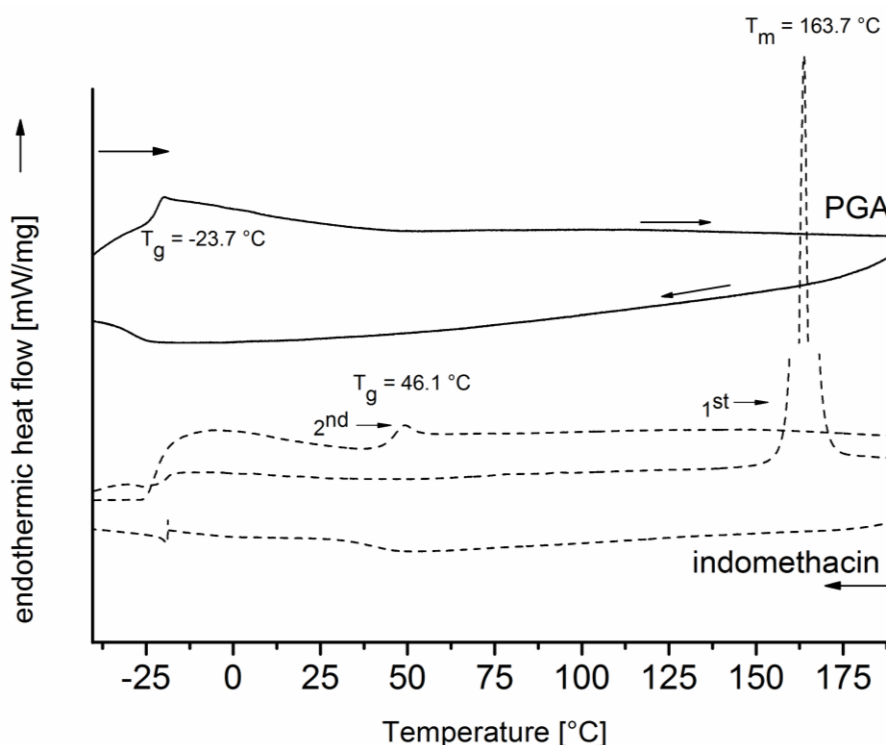
Figure 23. *DSC thermograms showing the thermal behavior of PGA (continuous line) and free indomethacin (dashed line) as bulk materials. The measurements were carried out with a heating/cooling rate of 5 K/min.*

Similar to the poly(glycerol adipate) backbone, the three grafted polymers are amorphous and showed no first order phase transition (Figure 24). It is obvious that the glass transition temperature is increasing from the PGA backbone to PGA-IDMC 100 % due to the sterical hindrance resulting in lower segmental mobility. These observations coincide with those of the macroviscosity measurements (Section 4.1.5).
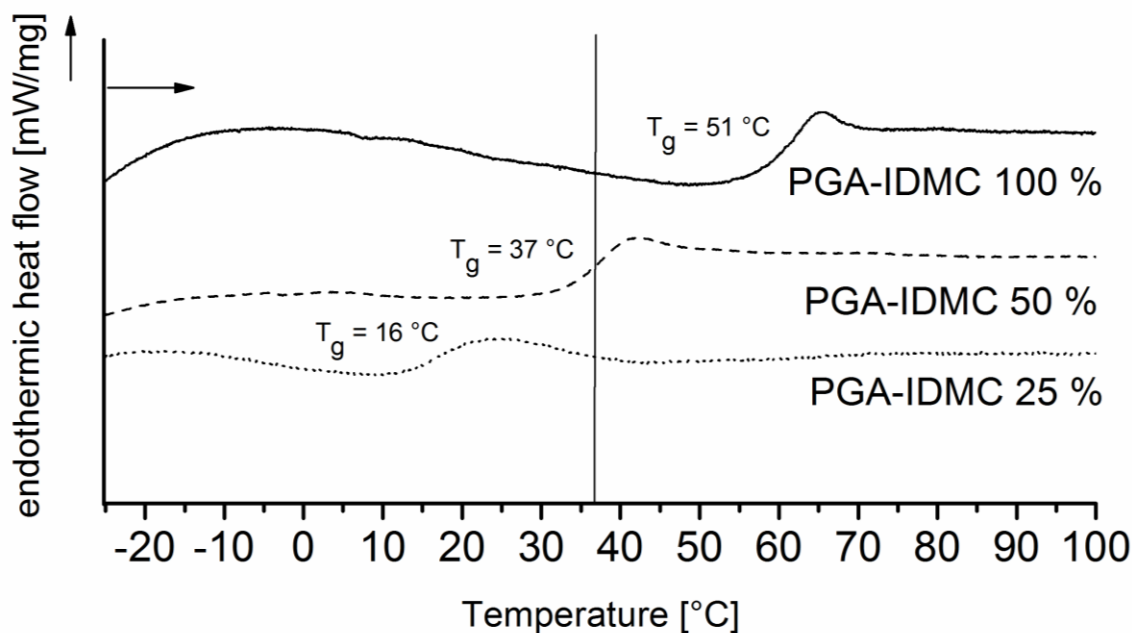
Figure 24. *DSC thermograms showing the thermal behavior of PGA-IDMC 25 % (dotted line), PGA-IDMC 50 % (dashed line) and PGA-IDMC 100 % (continuous line) as bulk materials. The measurements were carried out with a heating/cooling rate of 5 K/min.*

It was reported, that indomethacin and nifedipine are soluble or partly soluble in different polymers like polyvinyl pyrrolidone (PVP), polyvinyl acetate (PVAc) and their co-polymer (PVP/VA) [134]. To be sure that the observed shifts in the glass transition temperatures are due to covalently bound indomethacin, physical mixtures of PGA and indomethacin were prepared by cryo-milling (Section 3.7.1) in the ratio (w/w) of PGA to indomethacin equal to PGA-IDMC 25 and 100 %. Indomethacin is a hydrophobic drug; it should be less soluble in hydrophilic PGA. The results are shown in the following table (Table 10).

Table 10. *Glass transition temperature (T_g) and melting points (T_m) of PGA, PGA-IDMC conjugates and physical mixtures (PM) of PGA and indomethacin. The data were collected by DSC measurements carried out at 5 K/min.*

Sample	T_g [°C]	T_m [°C]
PGA	-23.7	N/A
Indomethacin	46.1	163.7
PGA-IDMC 25 %	16	N/A
PGA-IDMC 50 %	36.8	N/A
PGA-IDMC 100 %	51	N/A
PGA-IDMC PM 25 %	-0.1	138.9
PGA-IDMC PM 100 %	18.5	153.1

For both physical mixtures clear melting peaks of indomethacin, induced by the presence of crystals could be observed. Nevertheless, a shift of the melting temperature of indomethacin as well as of the glass transition temperature of PGA was noticeable, due to polymer-drug interactions. It is also conceivable that there was an amorphization or conversion of indomethacin into α modifiaction by mechanical action. However, published research [135] showed that the γ modification is stable in short milling cycles, which was also used for the reasons mentioned above.

4.1.4 X-RAY DIFFRACTION

Another analytical method for the determination of polymorphs is the powder X-ray diffraction. As already mentioned the used indomethacin occurs in the γ form and is stable over short cryo-milling cycles. In order to support the obtained results of the DSC (Section 4.1.3), for all polymers and indomethacin powder, X-ray diffractograms were recorded. Figure 25 shows the diffraction patterns of the four mentioned polymers and indomethacin. Indomethacin (γ form) shows five main reflexes at 11.6° (A), 16.8° (B), 19.6° (C), 21.9° (D) and 26.7° (E) (Figure 25) which confirm the literature data [136]. The poly(glycerol adipate) backbone shows a slight and broad reflex at 20° (Figure 25, black line). This reflex might be caused by free carboxylic acid groups. These free functional groups may be responsible for a semi-crystalline organization of the polymer [137]. It has been observed that fatty acid modified poly(glycerol adipate) showed crystalline reflexes in the WAXS [77]. In contrast, indomethacin modified PGA is totally amorphous, independent from the degree of grafting. These results coincide with those of the DSC

measurements (Section4.1.3), where no melting peak could be recorded and only a glass transition was observed.
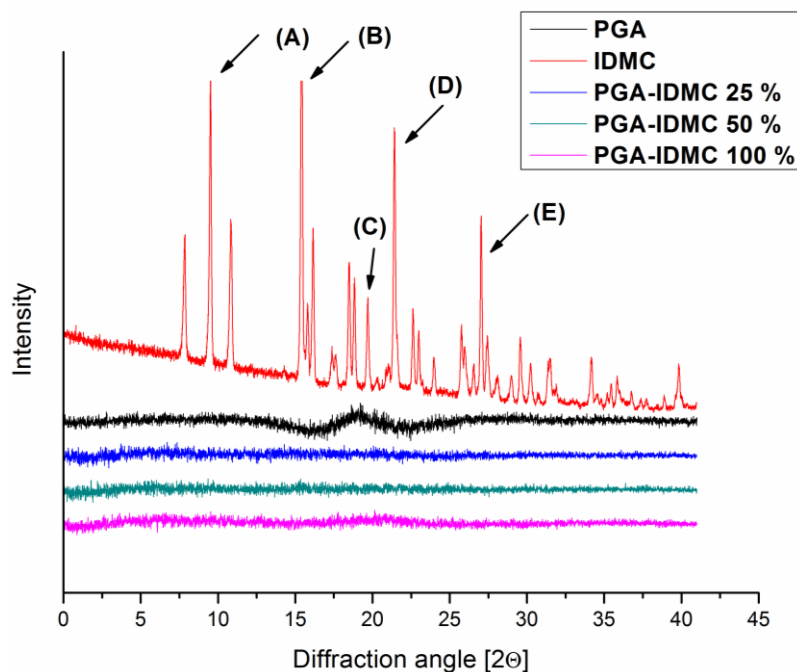
Figure 25. *X-ray diffraction of powdered samples of indomethacin, poly(glycerol adipate) and indomethacin grafted PGA, directly after preparation. The measurements were carried out at room temperature. Characteristic peaks of γ indomethacin are marked with (A)-(E).*

4.1.5 MACROVISCOSITY

Rheology is a study of flow and deformation of matter. The most important parameter for describing is viscosity, which is termed as the resistance to flow, and defined as relationship between stress and the deformation rate. Polymers show almost non-Newtonian behavior with shear thinning due to entangled macromolecules which begin to disentangle and orientate along the flow direction. Due to their structure they are more often viscoelastic in nature so the properties lie between the ones of elastic solids and viscous fluids [138]. Rheology is an excellent tool to characterize non-Newtonian material in order to control the parameter for further processing (e.g. extrusion) or forecasting the behavior at certain conditions, for example *in vivo*.

Judging only from the first impression, the four previously investigated polymers show differences in their shape and viscosity. It appears that with an increasing modification degree the viscous PGA becomes increasingly solid in texture.

Therefore, the macroviscosity was determined by exposing PGA and its three different conjugates to well-defined mechanical strain as described above.

The key attention has to be turned to the behavior of these polymers *in vivo*, therefore the measurements were carried out at 37 °C ensuring that the T_g of low and medium modified PGA is still achieved (Section 4.1.3). The differentiation between ideal-elastic and ideal-viscous systems is given as follows: In the case of ideal-plastic systems the loss angle δ (relationship between deformation and shear stress) is 0° because of the proportional connection of the displacement of the cone displacement and the counteracting force of the system. In contrast ideal-viscous systems show a loss angle δ of 90°. In practice, the properties are mostly between these two states, this is seen as a time-dependent relationship between the stress and the strain while deforming polymers. Storage modulus G' (elastic modulus) represents the part of energy stored in the polymer upon stress, loss modulus G'' (viscous modulus) in contrast expresses energy which is lost through dissipation [138]. The relationship between G' and G'' indicates whether the polymer behavior is more elastic or viscous at distinct conditions. To study only intact polymer structures, the first step was therefore to figure out from which deformation the polymer flows or the structure is destroyed. All samples were placed on a stationary plate and were deformed by oscillating cone geometry (Figure 11). Figure 26A shows the determined loss angle as a function of the deformation (shear rate 1 s^{-1}).

Grafted and non-grafted PGA showed an almost constant loss angle over the whole deformation range. PGA (δ=90°) shows ideal-viscous behavior. In contrast, the polymers become more elastic with increasing modification degree. For example, PGA-indomethacin 100 % (δ=78°) possesses 86 % viscous and 14 % elastic proportions. Therefore, no synthesized PGA-indomethacin conjugate shows ideal-elastic or ideal-viscous behavior. As expected, these polymers are viscoelastic, as are most macromolecules. Viscosity is the most important rheological parameter for describing flow. The complex viscosity describes the resistance to flow and is the relationship between defined stress and deformation rate. Results of complex viscosity η* studies (Figure 26B) confirm the loss angle results, namely that all investigated polymers have a wide viscoelastic range (LVR). Interestingly, the complex viscosity η* increases with growing molecular weight, for example η* of high modified PGA is 250-fold higher than η* of non-grafted PGA. To make a polymer flow the chains must have enough free space. This space is decreasing with increasing grafting due to the space claiming Indomethacin with its aromatic structures and large pendant groups [139]. Particularly noticeable is the

shear sensitive behaviour of PGA-IDMC 50 % from a deformation of 0.1 % and more (Figure 26B).
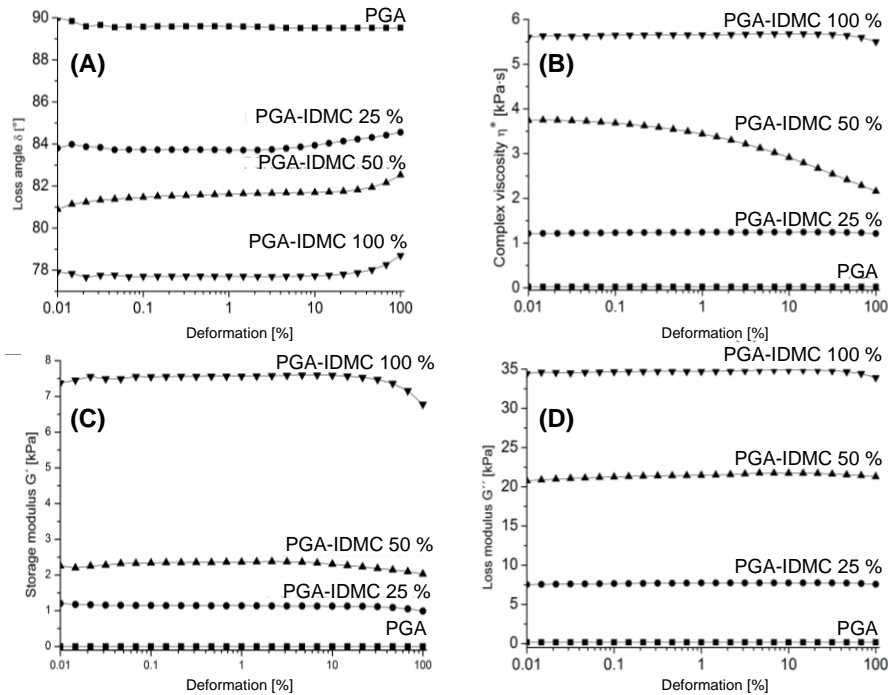
Figure 26. *Deformation dependence of loss angle δ (A), complex viscosity η* (B), storage modulus G'' (C) and loss modulus G'' (D) for PGA and different grafts. The measurements were carried out at 37 °C and a default shear rate of 1 s^{-1}.*

Figure 27 summarizes the results of the frequency sweep tests. The results of the deformation sweep tests showed that is irrelevant at which deformation the frequency tests are carried out (linear viscoelastic range). A constant deformation of 1 % was set and the shear rate was gradually increased. As expected, PGA behaved differently compared to the grafted polymers during the frequency sweep test.

PGA behaved almost like a Newtonian fluid, viscosity is therefore a material constant and independent from deformation and shear rate.

The loss angle δ of PGA remained consistent over the whole range but marginally lower in comparison to the deformation sweep tests. As a result, PGA behaved viscous-elastically under shear stress. PGA-IDMC 25 %, 50 % and 100 % showed shear thinning behavior, the macromolecule chains which are possibly entangled began to orientate along the flow direction with increasing shear rate. Hence, shear viscosity of polymers is strongly dependent on the shear rate.

A typical shear viscosity curve consists of four phases: 1st Newtonian plateau (no shear viscosity), transition area, shear thinning and transition to the 2nd Newtonian plateau (high shear rates) [139]. These theoretical phases are hard to determine, because very high shear rates are necessary to disentangle all polymer chains [140,141].

Figure 27B shows the shear thinning of the three different polymers. At low shear rates a small range of Newtonian plateau (zero shear viscosity) is directly turning into a transition area indicating the beginning of shear thinning. A considerable increase of the storage modulus G'' is noticed compared to the loss modulus G'' (Figure 27C). The polymers shift therefore from viscous-dominated to elastic-dominated behavior. Both curves are approximating each other over the frequency sweep. This is a typical behavior of polymers which often leads to a so called cross-over point [139], which is dependent on molecular weight, architecture and molecular weight distribution. In conclusion, due to the different polymer structures the rheological properties are very different and grafted-PGA is not comparable to non-grafted. The displayed results give a first impression of the macroviscosity but also create space for further investigations for example temperature, time-temperature, wider shear rate range dependence or study of microviscosity which is described in the EPR section at a later stage.
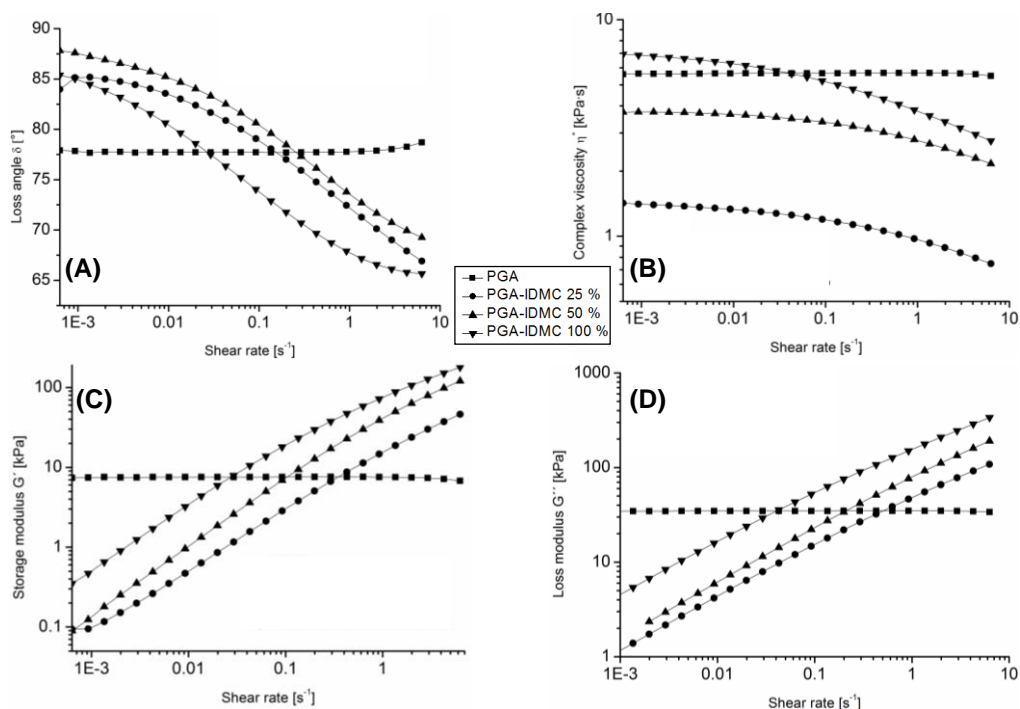
Figure 27. *Shear rate dependence of loss angle δ (A), complex viscosity η* (B), storage modulus G' (C) and loss modulus G'' (D) for PGA and different grafts. The measurements were carried out at 37 °C and a default deformation of 1 %.*

4.1.6 STATIC CONTACT ANGLE

The hydrophilicity is an important parameter for the polymer's interaction with the environment. Contact angle θ measurements were carried out in order to investigate the wettability properties of the new polymers. These should help to predict the hydrophilicity and the behavior in water during *in vitro* release studies or in the human body. It is very important to strictly adhere to the measurement times because of the time dependency of the static contact angle θ. The measurements were carried out directly after spotting the water drop on the polymer film and the contact angle of the same probe was measured 2 mins later to show to different time points otherwise the static contact angle measurements are just a snap-shot. The short time interval was chosen because of the rapid change of the contact angle especially during the measurements of the PGA films because of its hydrophilicity and ability to swell although it is not water-soluble [142]. These resulting θ values are summarized in Table 11.

Table 11. *Mean static contact angle values (± SD) of water (8 µl) against poly(glycerol adipate) and PGA-IDMC conjugates with different degree of grafting as bulk. All polymers were used as small films. Measurements were carried out at room temperature directly and after 2 mins of droplet placement (n=3).*

Polymer	Θ [°]; t = 0 min	Θ [°]; t = 2 min
PGA	55 ± 0.5	10 ± 2.0
PGA-IDMC 25 %	62 ± 0.9	55 ± 1.1
PGA-IDMC 50 %	79 ± 0.6	73 ± 0.8
PGA-IDMC 100 %	90 ± 1.0	87 ± 0.4

PGA is an amorphous polymer which is not water soluble but it swells to a considerable extent [142]. The θ value for the PGA polymer backbone of the current study is comparable to the value published by Taresco *et al.* [70]. It was expected that polymers with higher indomethacin substitution degrees are more hydrophobic due to the decreased number of free –OH groups and the introduction of hydrophobic groups. Indeed, the contact angles increased from 55° to 90° (time point 0 min) and from 10° to 87° (time point 2 mins) from the unmodified PGA backbone to PGA-indomethacin 100 % (Table 11). These results agree with the observed swelling behavior in water. Low modified PGA swelled to about 20 %, but polymers with higher modification degrees did displayed hardly any swelling. The time dependent change of the contact angle θ was

quite different. Due to its high hydrophilicity, PGA was almost entirely wetted after 2 min. For the polymer conjugates with indomethacin, the contact angle θ did changed more slowly and, depending on the degree of grafting, to a much smaller extent.

4.1.7 PREFORMED IMPLANTS

The preformed implants were prepared using the heating press showed in Figure 12. 50 mg of each polymer were pressed. The preformed implants are shown in Figure 30 below. The diameter of the implants is determined by the used press (5.5 mm for all used polymers). However, there are differences in the resulting height. For the same mass, the height of the PGA-IDMC 25 % implants is 3.3 mm, the heights for medium and highly modified PGA-IDMC are similar and 4.6 and 4.4 mm respectively. The visual appearance is also different and clearly visible in Figure 30. The implants out of PGA-IDMC 50 and 100 % are light yellow and solid, whereas the PGA-IDMC 25 % molding is much softer and somewhat less transparent, these observations are in line with the rheological measurements (Section 4.1.5) and may be caused by the exceeded glass transition temperature of PGA-IDMC 25 % at room temperature.

PGA-IDMC 100 %   PGA-IDMC 50 %   PGA-IDMC 25 %
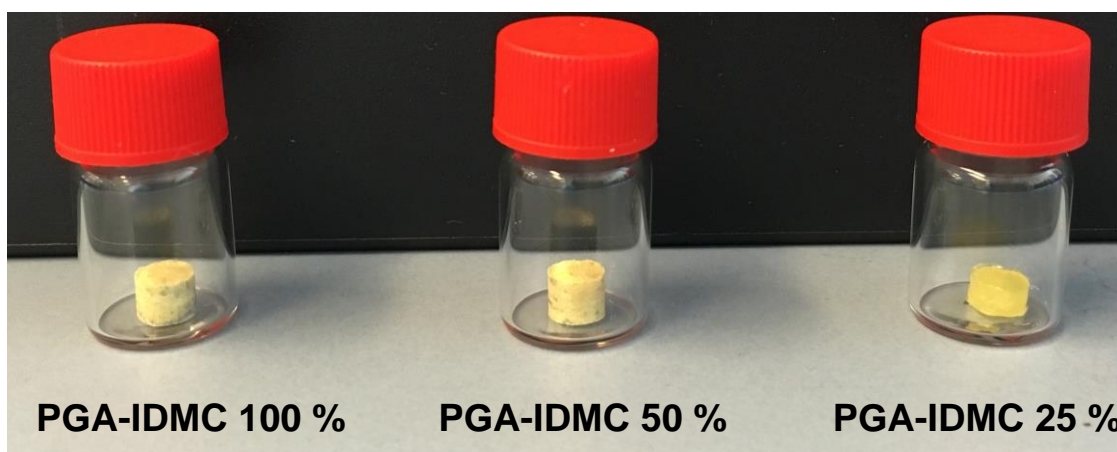
Figure 28. *Optical appearance of preformed implants out of different poly(glycerol adipate)-indomethacin conjugates, directly after preparation.*

4.1.7.1 *IN VITRO* RELEASE

The determination of the *in vitro* drug release is important to assess the therapeutic benefit of the synthesized prodrug and to plan and prepare further *in vivo* experiments. The dialysis tube method was therefore chosen. The implants were placed in the dialysis tubes described above (Section 3.4.3, p. 37), in order to separate released indomethacin from the remaining implant. Another advantage of this method is that the bags float in the

release medium and the implants can be wetted evenly from all sides. However, this release system also has disadvantages that have been critically discussed in the past. It was debated whether the release from the DDS is determining the release speed or the release from the dialysis bag [143,144]. Another important component that can impact the release rate is the volume of the release medium. Perfect sink conditions would be desirable, which would mean an infinite volume of release medium. *In vitro*, these conditions cannot be achieved. So one chooses the volume that the released concentration of the drug is less than 10 % of the saturation concentration or the full dose of drug should be dissolvable in 20-30 % of the media volume [145]. Due to the covalent bonding between indomethacin and poly(glycerol adipate) there was no initial burst release, in contrast to the described data by Thompson *et al.* for ibuprofen conjugated to poly(glycerol-adipate-co-ω-pentadecalactone) [146]. This allows the conclusion that indomethacin is quantitatively bound. Furthermore, the degree of drug loading could be considerably increased by using the PGA backbone. The release in pH 7.4 phosphate buffer is generally very slow (Figure 30B). However, slight differences between the individual polymers become apparent. The low modified polymer showed the highest rate of release, the highly modified polymer shows the lowest rate, due to the decreasing hydrophilicity (Section 4.1.6) which is associated with poor wettability. The space keeping indomethacin molecules hinders the attack of water. Another reason for the slow release rate is the ester bond used for coupling of indomethacin. Ester bonds are hydrolysable ($t_{0.5}$ = 3.3 yrs) but in contrast to other bonds such as poly(ortho esters) ($t_{0.5}$ = 4 h) or poly(anhydrides) ($t_{0.5}$ = 0.1 h) they are relatively stable in aqueous media at neutral pH [147]. For PGA-IDMC 25 %, only about 0.7 % (w/w) of indomethacin could be released within 28 days. Similarly low release rates have already been reported by Qian *et al* for poly[*N, N*-bis(2-hydroxyethyl) naproxenamide-*co*-sebacate] (PNSC) [148]. As a control experiment, the release of indomethacin from PGA/IDMC physical mixtures (PM) was investigated, which contained the same amount of active ingredient as the prepared conjugates. A similar release pattern was observed for all samples in the case of the physical mixtures of the PGA backbone with different indomethacin loads (Figure 30A, p. 61). After a small burst of a few percent (<10 %), an almost linear release profile was observed. The release was completed within 20 days. The PGA cylinders did not disintegrate during the release, hence, diffusion and not erosion is a key factor for indomethacin release from the physical mixtures. Ester hydrolysis can be catalyzed either acidic or by base [149]. Because inflammatory microenvironments [150] are often slightly acidic, release experiments were conducted at pH 4.75. Due to the reduced pH

value, the ester cleavage is increased, so after 28 days up to 16 % could be released (Figure 30C). Because enzymes might also contribute to the drug release *in vivo*, indomethacin release from the polymer conjugates in the presence of lipase *in vitro* was studied. Lipase from *Pseudomonas* spez. was chosen with reference to the results published by Marten *et al.* [151]. They described well hydrolytic activity of the enzymes for aliphatic polyesters at pH 7.0 at 37 °C, therefore it was important to keep the pH always in an appropriate range. The slight pH difference in contrast to the phosphate buffered trials was acceptable. The presence of lipase caused a clear acceleration of the release rate (Figure 30D). Around 25 % (substitution degrees 25 and 50 %) or around 45 % (PGA-indomethacin 100 %) of the drug were released within one month. It can therefore be concluded, that indomethacin release from the PGA-drug conjugates is very slow at neutral conditions. Lower pH-values and enzymes accelerate the release rate clearly. Overall, the release rates are promising for *in vivo* applications. The active ingredient was stable over the entire observation period (Figure 29).
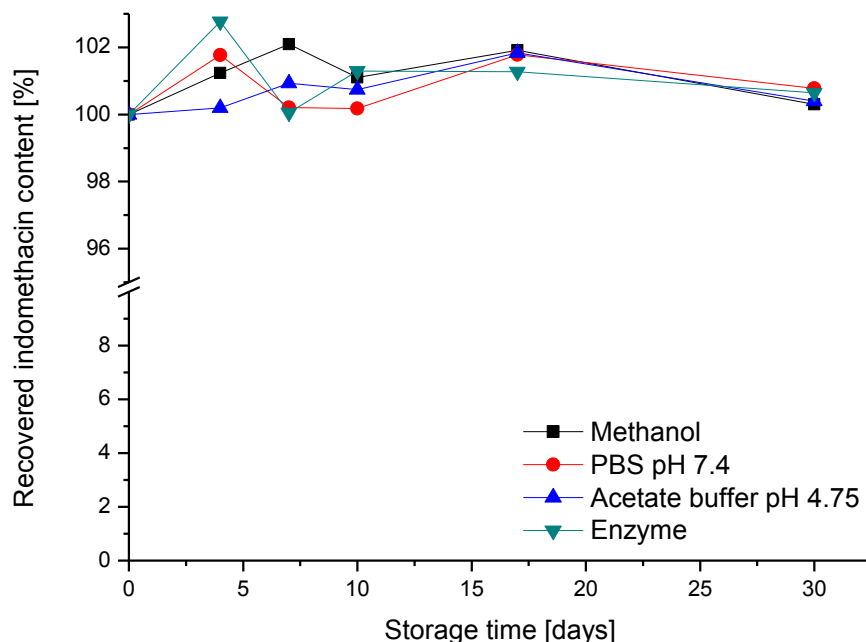
Figure 29. *Stability of indomethacin in different media monitored over 30 days at room temperature under light protection.*
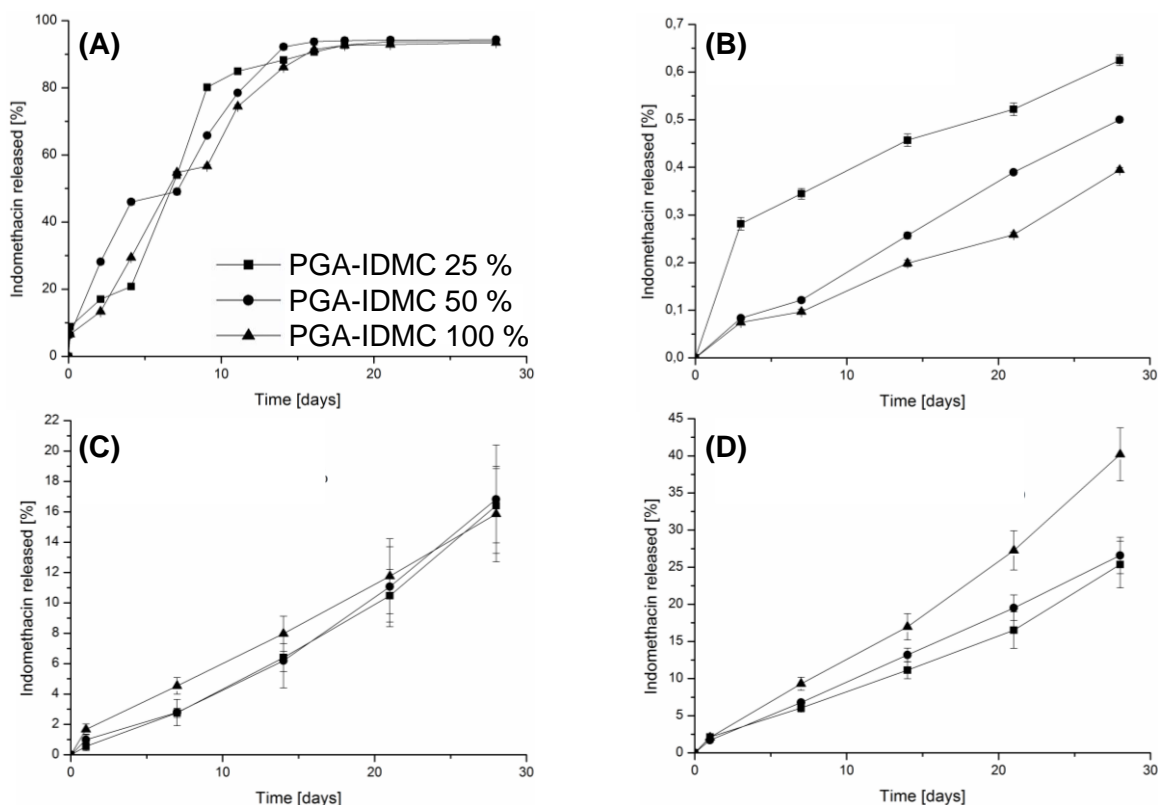
Figure 30. *Cumulative release % (w/w) of indomethacin from PGA-indomethacin physical mixtures in pH 7.4 phosphate buffer (A), PGA-indomethacin conjugates with different modification degrees in pH 7.4 phosphate buffer (B), pH 4.75 acetate buffer (C) and pH 7.0 sodium chloride solution containing lipase from Pseudomonas sp. (D). The release was carried out at 37 °C, over 28 days. Note the difference scaling of the y-axis.*

4.1.7.2 ELECTRON PARAMAGNETIC RESONANCE

To get a deeper insight into the release mechanisms EPR measurements were performed (Section 3.2.10). Therefore, the hydrophilic spin probe 4-Hydroxy-TEMPO-d17 (Figure 31) was incorporated into the preformed implants.
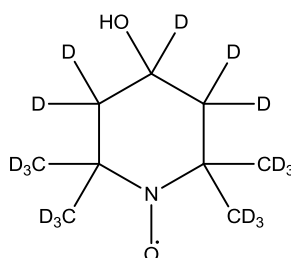
Figure 31. *Chemical structure of 4-Hydroxy-TEMPO-d17.*

The number of lines in the EPR spectrum depends on the number and type of nuclei interacting with the unpaired electron. A typical EPR spectrum is shown in Figure 32 with

the relevant parameter for the subsequent evaluation of the spectra. The spectra are usually recorded as first derivative.
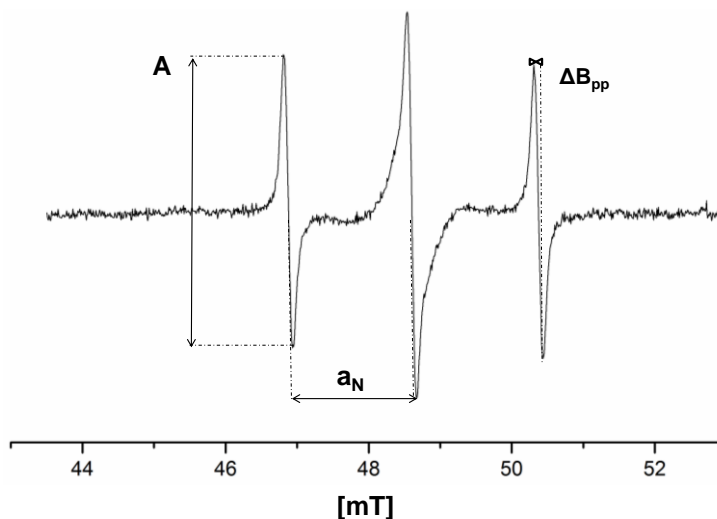
Figure 32. *In vitro L-Band EPR spectrum of 4-Hydroxy-TEMPO-d17 in double distilled water at room temperature illustrating the typical EPR parameter A (signal amplitude), a_N (hyperfine splitting constant) and ΔB_{pp} (peak to peak line width).*

The hyperfine splitting (a_N) provides information about the local environment of the spin probe and increases with increasing polarity [152]. Further information about the local environment of the incorporated spin probe give the amplitudes of mobile and immobile peak, it becomes larger with increasing mobilty of the spinprobe. Moreover, the peak to peak line width (ΔB_{pp}) becomes smaller with increasing mobility.

In following the L-Band EPR spectra of PGA-IDMC 25, 50 and 100 % preformed implants (containing 4-Hydroxy-TEMPO-d17) exposed to three different release media over 240 h are shown. At time 0 h, directly after incorporation, the spin probe is immobile and caused strong line broadening due to the restricted motion in a highly viscous environment [153] showing one large amplitude (Figure 33 - Figure 35, 0 h, triangle symbol). In the further measurements an external standard (N15PCM, Figure 33 - Figure 35, star symbol) was used for potential semi-quantitative calculations. For PGA-IDMC 25 % preformed implants, a slight and wide mobile peak of 4-Hydroxy-TEMPO-d17 appeared due to the ingress of buffer after 6 h (Figure 33A). In the further course of the measurements it is obvious, that the mobile peak appears not sharp over the whole period. The mobile peak remains asymmetrically and wider than the peak of the internal standard, therfore it is likely that a large amount of incorprated spin probe

remained immobile after 240 h. The signals are generally weak. For PGA-IDMC 50 % preformed implants the starting point is similar. The ingress of buffer caused an increase of mobility of the incorporated spin probe already after 6h (Figure 33B). In contrast to the above mentioned observations, all peaks appear very sharp (Figure 37) and all amplitudes are nearly equal already after 6 h up to 240 h. Also for PGA-IDMC 100 % the incorporated spin probe became mobile already after 6 h (Figure 33C). Over the entire measurements the shape of the peaks at the different times remained similar and the amplitudes of the incorparated spin probes are larger than those of the internal standard at any time. Even after 240 hours, a large proportion of spin probe remained immobile. In addition, the release medium was studied using an X-Band spectrometer and no spinprobe signal could be detected.
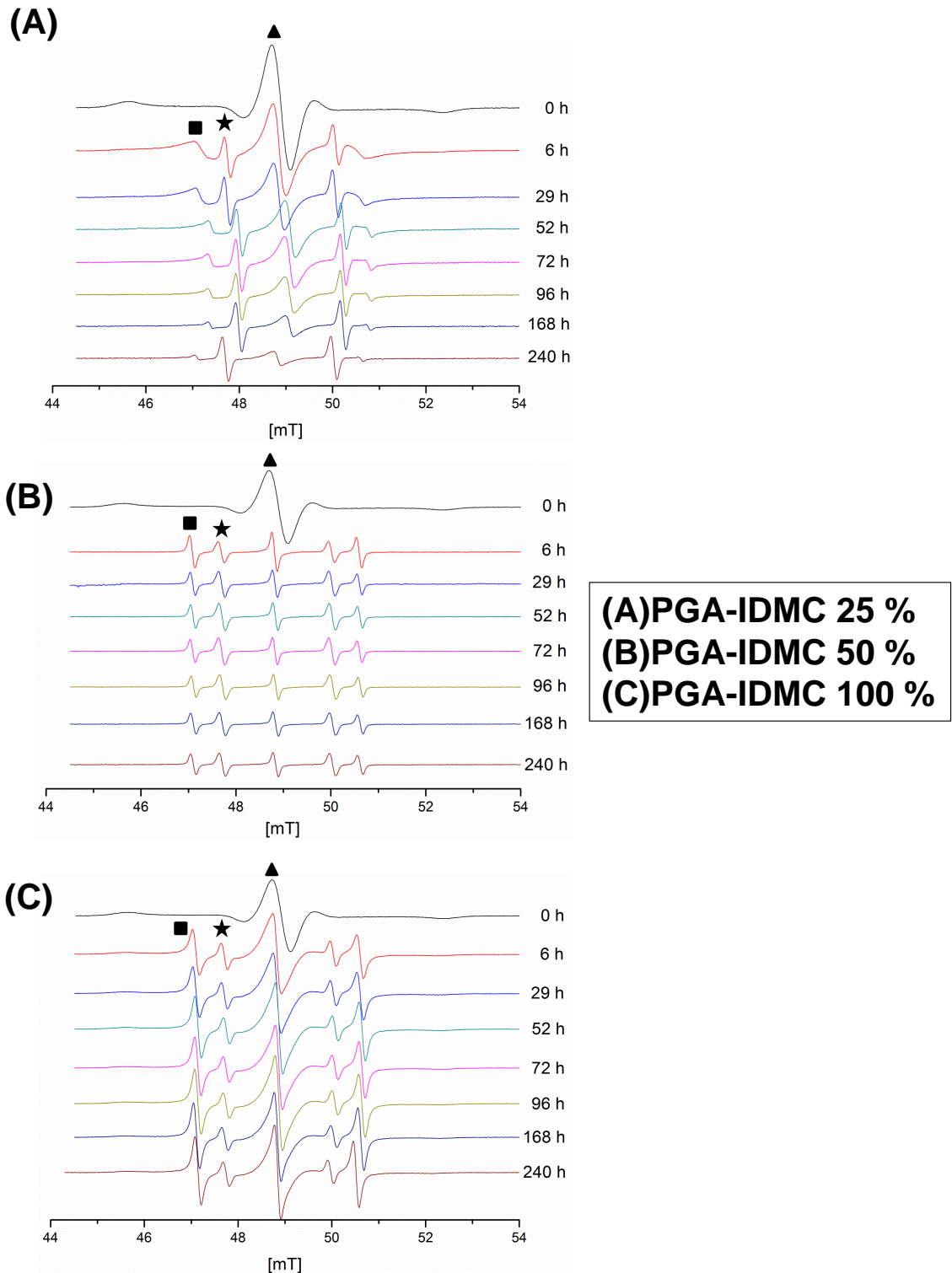
Figure 33. *EPR spectra (L-band) of 4-Hydroxy-TEMPO-d17 loaded preformed implants of PGA-IDMC grafts with different degrees of modification exposed to PBS pH 7.4 over 240 h. The measurements were carried out using 3-carbamoyl-proxyl-1-^{15}N (N15PCM) as external standard at room temperature. The star marks the peak of N15PCM, square mobile and triangle immobile lines of 4-Hydroxy-TEMPO-d17.*
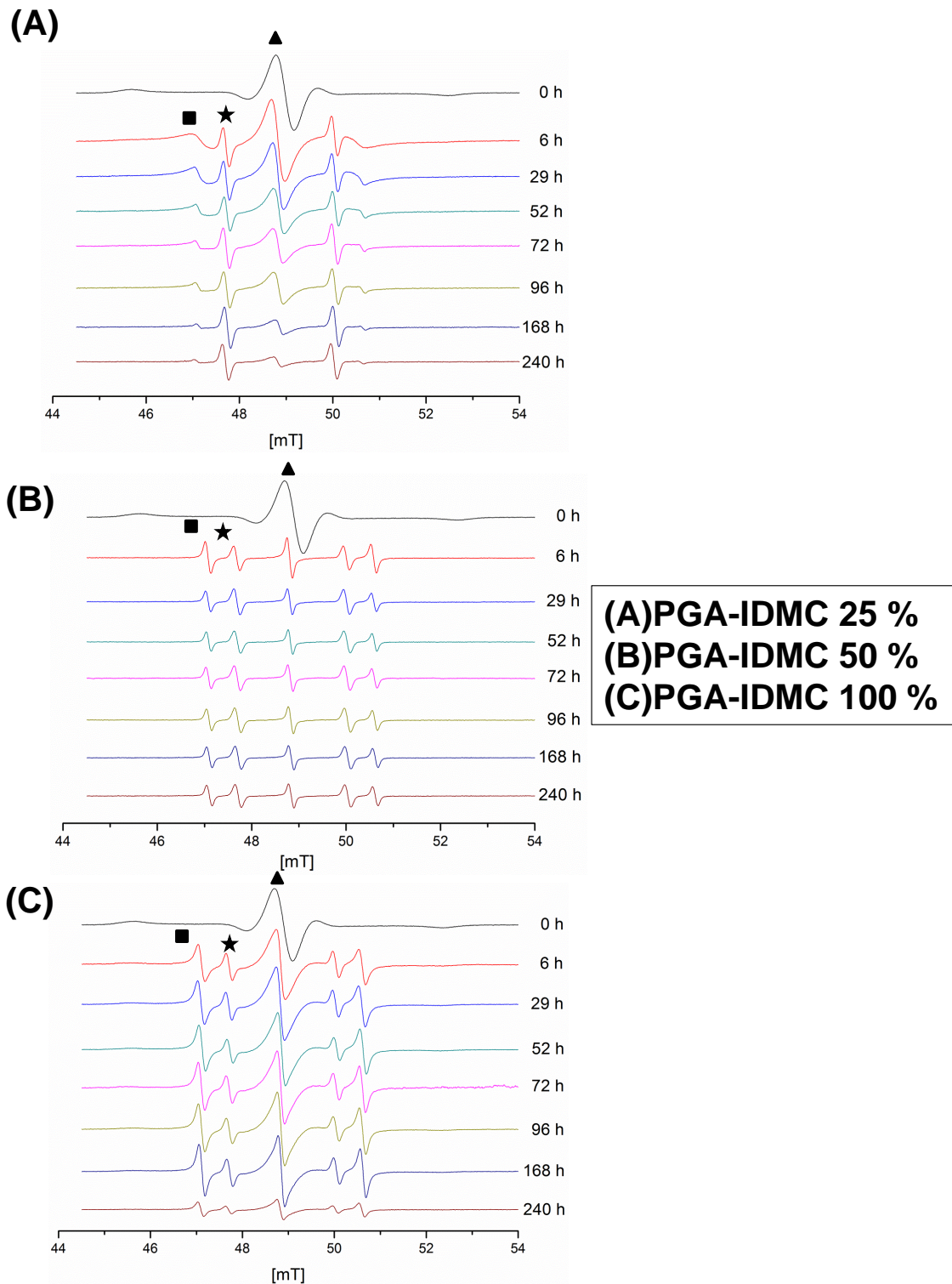
Figure 34. *EPR spectra (L-band) of 4-Hydroxy-TEMPO-d17 loaded preformed implants of PGA-IDMC grafts with different degrees of modification exposed to lipase from Pseudomonas spez. over 240 h. The measurements were carried out using 3-carbamoyl-proxyl-1-^{15}N (N15PCM) as external standard at room temperature. The star marks the peak of N15PCM, square mobile and triangle immobile lines of 4-Hydroxy-TEMPO-d17.*
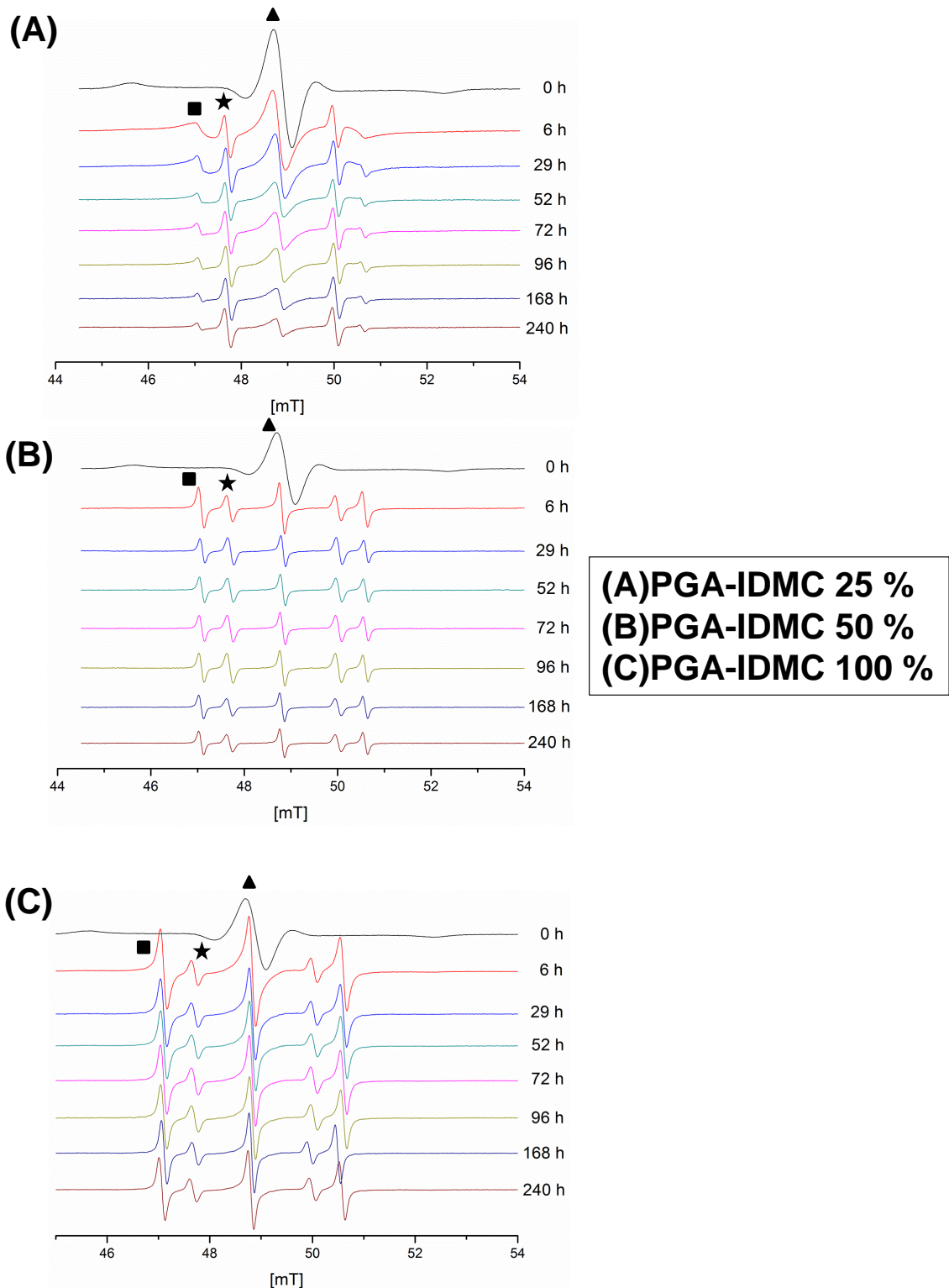
Figure 35. *EPR spectra (L-band) of 4-Hydroxy-TEMPO-d17 loaded preformed implants of PGA-IDMC grafts with different degrees of modification exposed acetate buffer pH 4.75 over 240 h. The measurements were carried out using 3-carbamoyl-proxyl-1-[15]N (N15PCM) as external standard at room temperature. The star marks the peak of N15PCM, square mobile and triangle immobile lines of 4-Hydroxy-TEMPO-d17.*
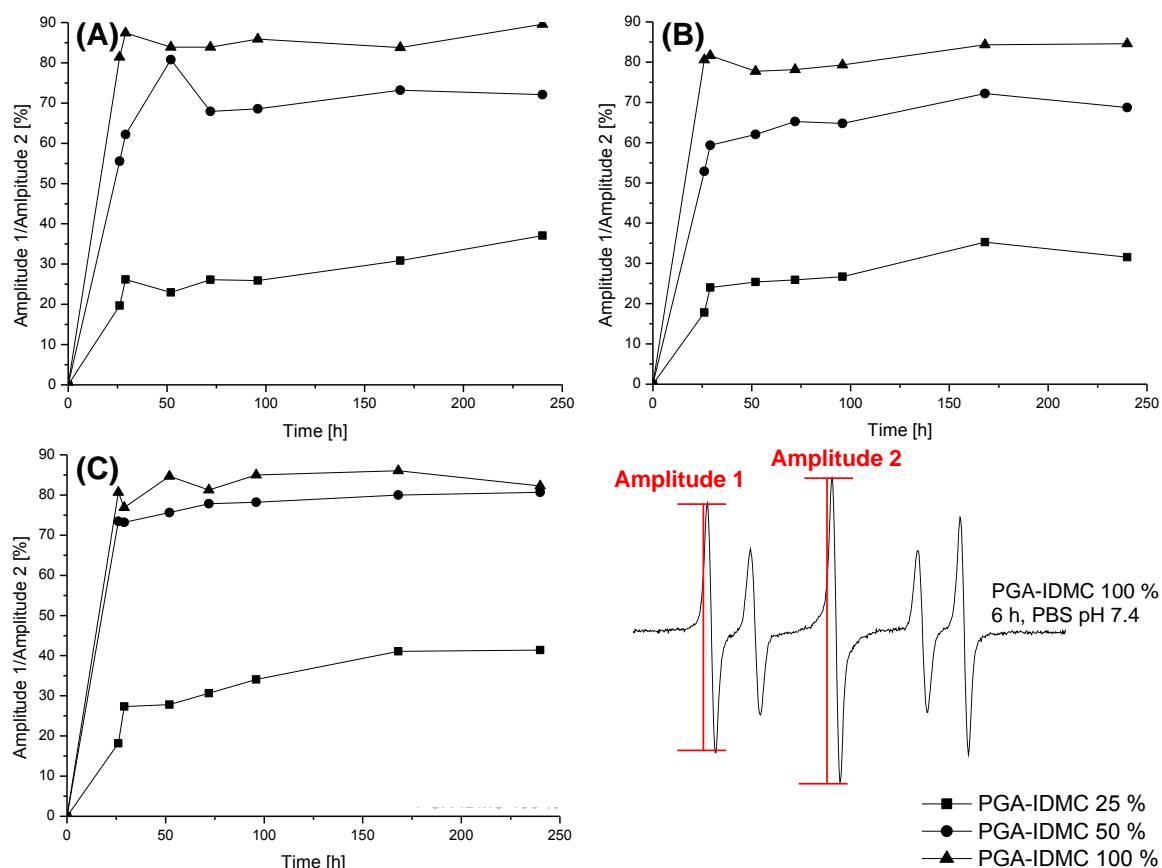
Figure 36. *Time dependent amplitude ratios of PGA-IDMC 25, 50 and 100 % preformed implants containing 4-Hydroxy-TEMPO-d17 exposed to PBS pH 7.4 (A), lipase from Pseudomonas spez.(B) and acetate buffer pH 4.75 (C) over 240 h. The ratios are based on the L-Band EPR spectra presented in Figure 33 - Figure 35 (star peak and triangle peak). Amplitude 1 and 2 were chosen as shown.*

Another important parameter to investigate the behaviour of incorporated spin probe is the evaluation of the amplitude ratios (Figure 36) based on the above shown EPR spectra (Figure 33 - Figure 35). The amplitude ratio is large, when the spin probe is mobile and largest for high modified PGA. 4-Hydroxy-TEMPO-d17 incorporated in PGA-IDMC 25 % became slowly mobile what is shown by a small amplitude ratio after 240 h and hardly detectable mobile peaks in the L-Band spectra (Figure 33 - Figure 35). Moreover, the peak width ΔB_{PP} is small and constant over the whole period of the experiment (Figure 37).
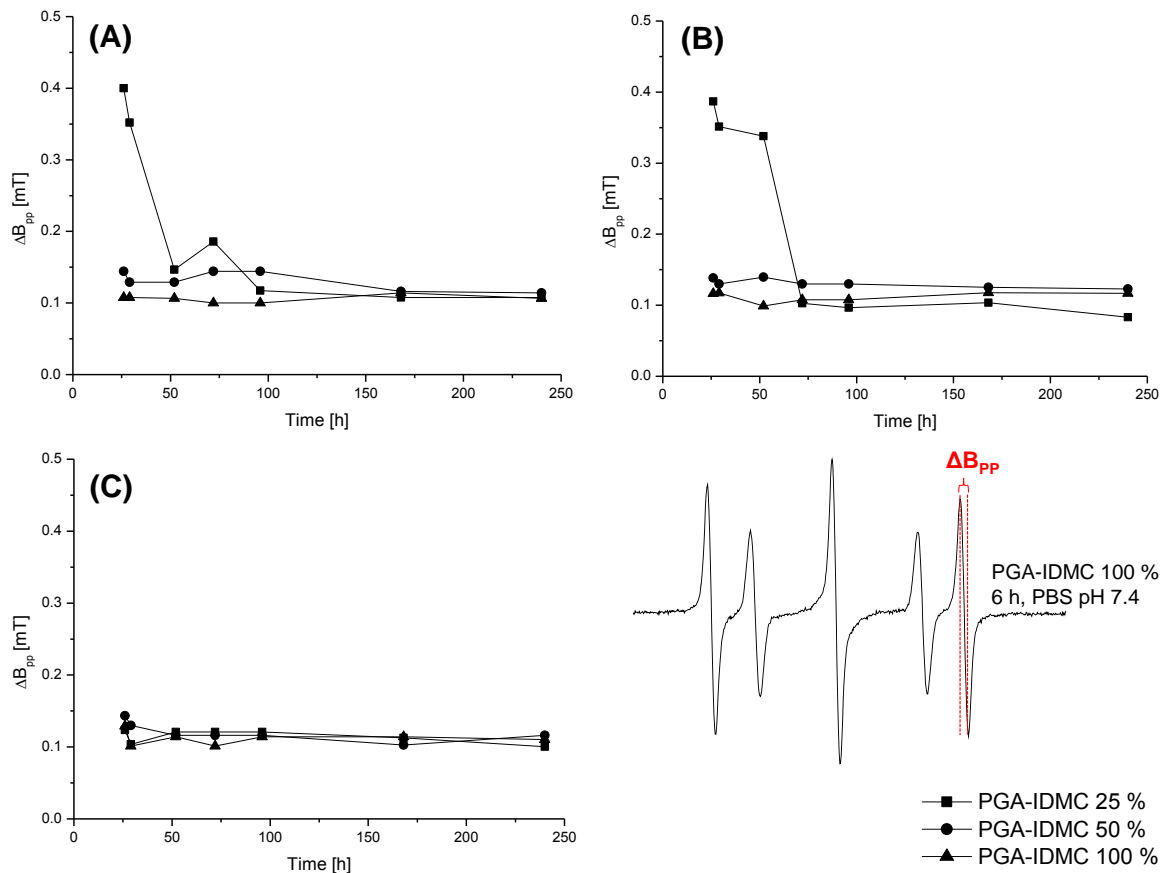
Figure 37. *Time dependent line width ΔB_{PP} of PGA-IDMC 25, 50 and 100 % preformed implants containing mobile 4-Hydroxy-TEMPO-d17 exposed to PBS pH 7.4 (A), lipase from Pseudomonas spez.(B) and acetate buffer pH 4.75 over 240 h. The data are based on the L-Band EPR spectra presented in Figure 33 - Figure 35.The line width ΔB_{PP} was calculated from the shown peak.*

Based on the presented data, the following assumptions can be made. PGA-IDMC 25 % is the most hydrophilic polymer (Section 4.1.6). Possibly the spin probe is dissolved in a mixture of polymer and buffer and therefore the mobility is less, exposed by a low amplitude ratio (Figure 36) and in general weak signals (Figure 33 - Figure 35). PGA-IDMC 50 % has hydrophilic and lipophilic domains causing the the ingress of buffer and thus a fast mobility of incorporated spin probe. PGA-IDMC 100 % is the most lipophilic polymer. Buffer can still penetrate into the preformed implant but is phase separated from the polymer. This results in a clearly mobile spin probe combined with a large proprtion of immobile spin probe.

4.2   NANOPARTICLES

The combination of a small size (e.g. Nano-Drug Delivery Systems (Nano-DDS)) and controlled release is difficult to achieve, even with solid particles. For example, diffusion coefficients of many drugs in poly(lactide-co-glycolide) (PLGA) are around 10^{-12} cm^2/s [154–156] and much higher in polymers with lower glass transition temperatures (e.g. in polycaprolactone 10^{-8} cm^2/s) [157]. According to the Einstein-Smoluchowski equation with the assumption of a diffusion coefficient of $2*10^{-12}$ cm^2/s, drugs diffuse in average in PLGA within 100 s a distance of 200 nm. However, it takes them more than 11 days to travel a distance of 20 μm. Therefore, diffusion controlled release is reasonable for PLGA microparticles, but unlikely for nanoparticles. Controlled release from Nano-DDS can be achieved either by a very strong association of the drug with the carrier or by means of a very low solubility, where the release is dissolution controlled by the low value of the saturation concentration, which triggers the rate of dissolution according to the Noyes-Whitney formula. This principle has been transformed into clinical practice with the liposomal encapsulation of poorly soluble doxorubicin sulfate [158]. The poorly soluble drug salt forms a nanosuspension inside the liposomes with a rigid shell of saturated phospholipids (partially PEGylated). A strong association of the drug with the carrier which withstands the numerous possibilities of alternative interactions within a complex *in vivo* environment is hard to achieve by non-covalent interactions. However, the formation of covalent bonds offers an excellent opportunity. The field of polymer based systems for parenteral controlled release applications is dominated by polylactide (PLA) and poly(lactide-co-glycolide) (PLGA). Both polymers are not optimal candidates for polymer drug conjugates due to the lack of functional groups in the polymeric backbone [159,160]. Covalent linkage of drug molecules is only possible at the end groups of the polymer chains and therefore, the loading capacity is poor. Problems of PLA/PLGA DDS which are derived from the highly acidic monomers lactic and glycolic acid include (i) autocatalytic polymer degradation with difficult to control drug release rates, (ii) formation of highly acidic microenvironments (up to pH 2) inside the DDS which favors drug degradation prior to release. For these reasons, the search is constantly going on to formulate various active ingredients as conjugates with new polymers. Examples include biodegradable polyesters containing ibuprofen and naproxen as pendant groups [161] or salicylic acid-based polymers (SAA) which are hydrolytically degradable into salicylic acid and adipic acid [162].

Alternative linear biodegradable polymers with attractive and tunable properties can be obtained by enzymatic linkage of polyols and dicarboxylic acids. For example, poly(glycerol adipate) (PGA) is a promising and biodegradable platform for new nanoparticulate DDSs [72]. PGA is a linear polyester with free pendant hydroxyl groups which remain after the enzymatic esterification of the primary alcohol groups of glycerol with adipic acid. They give the opportunity for further functionalization. So far, the research for grafted poly(glycerol adipate) derivatives was focused on fatty acid modified PGA [72,76,77,79,142,163]. Very recently also amino acid modified poly(glycerol adipate) derivates have been reported as promising candidates for pharmaceutical applications [164]. Weiss *et al.* presented a wide spectrum from lauric to behenic acid modified graft copolymers in 2012. They reported that the texture of these polymers can be tuned from viscous to solid depending on the chain length of the fatty acid and the degree of grafting. Furthermore, nanoparticles (NPs) have been produced successfully with interesting, partly cube like structures and an internal substructure similar to a cubic phase [76,77]. Also first *in vivo* tests were carried out by Weiss *et al.* 2018. Stearic acid modified PGA nanoparticles were prepared containing a non-covalent, physically dispersed lipophilic fluorescence dye DiR. In a second group the PGAS NPs were coated with N-(2-hydroxypropyl)methacrylamide (HPMA) covalently attached with the fluorescence dye DY676. The nanoparticles were well tolerated by mice after intravenous injection. Interestingly, fluorescence signals were obtained in the bones for non-coated PGAS NP. Besides, PGAS NPs accumulated in the ovaries and the adrenal glands [82,83], confirming similar observations made for PLGA nanoparticles and nanocapsules [82,83]. Due to their biodegradability and biocompatibility PGA DDSs are therefore a valuable contribution to the field of polymer therapeutics for parenteral application. This statement is confirmed by the experiments of Suksiriworapong *et al.* which demonstrated promising results for the first nanoscaled poly(glycerol adipate)-anticancer conjugate with methotrexate [165].

The first PGA based drug conjugate was described in 2009 [146]. In this study, ibuprofen was conjugated to poly(glycerol-adipate-co-ω-pentadecalactone). A burst release between 13-18 % was observed. Recently the synthesis and characterization of the first poly(glycerol adipate)-drug conjugate [166], which increases the drug load in relation to the above mentioned poly(glycerol-adipate-co-ω-pentadecalactone) derivates was described. In this study, indomethacin was covalently bound to the PGA backbone and afterwards a precise characterization was carried out including first release studies from the bulk polymer [166]. Indomethacin is an indolic acid derivative and potent inhibitor of

both cycloxygenase-1 (COX-1) and cyclooxygenase-2 (COX-2). Therefore, indomethacin has many applications. Best known is the antiphlogistic effect [91], which is the reason for the wide use of the drug to treat rheumatoid arthritis [92]. Moreover, it was also reported that indomethacin nanoparticle formulations reduced the corneal toxicity of indomethacin eye drops, which are used after cataract extraction in order to decrease postoperative inflammation [94]. A new polymer based nanoparticle formulation with high loading of indomethacin might be a precious contribution to this important field of application. In addition to that, also antitumor activities [96,167] have been reported. Bernardi *et al.* developed indomethacin nanocapsules using poly(ε-caprolactone) and capric/caprylic triglyceride for the treatment of glioblastoma in 2009. The use of this potential drug is highly limited by its side effects like gastrointestinal lesions after oral application [168]. Therefore, the development of additional advanced parenteral indomethacin delivery systems is highly desirable to develop further options for the above mentioned fields of application. With respect to the most suitable particle sizes for passive accumulation in inflamed tissue and the safety for intravenous injection, particles sizes below 300 nm were envisaged [169–171].

Ideally, drug conjugation enhances bioavailability and plasma half-life. The drug should be protected against enzymatic degradation or unspecific cellular uptake by modified pharmacokinetics (PK) in the whole body at the same time. Moreover, the conjugation should lead to reduced antigenic activity and the possibility to prepare advanced drug delivery systems. In 2012, stearic acid modified PGA was used as NP platform for the incorporation of different anti-inflammatory drugs. The drug loading was very low (1-2 % (w/w)) and a controlled release over two weeks was reached, with a high initial burst of about 20 % [79]. The focus of the current study was the preparation and characterization of nanoparticles of indomethacin PGA conjugates with different degrees of drug substitution. Laser based particle sizing (PCS and NTA), zeta potential and TEM measurements were carried out to characterize the nanoparticles. Biological characterization included cell viability and hemolytic activity. Indomethacin is known for its high hemolytic activity [172]. Due to this, the application is limited to oral, dermal and rectal administrations. It was therefore the aim to develop a non-hemolytic prodrug for intravenous application. Moreover, first release experiments were carried out over 15 days. In vitro release studies of Nano-DDS are not trivial because of the difficulty to separate the released drug from the Nano-DDS. A special setup (using nonporous aluminum oxide membrane with a high porosity) was developed to overcome the

limitations of dialysis based release studies (e.g. the slow drug diffusion through the membrane).

4.2.1   PREPERATION OF NANOPARTICLES

PGA-IDMC based nanoparticles have been prepared by modified interfacial deposition method [103]. Fatty acid modified poly(glycerol adipate) nanoparticles could be prepared without any surfactants, just by using a modified interfacial deposition method [76]. Attempts to apply this method with PGA-IDMC as part of this thesis were not successful. Therefore, Poloxamer 188 and poly(vinyl alcohol) were chosen as emulsifiers. Already small contents were sufficient to prepare nanoparticles. The preparation of nanoparticles was optimized further and made reproducible by the use of a syringe pump as already described in detail (Section 3.3.1).

4.2.2   PHOTON CORRELATION SPECTROSCOPY

PGA-indomethacin nanoparticles were prepared using an interfacial deposition method [103]. Fatty acid modified poly(glycerol adipate) nanospheres could be prepared without any surfactants, just by a modified interfacial deposition method [76]. Furthermore, the influence of the emulsifier concentration on the particle size (Figure 38) was investigated. It was possible to produce nanoparticles with narrow size distributions in the range of 160 to 220 nm, which is in the desired size range (below 300 nm). The described particles were slightly larger than stearic acid modified poly(glycerol adipate) NPs (100 – 130 nm) [78] and comparable to the recently described z-averages for 10 %MTX-PGA NPs in pH 7.4 medium (around 200 nm) [165]. Larger particle sizes were observed for Poloxamer stabilized nanospheres made out of PGA-IDMC 25 mol% and PGA-IDMC 50 mol% (Figure 38). In contrast to highly modified PGA, the lower and medium grade substituted poly(glycerol adipate) polymers swell in water due to their higher hydrophilicity [166]. These lower substituted polymers show higher surface activity [166] and they are expected to be present at a higher degree at the interface, which might decrease the stabilization at the interface. PVA was, in contrast to Poloxamer, able to stabilize also the low and medium substituted polymers. Most likely, it has a higher affinity to the interface and a lower degree of exchange between the interface and the aqueous bulk phase. Recently it has been observed that Poloxamer or Tween stabilized PLGA nanoparticles are digested by lipase, but PVA stabilized PLGA nanoparticles are not [173]. Most PDI values were between 0.1 and 0.2 which indicates narrow size

distributions. These values were comparable to other PGA based nanoparticle formulations [165].
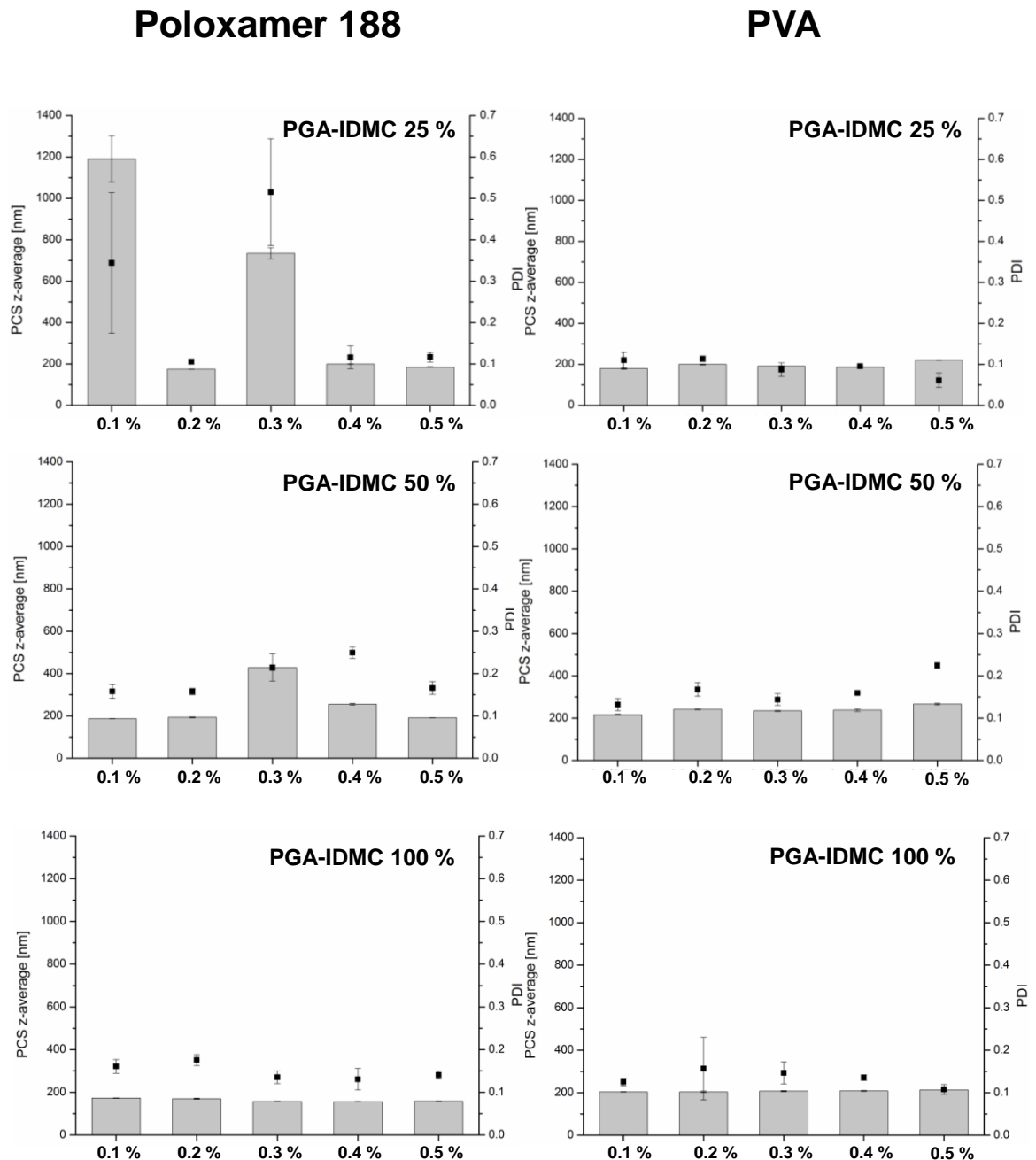
Figure 38. *PCS z-average and PDI of PGA-indomethacin nanoparticles using Poloxamer 188 and poly(vinyl alcohol) as emulsifiers (0.1 – 0.5 %) in double distilled water. Data represent mean values ± standard errors (SE); n=3. z-average▭ ,PDI ■*

In addition to the particle size directly after preparation (Figure 38), the particle stability after lyophilization and subsequent storage over 4 weeks in the fridge (5 °C) was investigated (Figure 39). The aim was the development of a ready to use formulation. Therefore, PGA-IDMC NP with different degrees of modification were prepared as already described (Section 3.3.1) and sucrose 10 % (w/v) was added as cryoprotectant [174,175] and isotonizing additive. Lyophilization is a common method for sensitive materials. Therefore, the samples were rapidly frozen with liquid nitrogen under the eutectic temperature; the cryoprotectant prevents the particles from collapsing. Afterwards the formulations were lyophilized according to the procedure described above (Section 3.7.1). After 4 weeks at 5 °C and light protection, the particles were redispersed in double distilled water and size was measured again using dynamic light scattering. All formulations could be redispersed quantitatively and no cake could be observed. Accordingly, the formulations can be regarded as stable over the monitored time. The formulations can therefore be stored dry and resuspended immediately before the application.
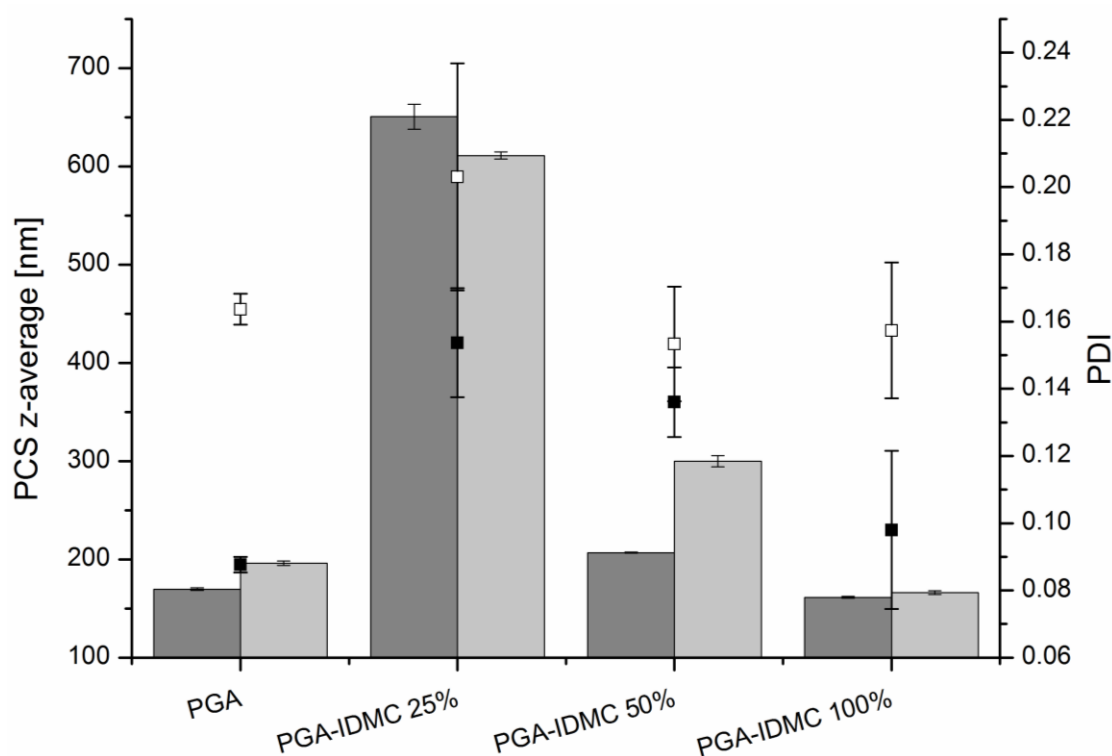
Figure 39. *PCS z-average and PDI of Poloxamer 188 0.3 % (w/v) stabilized PGA-IDMC NP with different degrees of grafting directly after preparation (dark gray bars and black boxes) and after lyophilzation, followed by storage at 5 °C for 4 weeks (light gray bars and white boxes).*

4.2.3 NANO TRACKING ANALYSIS

Nanoparticle tracking analysis calculates the particle size of the diffusion track of each single particle, according to the modified Stokes-Einstein Equation (Section 3.3.2.2). Therefore, it is a complementary method for particle size measurement of the selected formulations. Selected results are shown in Figure 40. The greatest advantages of the NTA are the high peak resolution, low influence of large particles on the results and the individual particle sizing in contrast to the DLS. On the other hand an experienced operator is required and the measurements are less reproducible [106]. Nanoparticle tracking analysis (NTA) was used as a complementary method of particle sizing. NTA calculates the particle size of every single particle using the diffusion track via a modified Stokes-Einstein equation [106,105]. The results are shown in Figure 40.
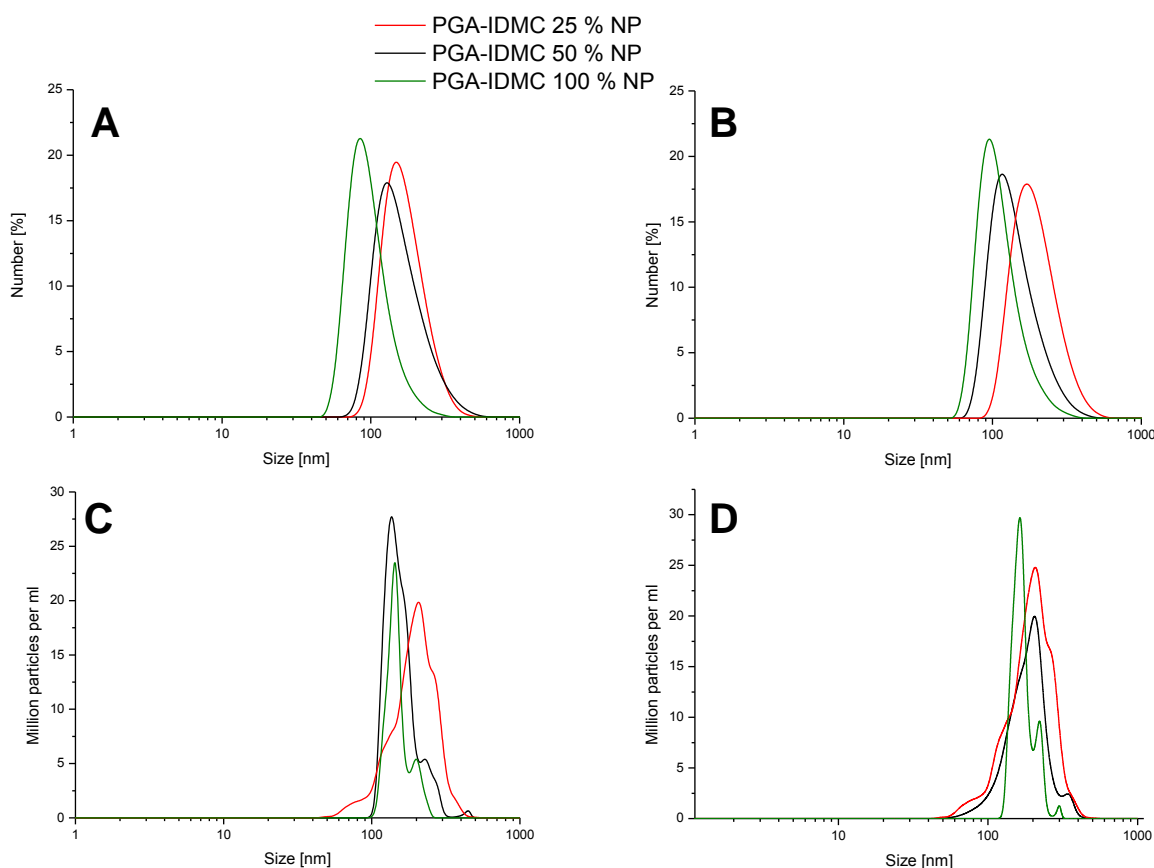
Figure 40. *Particle number weighted size distribution of PGA-IDMC nanoparticles with different degrees of grafting stabilized with 0.4 % PVA (B and D) and Poloxamer 188 (A and C) respectively. Particle size measured with NTA (C and D); Particle size measured using DLS (A and B).*

In the study, the results of NTA and photon correlation spectroscopy are in good agreement which gives confidence to the results of both methods.

4.2.4 ZETAPOTENTIAL MEASUREMENTS

The Zeta potential of Poloxamer 188 stabilized PLA nanospheres changed to positive values after dilution with slightly acidic buffer for incubation (1:10 Sörensen buffer pH 4.9) due to protonated carboxyl end groups [176]. A positive zeta potential was also observed in our samples for the 0.3 % Poloxamer stabilized PGA-IDMC 25 % nanospheres in Sörensen buffer pH 4.9 (Figure 41, left column 4). Incubation of the same nanosphere composition in Sörensen buffer pH 6.8 leads to a negative zeta potential (Figure 41, left column 5). These observations indicate that the environmental pH is very important for these particular samples. Other Poloxamer stabilized samples and all PVA containing samples are less dependent on the pH, because both Sörensen buffers led to similar zeta potential values (Table 1-6 in Supplement). Striking is the very negative zeta potential (between -40 and -50 mV) of PGA-IDMC 50 % nanoparticles stabilized with 0.3 % Poloxamer 188 (Figure 41). These values are comparable to the published data for stearic acid modified PGA nanospheres which could be produced without any surfactant [78]. It is also surprising that this composition, despite the highly negative zeta potential had the highest particle size and lowest stability.

Zeta potential measurements do not measure the charge of the particle surface, but the charge difference between the shear plane and the bulk liquid. The zeta potential depends on the charge distribution on the particle and the thickness of the shear plane. Surfactants might influence both parameters. The highly negative zeta potential might result from the adsorption of Poloxamer molecules which increase the thickness of the shear plane.

PVA has been used widely in biodegradable nanospheres formulations (0.5 to 10 % (w/v)) and is known to have a high shielding effect and almost neutral zeta potentials [177,178]. PVA itself is not biodegradable, it is adsorbed on the surface of the nanospheres and cannot be removed completely from the particle surface by washing [179]. Therefore, very low amount of PVA was used to prepare stable nanosphere dispersions. Already 0.1 % (w/v) PVA (Table 2, 4 and 6, supplementary data) was sufficient and the zeta potential was almost neutral indicating a PVA saturated particle surface. The near neutral zeta potential of all PVA stabilized samples shows the high affinity of PVA to the nanosphere interface.
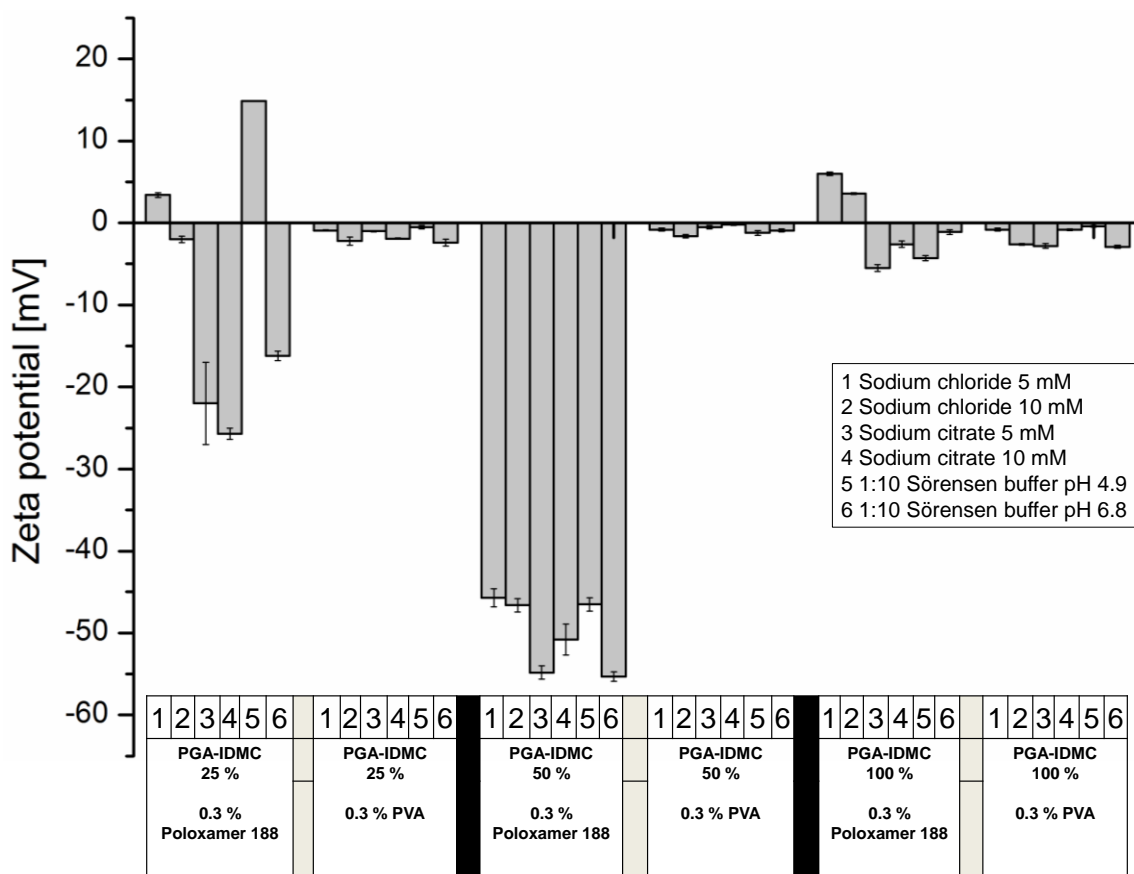
Figure 41. *Zeta potential of PGA-IDMC conjugate NP stabilized with 0.3 % (w/v) Poloxamer 188 or PVA, respectively. The measurements were carried out at 25 °C in different buffer solutions (marked with 1-6). Equilibration time was 180 s in the Zetamaster.*

4.2.5 TRANSMISSION ELECTRON MICROSCOPY

Particle size and shape were investigated through negatively stained samples using transmission electron microscopy. Heavy atoms scatter electrons more than light one, uranyl acetate was therefore used for contrasting. Uranyl acetate gives finer grain than those using others, except uranyl format [180]. Moreover it is stable for more than one year [181].

The information of the particle shape in particular is essential for the interpretation of the particle size data because the described methods assume spherical particles. Furtermore particle shape is very important for the *in vivo* distribution and interactions with cells. The spherical shape of poly(glycerol adipate) based nanoparticles was reported previously [72]. Later on, non-spherical shapes were found for stearic acid modified poly(glycerol adipate) [76]. All prepared nanoparticles appeared spherically

which is the most common structure of particulate systems, due to minimized surface energy (Figure 42). Only for nanoparticles produced of low modified PGA-IDMC (Figure 42A and B) non-spherical particles were found. This could be caused by the soft polymer texture which was described before [166]. Moreover, aged nanoparticles of selected samples were investigated. Therefore, the aqueous nanoparticle dispersions were stored in fridge for one week. These particles (Figure 42C and F, white arrows) showed irregularities on the surface, which could be caused by degradation of the polymer. Furthermore, it is noticeable that the contrast for these particles was weaker. They also appeared brighter. Under ideal conditions, the stain agent should not react with or bind with specimen. For this case, the background of the image appears dark and the particles brighter [182,183]. However, the staining agent will be bound to negatively charged molecules such as indomethacin or free carboxy groups or for example proteins, lipids and nucleic acid phosphate groups which was published before [184]. In this case, the conditions are reversed and the background appears brighter and the image darker and it should be more aptly called "positive staining" [182]. Comparable positive stained images have already been published for PGA-S85 based nanoparticles [77]. During aging, indomethacin is released (Section 4.2.7), which is negatively charged in solution and is able to bound positively charged uranyl. The free indomethacin is located outside of the particle, therefore the particles appear as classic negatively stained image and the surrounding appears darker, where free indomethacin is suspected. In general, nanoparticles from medium and high modified poly(glycerol adipate) showed spherical shape, therefore it can be concluded from this that the prior shown particle data displayed correct results. Furthermore, spherical particles are preferable for the application *in vivo* because of their linear flow within blood vessels [185]. At this point, it should be mentioned that transmission electron micrographs show only two-dimensional projections and the preparation techniques always have a big influence on the particle orientation.
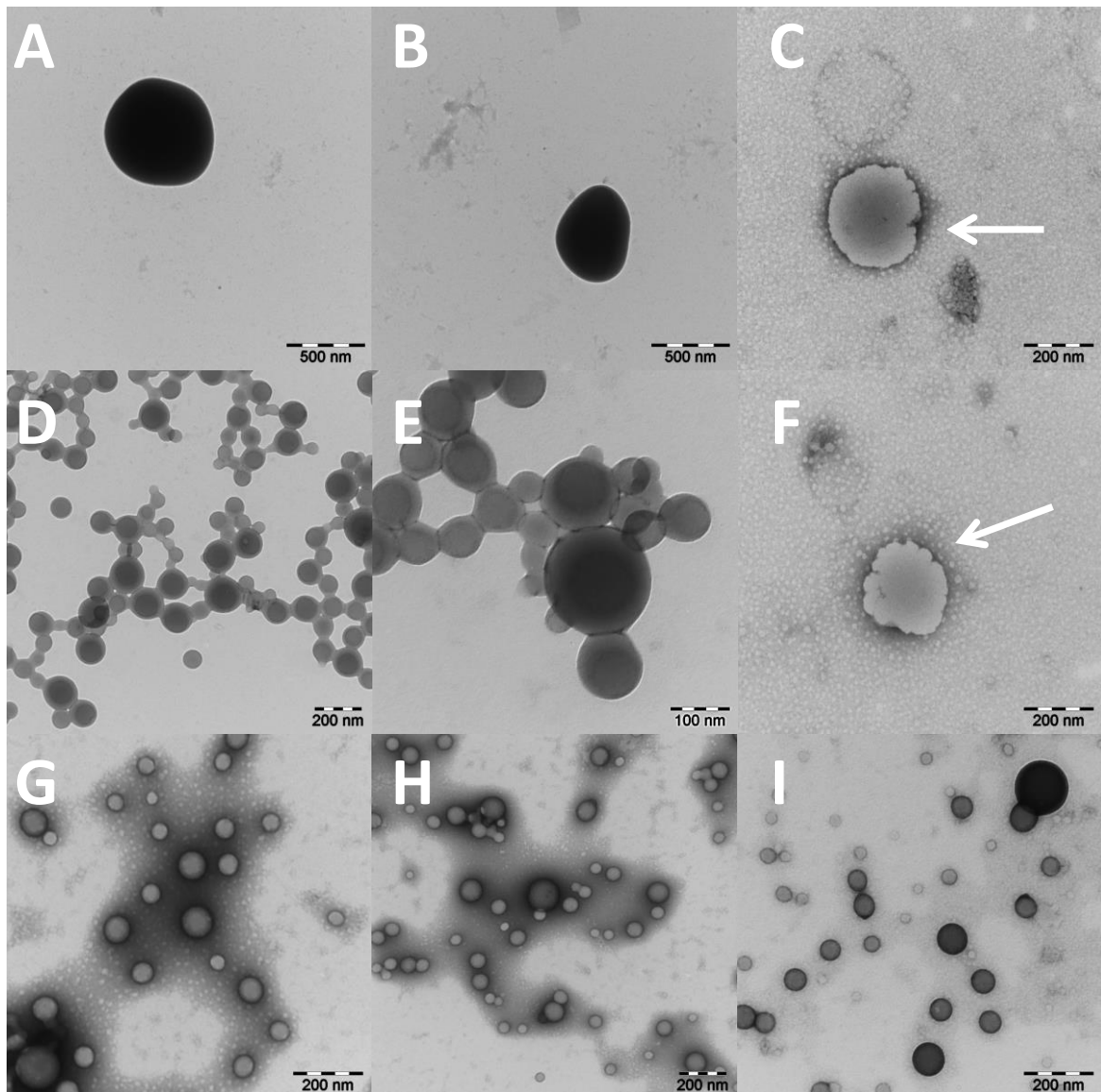
Figure 42. *Transmission electron micrographs of negatively stained (uranyl acetate) PGA-indomethacin nanoparticles. (A) and (B) PGA-IDMC 25 %; (C) and (F) aged (one week) PGA-IDMC 25 %; (D) and (E) PGA-IDMC 50 %, (G-I) PGA-IDMC 100 %. Note the different scale bars.*

4.2.6 HEMOLYTIC ACTIVITY AND CYTOXOCICTY ASSAY

With regard to the further development and future intravenous administrations and for comparison with the non-conjugated drug, the hemolytic activity of the nanosphere formulations and the free drug were determined by incubating freshly separated RBCs with nanoparticle dispersion (1 mg/ml) or 1 mM indomethacin solution (in PBS) for 1 h at 37°C. Assuming total indomethacin release in the NP dispersions, the indomethacin concentrations for the grafted polymers would be as follows: PGA-IDMC 25 % equal to 1 mM IDMC, PGA-IDMC 50 % equal to 1.31 mM IDMC, PGA-IDMC 100 % equal to 1.51 mM IDMC. Hemolytic activity was determined as a proportion of total hemolysis triggered by 2 % (w/v) aqueous SDS solution (positive control). The value of PBS (negative control) was set as zero. The evaluation of the results is based according on ASTM F756-08 standards [186]. Hemolysis is classified as follows, non-hemolytic 0-2 %, slightly hemolytic 2-5 % and hemolytic >5 % of released hemoglobin. Therefore, nanospheres based on PGA-IDMC 50 mol% and 100 mol% are non-hemolytic, NP based on low modified poly(glycerol adipate) are between slightly hemolytic and hemolytic (Figure 43). The nanoparticles made out of the polymer backbone and the solution of free indomethacin, were hemolytic. Furthermore, it is interesting to note that the hemolytic activity decreased with increasing drug loading. This could be caused by the reduced amount of free hydroxyl groups leading to a decreasing amphiphilic character which was reported in a similar way before for fatty acid modified poly(glycerol adipate) derivate [78]. Therefore, especially nanoparticles made out of highly modified poly(glycerol adipate) are promising because they combine high drug loads with low hemolytic activity.
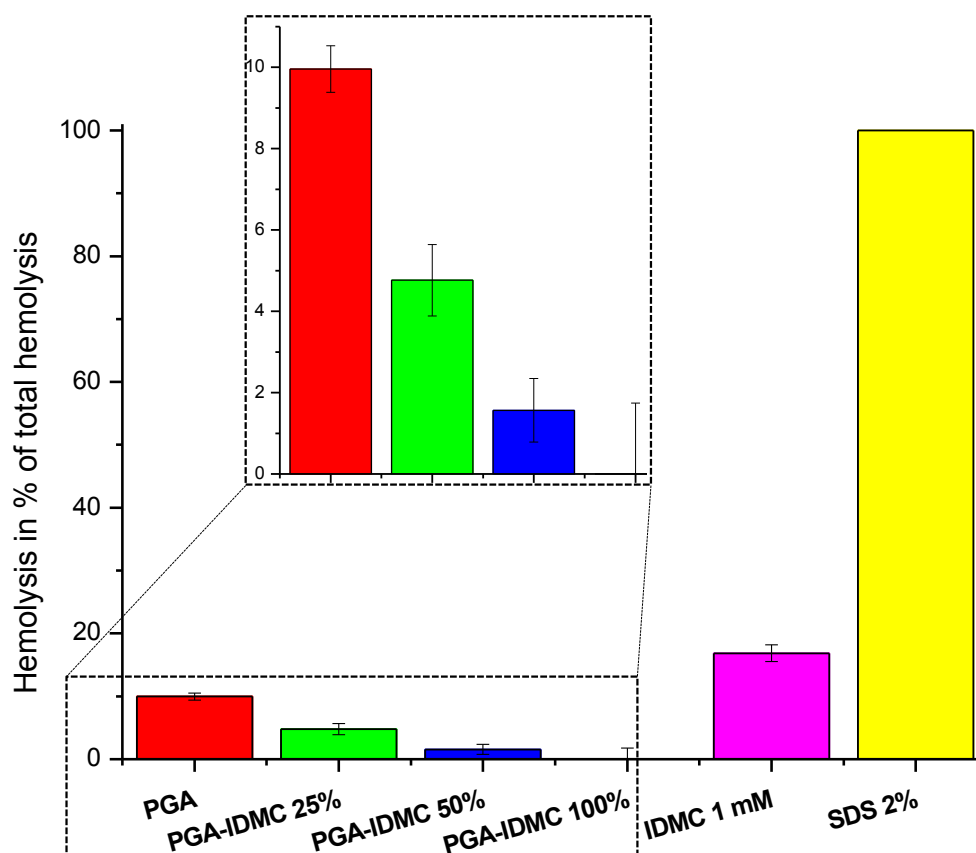
Figure 43. *Hemolytic activity of PGA nanoparticle dispersion (1mg/ml), PGA-IDMC conjugates with different degree of grafting (1 mg/ml) and free indomethacin 1mM (IDMC) as a proportion of total hemolysis (measured after incubation with 2 % SDS solution), data represent means ± standard deviation (SD); n=3. Measurements were carried out at 380 nm.*

To achieve a greater diversity of the cytotoxicity of the PGA based nanoparticles the tests were carried out using three different cell types (human lung carcinoma cells (A549), human cervical cancer cells (HeLa) and cells from the kidney of sus scrofa (LLC-PK1)). As described above, nanoparticle dispersions were added to the wells. After incubation for 24 h at 37°C, alamarBlue® was added and the incubation was repeated for 1 h. Non-treated cells served as negative control and were defined to have 100 % viability. Cells treated with dimethyl sulfoxide (DMSO) served as a positive control, set to zero percent. The amount of fluorescence is proportional to the number of living cells and corresponds to the cells metabolic activity. Therefore, nonviable cells have a lower metabolic activity and thus generate a lower signal than healthy cells. AlamarBlue® was chosen because of the previously reported improved sensitivity and performance when compared to MTT assays [187].

High cell viability over the tested range was observed for all polymer conjugates (Figure 44). The polymer conjugates, especially the highly modified polymers combine high drug load, low hemolytic activity and low *in vitro* toxicity in various cell lines.

The cytotoxicity of free indomethacin is discussed differently in the literature. Some reports indicate high cytotoxic effects [172], others indicate low cytotoxic effects [188,189]. The reasons remain unclear. Therefore, cell viability studies for free indomethacin (0.1 – 40 µg/well) using the three mentioned cell lines were conducted. For free indomethacin a clear decrease of cell viability of all three cell lines was visible at higher amounts of the free drug (Figure 45). Cell viabilities were below 40 % for all three cell lines. Polymer conjugates showed much higher values (80-100 % survival for 40 µg polymer loadings).

A comparison of the free drug with the polymer conjugates could be based on the total mass. However, this would imply different drug contents due to the different drug loadings. Therefore, cell toxicity was plotted against the indomethacin load (Figure 45). In the case of A549 cells, advantages of the drug conjugates were observed for drug loads larger than 10 µg (Figure 45). Also the results of the LLC-PK1 cells indicated a higher toxicity of the free drug. The results with the HeLa cells are less conclusive. Reasons might be the different sensitivity of the cells and the scattering of the data. However, the main goal of this study was the development of an i.v.-injectable nanodispersion of a biodegradable indomethacin polymer conjugate with controlled release properties and low toxicity and hemolysis. Whether or not the toxicity of the conjugated drug is different from free indomethacin is interesting, but of secondary importance as long the drug conjugates are nontoxic. Based on the good results of the hemolysis test and the cell toxicity study, it was concluded that the PGA-IDMC nanodispersions are suitable candidates for further *in vivo* investigations (Section 4.2.9).
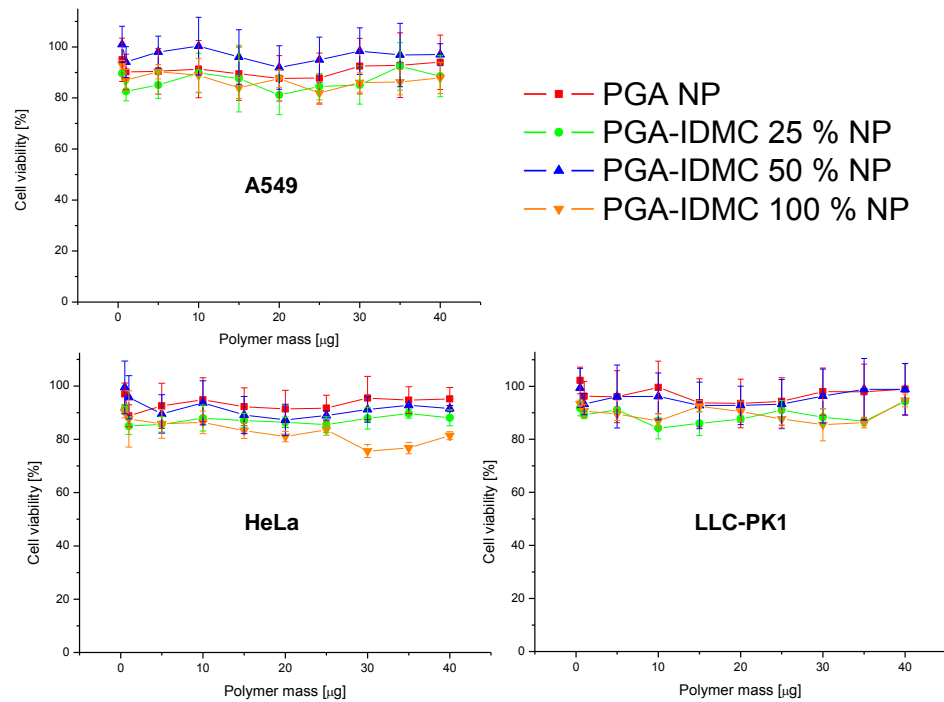
Figure 44. *Cell viability of A549 cells (top, left), HeLa cells (bottom, left) and LLC-PK1 cells (bottom, right) after 24 h incubation with PGA and different PGA-IDMC conjugate nanoparticles in different amounts. Cell viability was determined after incubation with alamarBlue® via fluorescence. Mean values and standard deviation are shown (n=6).*
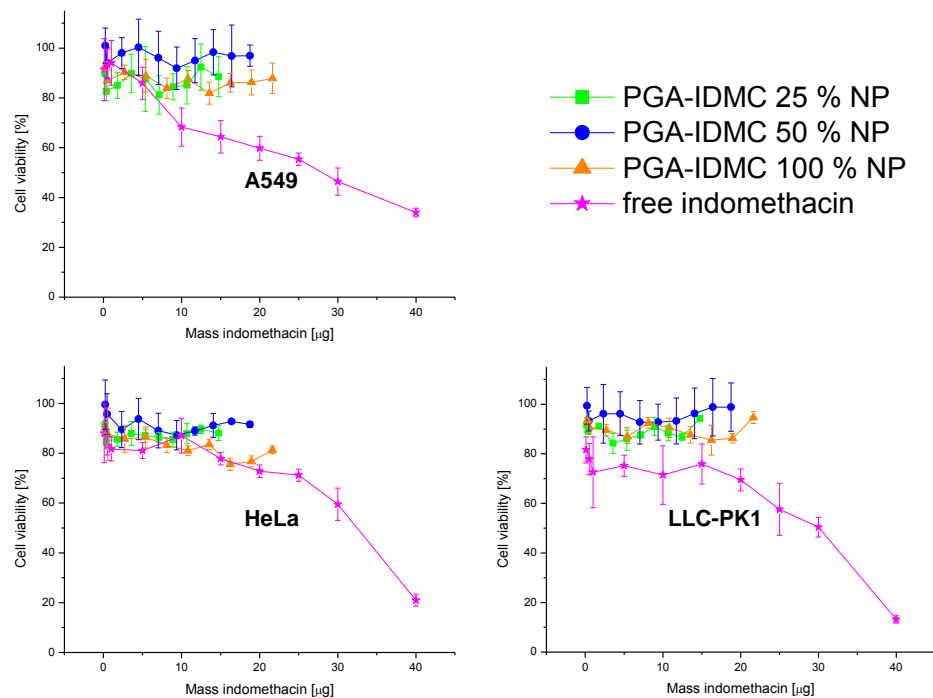
Figure 45. *Cell viability of A549 cells, HeLa cells and LLC-PK1 cells after 24 h incubation with PGA and different PGA-IDMC conjugate nanospheres in different amounts (total polymer mass). Cell viability was measured after incubation with alamarBlue® via fluorescence. Mean values and standard deviation are shown (n=6).*

4.2.7 *IN VITRO* RELEASE STUDY

In general, the evaluation of drug release from nanocarriers is difficult, due to the challenging separation of the free drug from the carrier. Most commonly, dialysis methods are used. The main disadvantage of the dialysis is the fact, that very often the overall kinetic is determined not by the drug release process from the Nano-DDS, but by the permeation kinetics through the dialysis membrane. Several scientists applied pressure to force the transport through the membranes and to come closer to a real release kinetic [190–192]. As a result, very fast release kinetics has been observed. A disadvantage of polymeric membranes is their sensitivity to solvents and pressure. A search was carried out for alternative materials with the following properties: (i) high porosity with defined nanopores; (ii) resistant against solvents and (iii) pressure resistance. The most systems are based on ultrafiltration. Based on these experiences, a release system for nanocarriers was developed. The construction of this device is described in detail above (Section 3.3.5). The core is the FlexiPor® nanoporous (20 nm) aluminum oxide membrane (SmartMembranes GmbH, Halle/Saale, Germany) which is shown in detail in Figure 46.
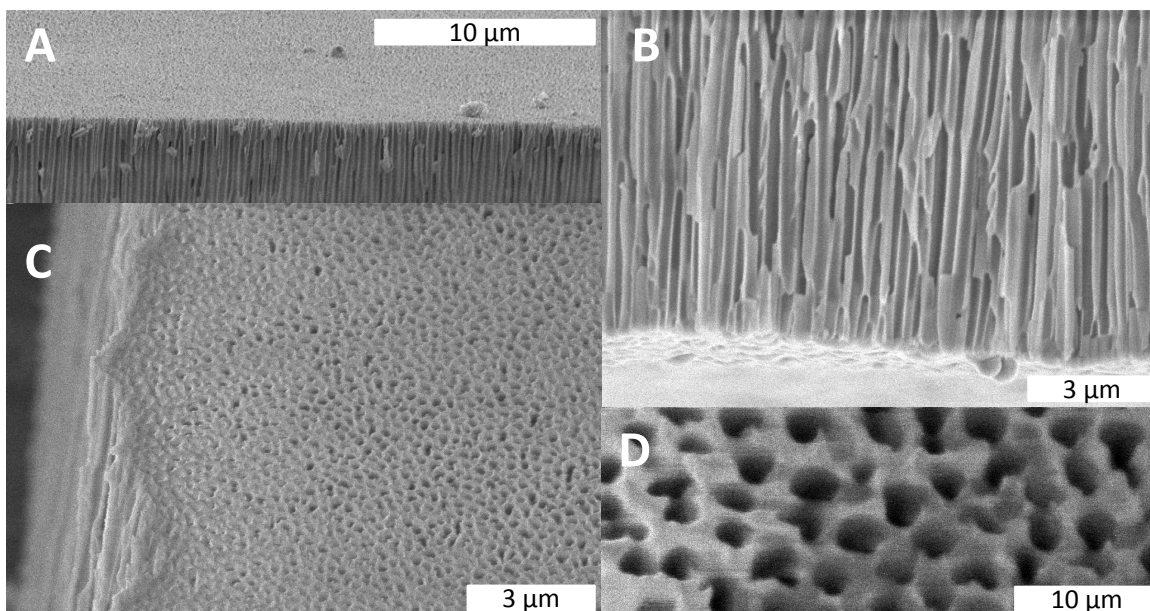
Figure 46. *ESEM micrographs of a FlexiPor® 20 nm membrane prior to use. Side view (A and B), back side (C) and front side (D). Back and front side were measured with a tilt of 45°.*

Drug adsorption to the membrane might be high because of the high surface area of the membrane which results from the high porosity and the small pore size. Two defined aqueous indomethacin solutions (8.5 and 12 µM) were filtered subsequently through the membranes. Indomethacin was quantified by HPLC. The recovery of 100 % could not be reached (Figure 47). Thus it is obvious that indomethacin is partly adsorbing on the membrane surface (Figure 47, left). Therefore, we could observe an increasing recovery rate with an increasing amount of filtered solution. This effect was independent from the investigated concentration of the stock solution, based on this the release results were corrected according to the recovery rates (Figure 47, right).
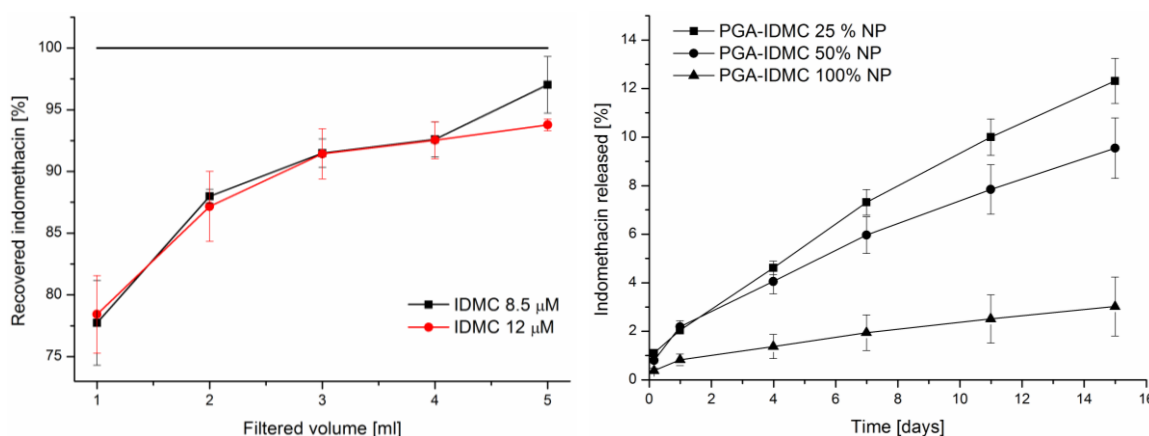
Figure 47. *Recovery of indomethacin after filtration of two different indomethacin solutions, through a FlexiPor® 20 nm membrane (left) and cumulative indomethacin release of PGA-IDMC nanoparticles with different substitution degree in pH 7.4 phosphate buffer over 15 days (n=3).*

Very low release rates have been observed with the bulk polymers *in vitro* (below 1 % of cumulative release over 30 days) [166]. Relative to the bulk polymers, the release rate from the nanospheres was higher, but still controlled and without any burst (Figure 12). This can be explained by the higher surface of nanospheres in contrast to preformed implants. The obtained release rates are comparable to the results reported for MTX-PGA NPs, where 17 % were released over 30 days in PBS pH 7.4 from 30%MTX-PGA NPs using a dialysis bag model [165]. Thereby, the surface for the hydrolysis of the ester bonds is much higher. Due to the higher hydrophilicity, the release rate is increasing with decreasing substitution degree. Furthermore, it should be mentioned that enzymes may have contributed to the release because the experiments could not be carried out under sterile conditions. However, the samples did not show any sign of bacterial growth, due to the preservation with sodium azide 0.02 % (w/v). The obtained release rates are low,

but recently published data of the release of covalently bond MTX from MTX-PGA NP [165] proofed an increase of the release rate by the influence of enzymes. This would lead to more clinical relevance.

The results described in this chapter (Section 4.2.7) have been developed in cooperation with Richard Krombholz during his practical year at the Martin-Luther-University, Halle (Saale) (11/2016 – 04/2017).

4.2.8 *IN VIVO* FLUORESCENCE IMAGING

To date, no poly(glycerol adipate) based drug conjugate has been applied *in vivo*. Therefore, the knowledge about the *in vivo* performance is very limited and can only be assumed from previously reported data of stearic acid modified poly(glycerol adipate) NPs [82]. The PGA-IDMC 100 % NPs performed especially well in the prior *in vitro* cytotoxicity tests in three different cell lines as well as in the hemolytic assay (Section 4.2.6). Therefore, these nanoparticle formulations were selected for first *in vivo* distribution studies using noninvasive *in vivo* fluorescence imaging. Distribution studies of both groups were performed in female as well as male hairless SKH1 mice. DiR is a lipophilic fluorescent dye and frequently used in previous studies on parenterally administered PLGA nanoparticles [83] and microparticles [193]. The results for the distribution of physically marked DiR PGA-IDMC 100 % nanoparticles are given in the following Figure 48. As expected, high fluorescence signals were detected in the liver already directly after injection (Figure 48, yellow arrow). This is a typical behavior for nanoparticulate formulations [194–196]. Mouse 4 showed no fluorescence signal in the liver due to high amount of formulation administered in the tissue during the intravenous application. The injection site showed high fluorescence signal intensity over the entire observation period. Therefore, the signals from other organs or regions could be hardly detected after a certain time due the automatically adjusted exposure time of the camera. The injection sites have been covered for the images captured after 48 and 72 h using a black plastic plate detect low signals from the liver also. However, fluorescence imaging is necessary for more detailed information about other involved organs and tissues *ex vivo*.
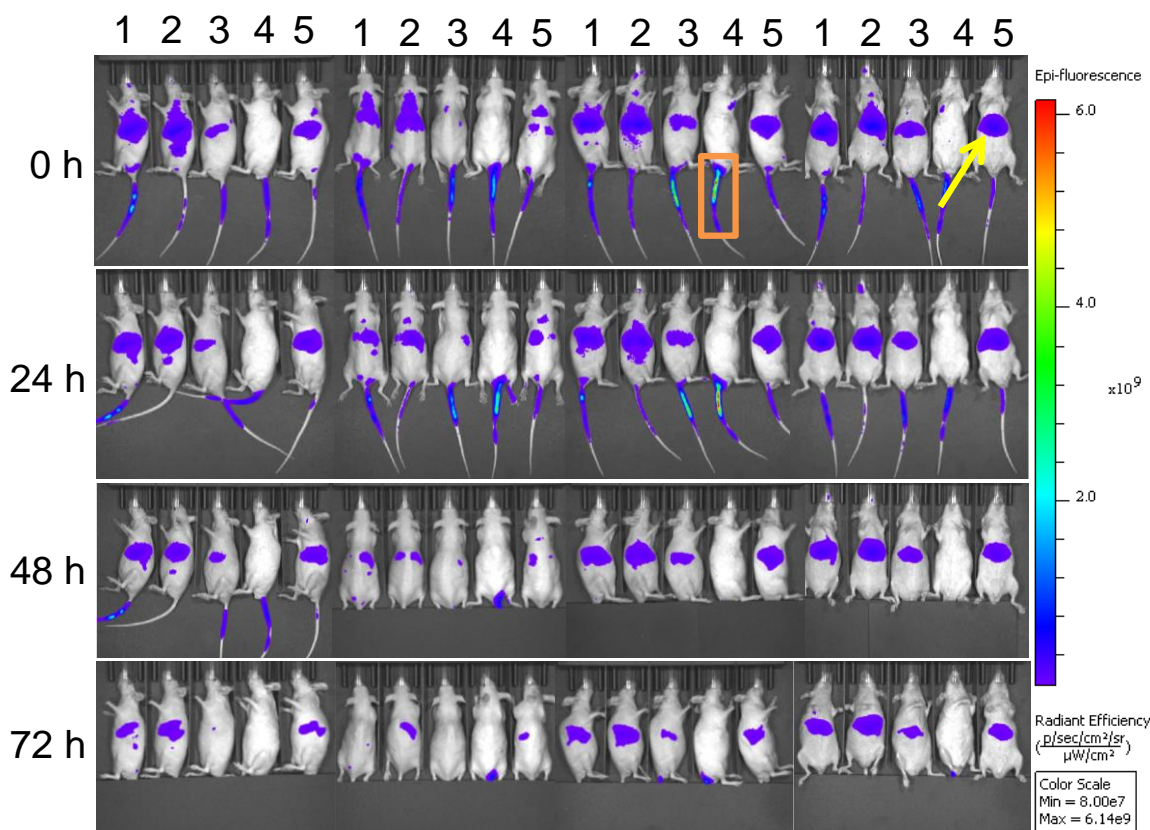
Figure 48. *Distribution of PGA-IDMC 100 % nanoparticles containing DiR in SKH1-Hr^{hr} (female – three mice from the left (1-3), male – two mice on the right (4,5)). The images were captured in four different orientations: left lateral side, dorsal side, right lateral side, and ventral side (from left to right). The biodistribution was analyzed directly after injection (0 h) and after 24 h, 48 h and 72 h. Orange frame indicates the injection site, yellow arrow the fluorescence signal in the liver.*

However, the distribution of DY-782 labelled PGA-IDMC 100 % NPs was more complex. DY-782 was chosen due to its NIR excitation wavelength as well as the possibility for covalent attachment to remaining free hydroxyl groups of PGA-IDMC 100 %. The dye was coupled using the same chemistry (Steglich esterification) which was used for the conjugation of indomethacin to the poly(glycerol adipate) backbone. The fluorescent dye DY-782 can therefore be regarded as a model drug and give indications for the release of indomethacin *in vivo*. The results are given in the following Figure 49. Learning from the DiR based experiments, the injection sites were covered from the beginning using the black plastic plate mentioned above. In contrast to DiR labelled NPs, the formulation showed a rapid accumulation in the kidneys (Figure 49, red arrows), the liver (Figure 49, yellow arrow), the lungs (Figure 49, orange arrow) as well as in the lymph nodes (Figure 49, green arrows). Especially the accumulation in the kidneys was reported prior for PGA based polymeric nanoparticles [82], but also for HPMA based nanoscale formulations

[197]. It is striking that strong fluorescence signals emanate from the kidneys, but no fluorescence could be observed in the bladder. That indicates a specific interaction between the fluorescent dye and the kidneys or between the polymer-conjugate and the kidneys. On the other hand, it is possible that the ester bond between DY-782 and polymer backbone is very rapidly enzymatically cleaved and the fluorescent dye is extremly rapidly renally eliminated. Urination of the mice cannot be controlled. Thus, there is the possibility, that no bladder signal could be observed due to the above-mentioned fact. However, the fluorescence intensity in the mentioned organs decreased rapidly after 24 h and it is therefore very likely that elimination occurs more often via the kidneys. Since differences in the distribution between the two groups were found, one mouse per group and sex were autopsied at the end of each experiment. Also two untreated (one male and one female) mice were autopsied and the autofluorescence of each tissue was subtracted from the treated ones.

Figure 49. *Distribution of PGA-IDMC 100 % nanoparticles containing covalently bound DY782 in SKH1-Hr^{hr} (female on the left, male on the right). The images were captured in four different orientations: left lateral side, dorsal side, right lateral side, and ventral side (from top to bottom).The biodistribution was analyzed directly after injection (0 h), and after 24 h. Untreated mice of both sexes were additionally monitored after 24 h (gray scale images).The arrows indicate the following organs: red = kidneys; yellow = liver; orange = lungs; green = lymph nodes.*

4.2.9 EX VIVO FLUORESCENCE IMAGING

During the *ex vivo* experiments all decisive organs were examined and rinsed before fluorescence imaging using phosphate buffer pH 7.4 to remove blood or excreta from the tissue in order to prevent autofluorescence. The extracted organs are schematically and clearly presented in Figure 50 (DiR NPs, below) and Figure 53 (DY-782 NPs). The highest fluorescence signal for DiR marked PGA-IDMC 100 % NPs was found in the liver, especially in female mice (Figure 51, A2) and a little lighter in male mice (Figure 52, A2). Even very high intensity could be observed in the spleen, at this point especially in male mice (Figure 52, A3). The accumulation of nanoparticles in the spleen is already known [82,198] and could be confirmed by the experiments carried out.
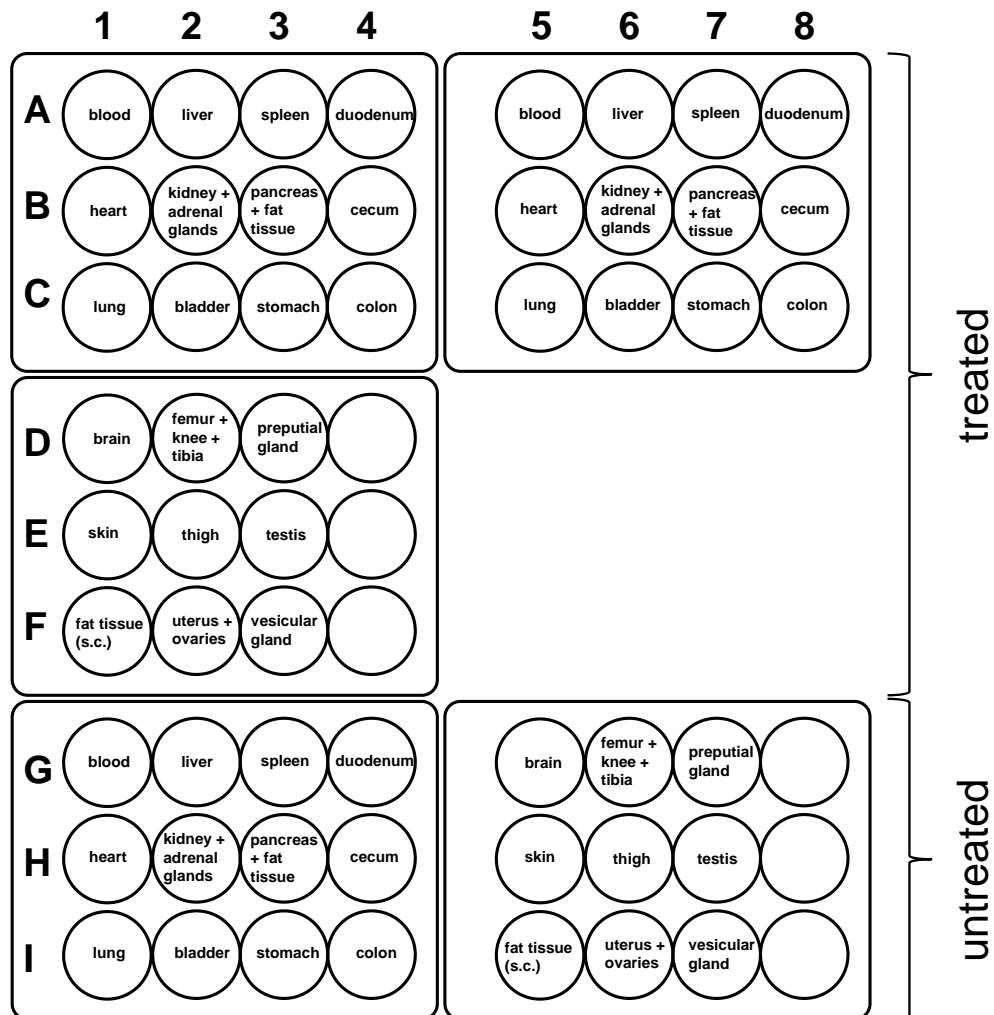
Figure 50. *Schematic illustration of the position of examined tissue after autopsy of SKH1-Hr^hr^ mice (male and female) treated with DiR marked PGA-IDMC 100 % NPs.*

Particularly eye-catching is the strong fluorescence signal in the uterus and especially in the ovaries (Figure 51; F2). This effect of nanoscale formulations has also been discovered before [199–202] and remains an exciting observation. Schädlich *et al.* provided interesting data about accumulation in detail [83]. The described enrichment in tertiary follicles, or in cells of the *corpus luteum* which could be proven by the unequal distribution of the fluorescence signal. There were presumptions that this is a dye specific phenomenon, however this was refuted very recently by Weiss *et al.* [82].
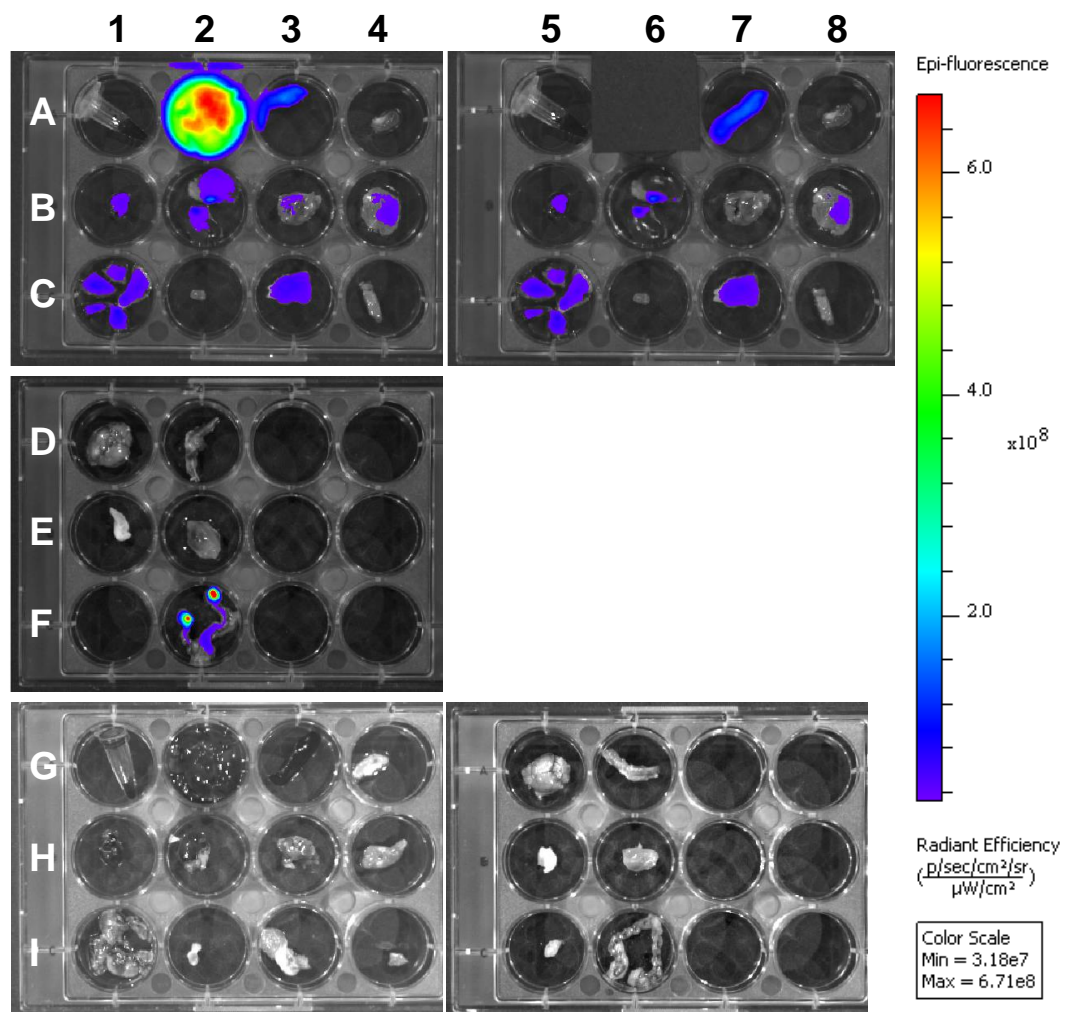
Figure 51. *Ex-vivo fluorescent images from extracted female SKH1-Hr^{hr} mouse organs, 72 hours after treatment with DiR marked PGA-IDMC 100 % NPs (lines A-F). Autofluorescence of organs of untreated female SKH1-Hr^{hr} (lines G-I) was subtracted from the treated mice. The liver (A6) was covered with a black plastic plate for one measurement in order to get higher fluorescence due to the automatically adjusted exposure time.*

They provided data showing accumulation in the ovaries using the fluorescent dye DY-676 and steric acid modified PGA NPs.
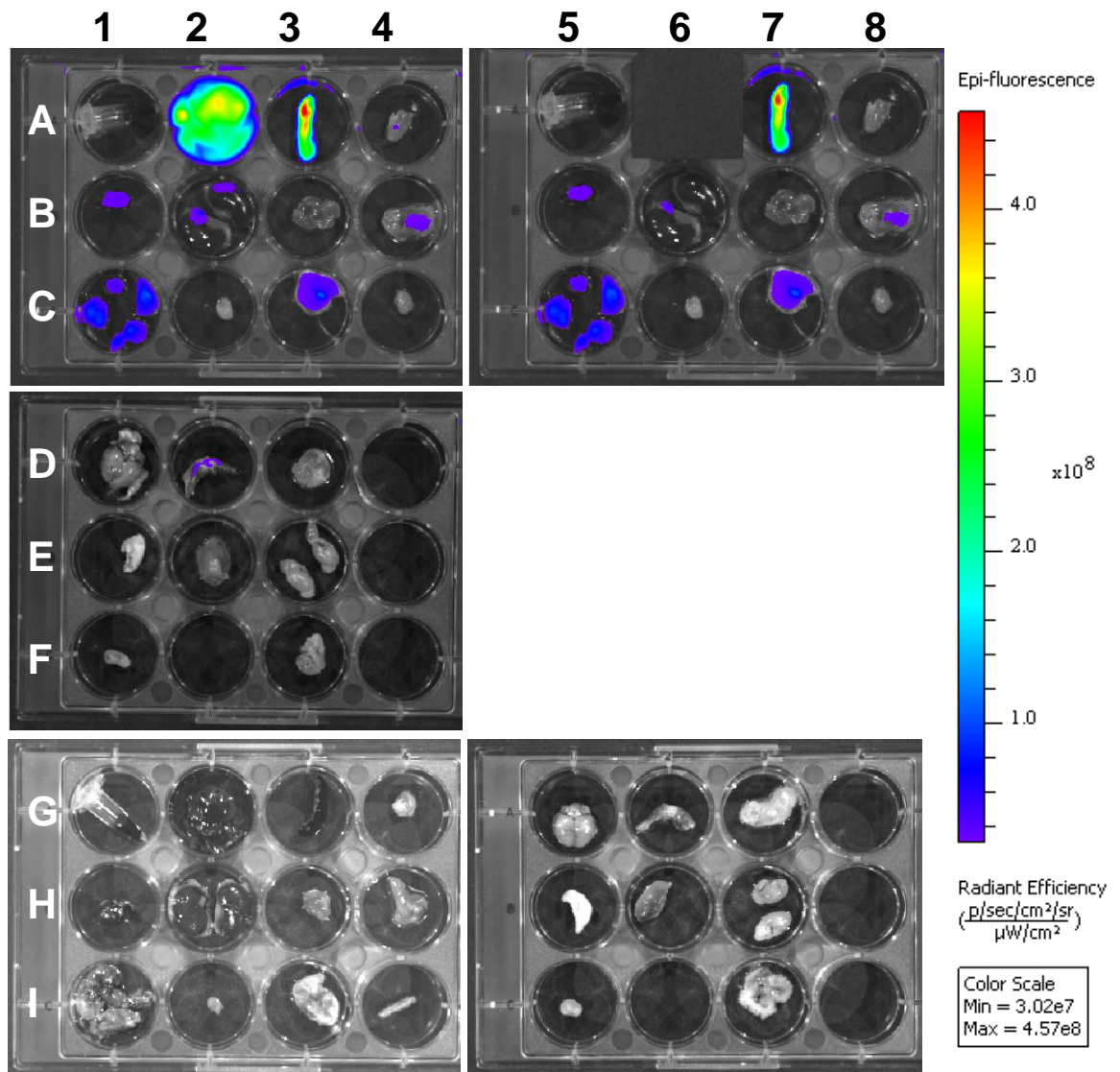
Figure 52. *Fluorescent images from extracted male SKH1-Hr^hr mouse organs, 72 days after treatment with DiR marked PGA-IDMC 100% NPs (lines A-F). Autofluorescence of organs of untreated female SKH1-Hr^hr (lines G-I) was subtracted from the treated mice. The liver (A6) was covered with a black plastic plate for one measurement in order to get higher fluorescence due to the automatically adjusted exposure time.*

The comparison of the distribution of particles, the two mentioned labeling options was the starting point of the present results. The results of the DY-782 marked female (Figure 54) and male (Figure 55) are shown in the images below. The more complex distribution from the in vivo imaging (Figure 49) could be confirmed *ex vivo*. In turn, signals were found in the liver (Figure 54 and Figure 55, A2), but in contrast to the DiR experiments

they were much lower. There was no fluorescence detectable in the spleen. The highest fluorescence intensity for this formulation was found in the kidneys (Figure 54 and Figure 55, B2). As there was no signal present in the bladder the polymer or the cleaved dye probably interaced with the tissue of kidneys. Various properties have already been mentioned so far which influence the cumulation in the kidneys. For example, high degree of grafting by drugs [203–205], functional groups or negative charge [206,207] of the nanoparticle formulations. Another component of the reticuloendothelial system are the lungs. Several articles have already reported that nanoparticles also accumulate in this tissue after intravenous administration. For example (methyl-2-14C-methacrylate) nanoparticles [194] or ^{14}C-polyhyxyl cyanoacrylate nanoparticles [208].
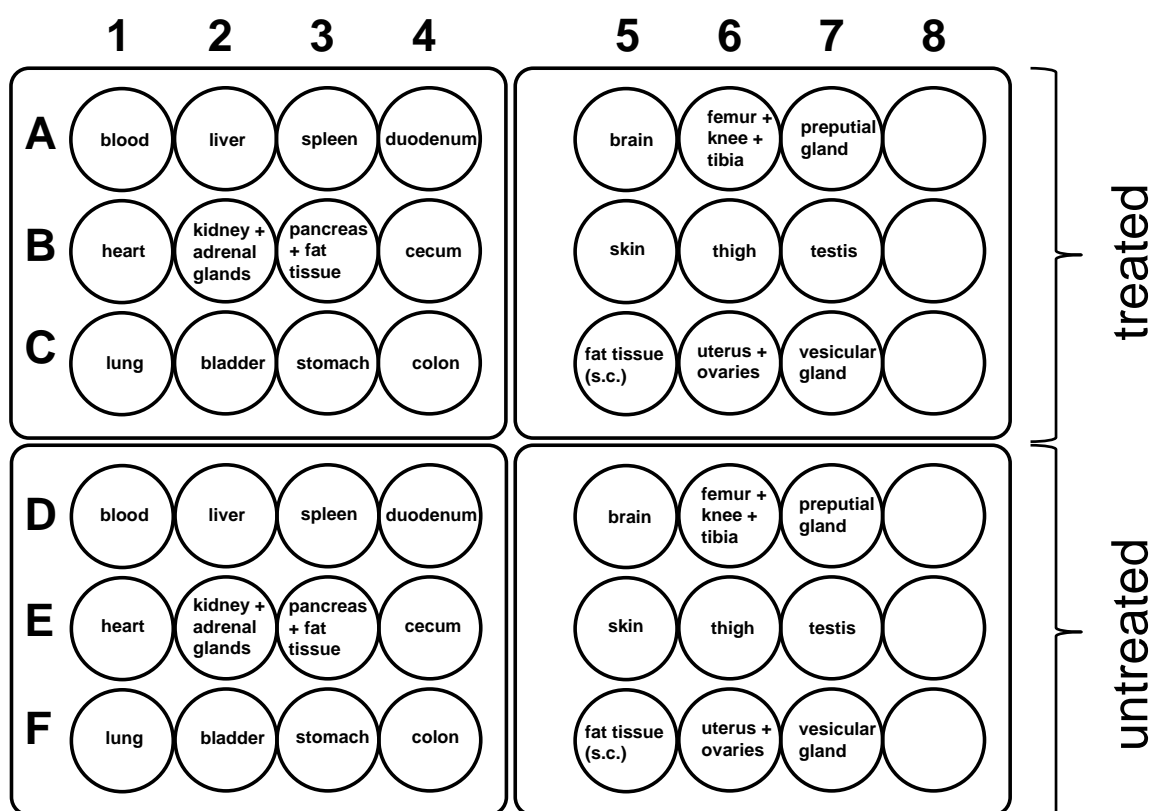
Figure 53. *Schematic illustration of the position of examined tissue after autopsy of SKH1-Hr^{hr} mice (male and female) treated with DY-782 modified PGA-IDMC 100 % NPs.*
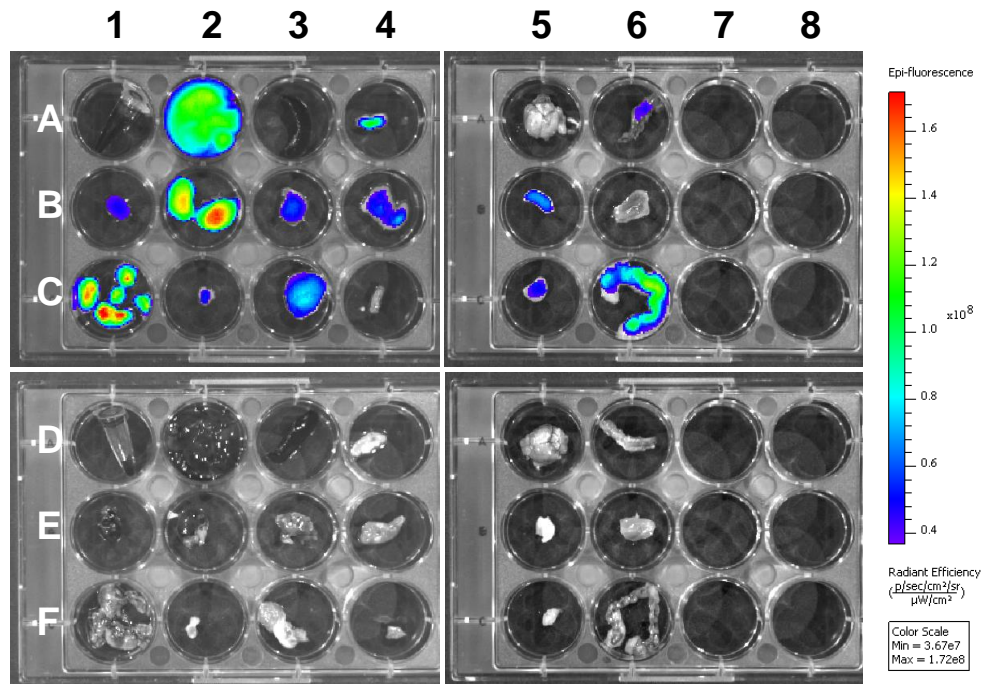
Figure 54. *Fluorescent images from extracted female SKH1-Hr^{hr} mouse organs, 72 hours after treatment with DY-782 modified PGA-IDMC 100 % NPs (lines A-F). Auto-fluorescence of organs of untreated female SKH1-Hr^{hr} (lines G-I) was subtracted from the treated mice.*
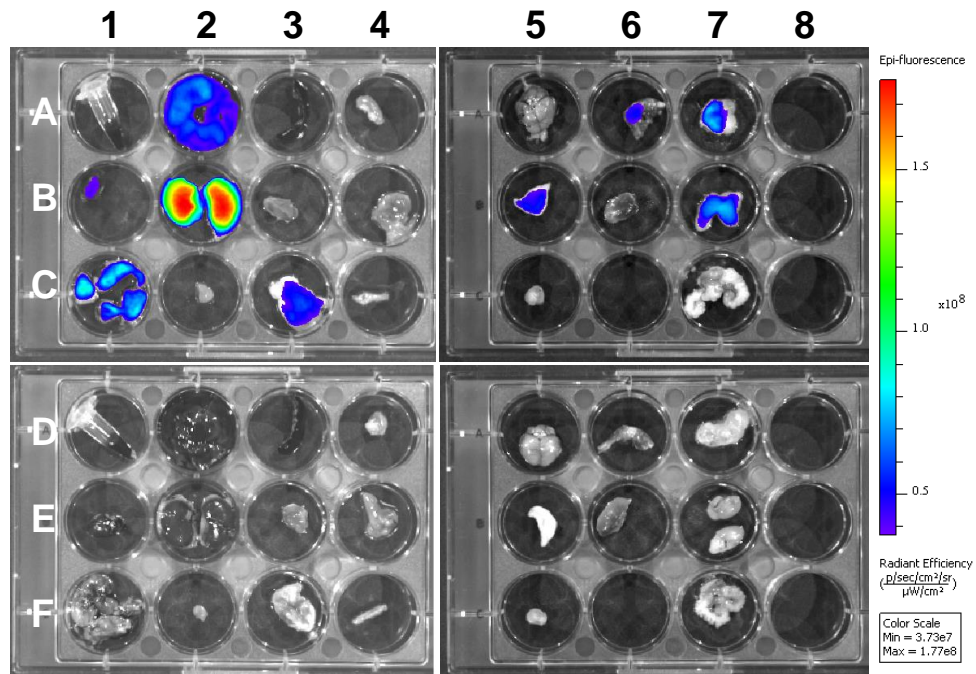
Figure 55. *Fluorescent images from extracted male SKH1-Hr^{hr} mouse organs, 72 hours after treatment with DY-782 modified PGA-IDMC 100 % NPs (lines A-F). Auto-fluorescence of organs of untreated female SKH1-Hr^{hr} (lines G-I) was subtracted from the treated mice.*

In addition to the signals from the kidneys, the highest intensities were found in the lungs (Figure 54 and Figure 55, C1). However, this behavior could not be confirmed with this intensity in the experiments with DiR marked particles. Further experiments have to be carried out to clarify whether this is a dye-specific phenomenon or not. Another possibility is that the autopsy was performed after 24 h (DY-782 NPs) or 72 h (DiR NPs). Perhaps the accumulation in the lungs is very fast, followed by a rapid decline. As already mentioned further investigations are necessary at this point.

The question of whether an accumulation could also be confirmed with covalently labeled nanoparticles proved to be intriguing. In comparison to the previous experiments, no accumulation in the ovaries (Figure 55, C7) could be observed. However, clear signals could be found in the uterus (Figure 55, C7), which are comparable in their intensity to those from the liver (Figure Figure 55, A2). This may be due to the shorter circulation time of the DY-782 marked nanoparticles. In addition, a time-dependent investigation of the accumulation in the individual organs would be a desirable object for further research.

In conclusion, the mentioned formulations were well tolerated by mice throughout the experimental period, confirming the obtained *in vitro* results (Sectio 4.2.6) now *in vivo*.

The evaluation of the test animals was carried out based on a prepared score sheet as per the German animal protection law (§ 31 Abs. 1 Satz 2 Nr. 1d TierSchVersV).

4.3 MICROPARTICLES

The dominating field of polymer therapeutics and especially the polymer-drug conjugates is the use as nanoscale DDS [4]. With the growing interest for new areas of application and diseases, such as infections [209] and inflammation [210] such as rheumatoid arthritis [211], there is also a need for innovative formulations outside the nanoscale range. NSAIDS are important drugs for the therapy of osteoarthritis and are often locally applicated directly into the synovial joint. To prevent mass phagocytosis, the application of microparticles is preferred [91]. In order to determine the potential of the PGA-IDMC conjugates for versatile applications, microparticles were produced and characterized in addition to the above described nanoparticles (Section 4.2).

The microparticles were prepared according to the oil-in-water method described above (Section 3.4.1) and involved several critical parameters that had to be taken into consideration during production:

- the polymer solution must be injected directly into the aqueous phase
- the blade stirrer must be adjusted to ensure decentralized stirring in the beaker
- the blade stirrer must be adjusted just a few millimeters above the bottom of the cup
- PTFE beaker
- vigorous stirring and slow injection
- aqueous 5 % (w/v) Poloxamer 188 solution

Under consideration of these core parameters it was possible to prepare microparticles out of PGA-IDMC 50 and 100 %.

4.3.1 STATIC LIGHT SCATTERING

Static light scattering is a basic method for particle size measurements of microparticle formulations. The resulting particle size distributions are usually characterized by $D_{(0.1)}$, $D_{(0.5)}$, $D_{(0.9)}$ and mean values [212]. The evaluation was carried out using the Fraunhofer theory, since the particles are not transparent and significantly larger than the wavelength (450 and 633 nm) of the light used during the measurements [213]. Therefore, no refractive indices of particles and dispersion medium are needed. Figure 56 shows the results of the characterization using SLS. The volume weighted particle size distribution of both polymers showed that the preparation of microparticles, using the method described above, was successful. The cumulative distribution curve of PGA-IDMC 100 % (Figure 56, black line) is noticeable steeper than the one of PGA-IDMC 50 % (Figure 56, red line). Accordingly, PGA-IDMC 100 % shows a narrower particle size distribution. However, both batches displayed a fraction of small particles in range between 2 and 20 µm, maybe caused bye the frequent washing in order to remove the stabilizer Poloxamer 188 (Section 3.4.1). PGA-IDMC 50 %, unlike PGA-IDMC 100 %, has an additional small fraction in the large size range between 800 and 2000 µm. A possible reason for this may in turn be the difference in hydrophilicity of the two mentioned polymers which has already caused slight differences in the size of nanoparticles (Section 4.2.2). The comparison of the characteristic particle indices (Table 12) clarifies the great difference between the two microparticle species. Both polymers have a relatively broad particle size distribution. However, the gap between $D_{(0.1)}$ and $D_{(0.9)}$ is lower and therofore the particle size distribution is narrower. These results will be confirmed in the following chapters by data of light microscopy and electron microscope images.

Table 12. *Particle size distribution of PGA-IDMC based MP with different degrees of modification. Data was determined by static light scattering under the assumption of spherical particles.*

Sample	$D_{(0.1)}$	$D_{(0.5)}$	$D_{(0.9)}$	$D_{(4,3)}$
PGA-IDMC 50 % MP	49.6 µm	112.6 µm	282.8 µm	140.8 µm
PGA-IDMC 100 % MP	39.7 µm	81.2 µm	147.8 µm	87.7 µm
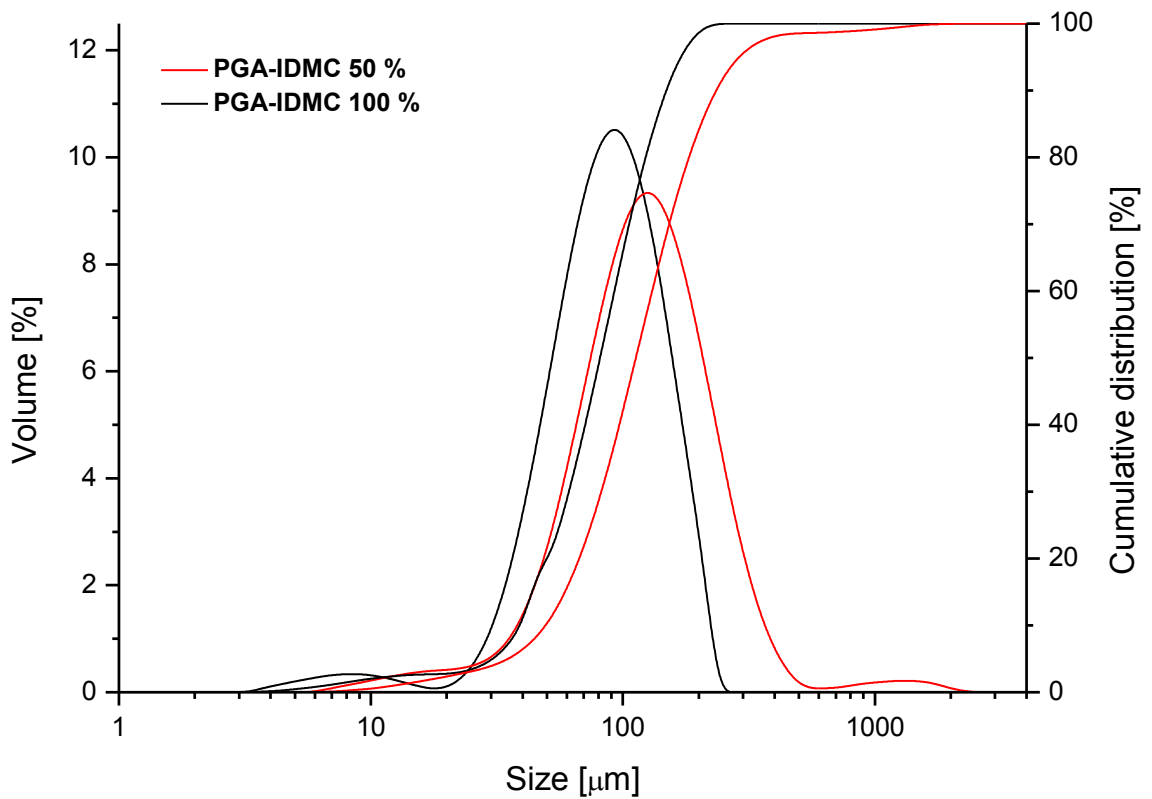
Figure 56. *Particle size distribution of PGA-IDMC 50 % MP (red line) in comparison to PGA-IDMC 100 % (black line) based microparticles determined by static light scattering.*

4.3.2 LIGHT MICROSCOPY

Prior to the electron microscopy, light microscopy was used to get an overview over particle size and shape of the nanoparticles. A selection is shown in the following Figure 57.
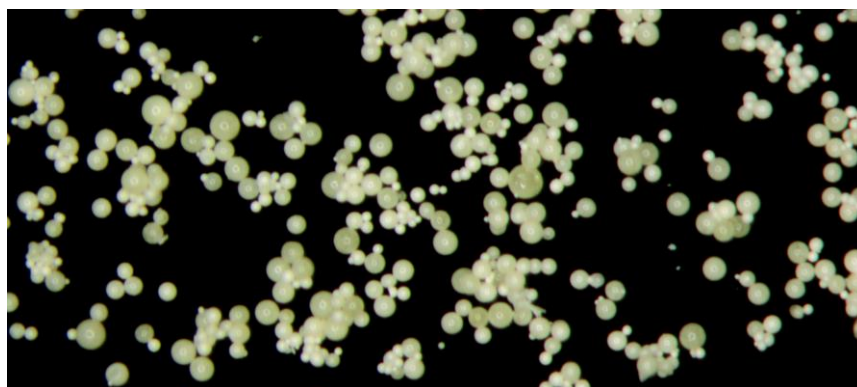
Figure 57. *Light microscopic images of PGA-IDMC 100 % MP using a reflected light microscope.*

All particles appeared spherical and yellowish which suggests that the laser-based size measurements were evaluated correctly.

4.3.3 SCANNING ELECTRON MICROSCOPY

The results obtained by static light scattering should be supported by scanning electron micrographs. Scanning electron microscopy is a common method for studying size and morphology of microparticles [214]. The following Figure 58 and Figure 59 show the results of the SEM measurements for PGA-IDMC 100 %, which were selected due to their narrower size distribution acoording to the SLS results (Section 4.3.1). All particles appeared spherical, which is important for the correct evaluation of the results of static light scattering (Section 4.3.1). The fraction of small particles from the SLS measurements (Figure 56) could also be confirmed by the electron micrographs (Figure 58D and G). They are therefore particles, and not non-covalently bound indomethacin crystals. Moreover, the images provide interesting insights into to morphology of the particles. To study the nuclear structure of these particles, some were destroyed with a razor blade. These images are shown in Figure 59. Methylene chloride is a very desirable organic solvent which is often used for the preparation of microparticles using the O/W-method due to its low water solubility [215]. This normally leads to a fast

precipitation and regular surface due to the fast efflux of the organic solvent. Although methylene chloride was used as organic solvent, the morphology of the examined particles deviates from this general case. Due to the high Poloxamer 188 concentration of the aqueous phase (5 % (w/v), the solubility of methylene chloride in water is increased and as a result a proportionate amount of water was used (1:20). Therefore, the polymer formed a shell-like structure around the particles with a hollow core (Figure 59G) [216]. Finally, the solvent was extracted from the core which led to the obvious structure. In general, solubilizers such as the water soluble PVP [217] and Pluronic[®] F127 [218] are known as extractable porogens. Moreover, during preparation and electron microscope measurements the particles were stored under vacuum conditions. This might also contribute to the very porous structure due to evaporation of residual solvents.
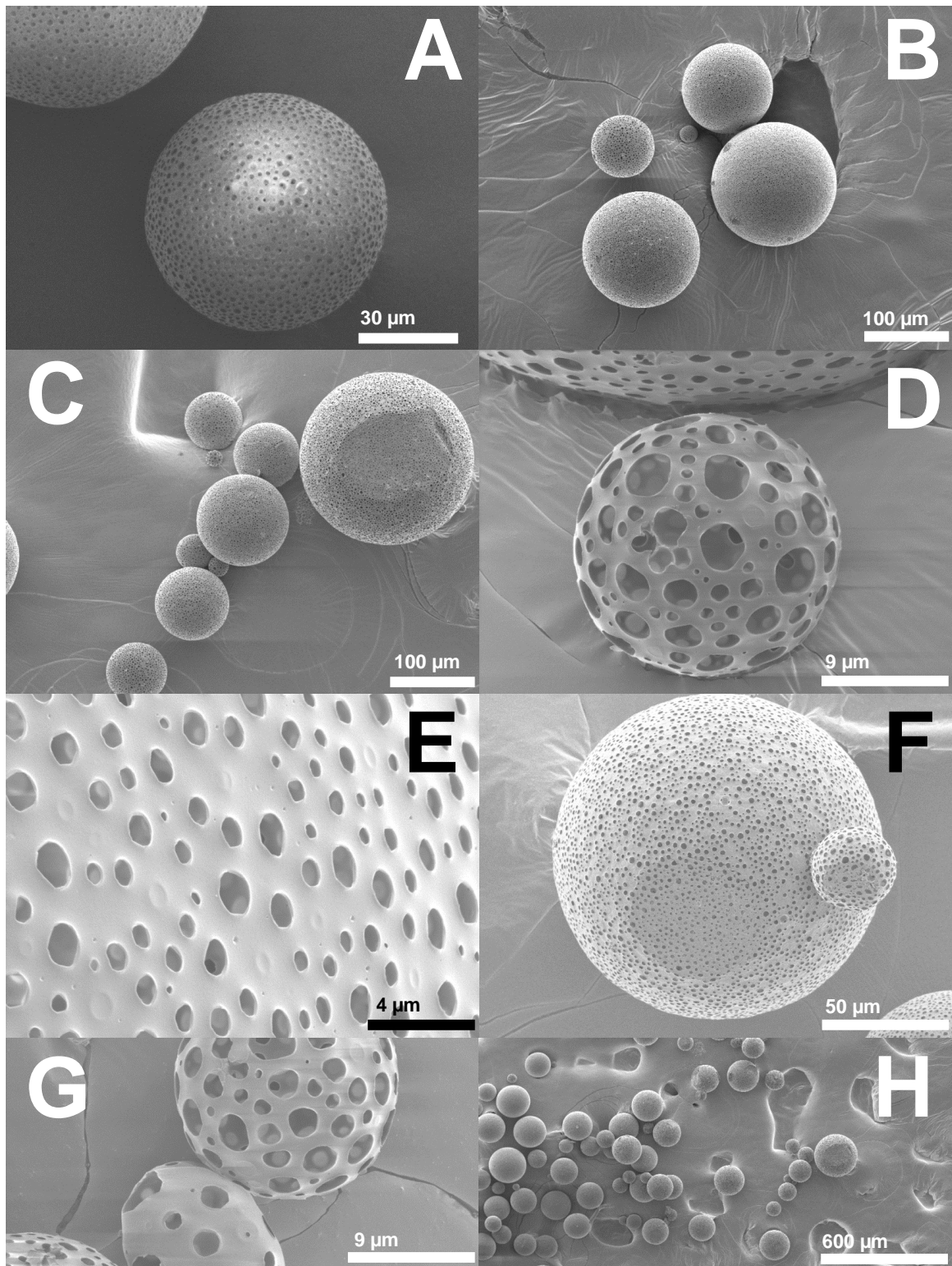
Figure 58. *Electron scanning micrographs of intact PGA-IDMC 100 % based microparticles, directly after preparation. The measurements were carried out under vacuum conditions.*
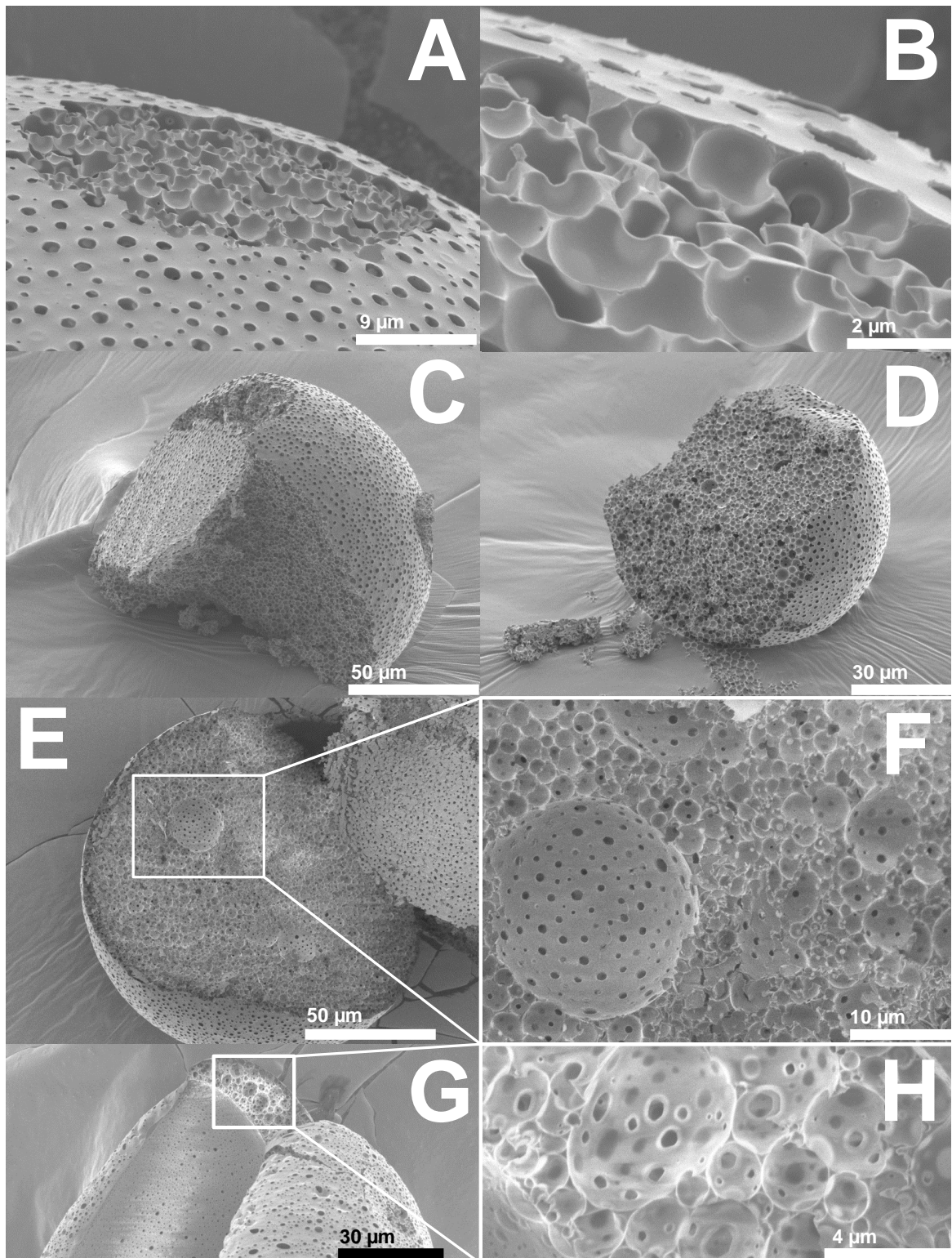
Figure 59. *Electron scanning micrographs of damaged PGA-IDMC 100 % based microparticles. The microparticles were damaged arbitrarily using a razor blade. The measurements were carried out under vacuum conditions.*

4.3.4 *IN VITRO* RELEASE

A determination of the indomethacin release *in vitro* for this microparticle-based DDS is necessary to be able to estimate the potential for later application *in vivo*. The following Figure 60 (below) shows the cumulative release of indomethacin over a period of three months. The release experiments were carried out in the style of the preformed implants (Section 3.2.11) in three different release media. The release rate in buffer (Figure 60A) is again very slow. Compared to preformed implants (Section 4.1.7.1) and nanoparticles (Section 4.2.7), the microparticle release rate lies in between. It can be assumed that the release rate depends on the surface of the DDS. Therefore, it is decreasing from nanoparticles, over microparticles to preformed implants. It is striking that the release rate is independent of the degree of modification for the release in buffer (Figure 60A). In the acidic environment, as well as under the influence of enzymes, a similar behavior emerges as for the previously described preformed implants (Section 4.1.7). The release is significantly accelerated.
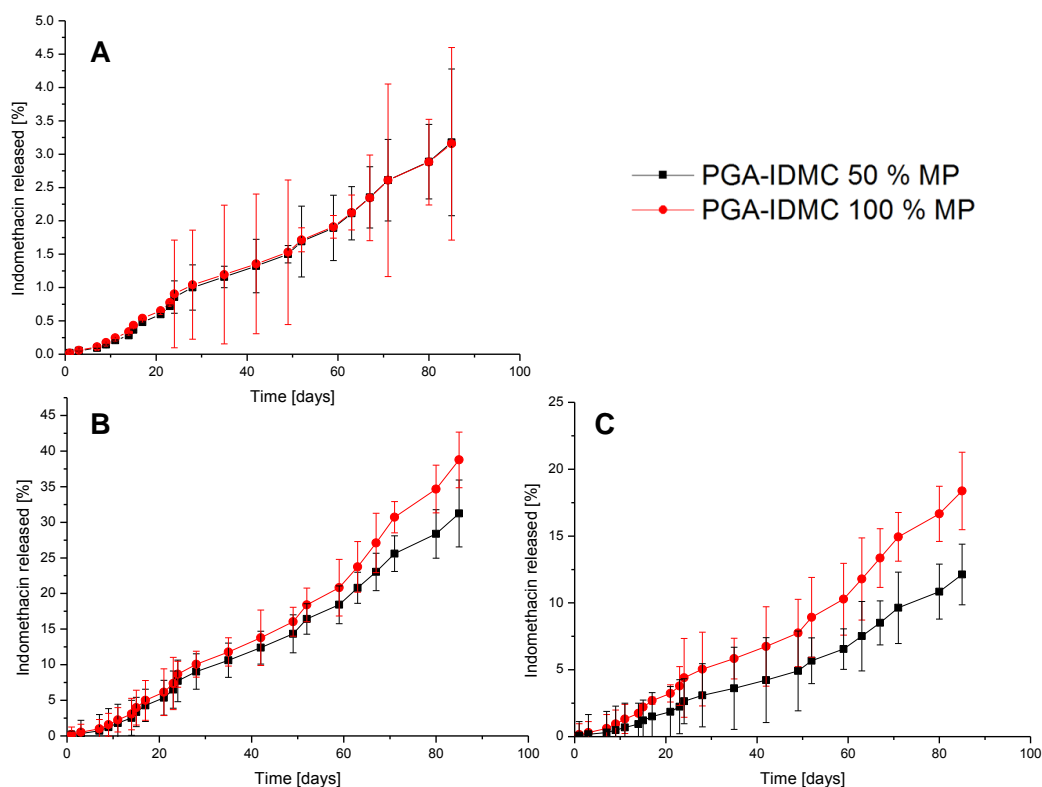
Figure 60. *Cumulative release % (w/w) of indomethacin from PGA-indomethacin microparticles with different degree of modification in pH 7.4 phosphate buffer (A), pH 7.0 sodium chloride solution containing lipase from Pseudomonas sp. (B) and pH 4.75 acetate buffer (C). The release was carried out at 37 °C over three months.*

5   <u>SUMMARY AND PERSPECTIVES</u>

The interest in polymer drug conjugates as a new platform for innovative drug delivery systems is steadily increasing. The potential of poly(glycerol adipate) as a basis for the development of drug conjugates was investigated within this work. Due to its high therapeutic relevance for various diseases, indomethacin has been selected as a suitable candidate for the synthesis of drug-grafted PGA derivates.

The linear polyester PGA was synthesized via an enzymatic polytranscondensation, using lipase from *candida antarctica* (CALB), from glycerol and divinyladipate. This esterification is selective on primary hydroxyl groups. Using the pendant OH-groups of poly(glycerol adipate) further modifications can be carried out. In a second synthesis step a simple, one-step reaction (Steglich esterification) was presented within this work for the covalent coupling of indomethacin. No complex linker or previous modification of drug on the one hand or backbone polymer on the other hand was necessary.

In the course of this work, indomethacin PGA conjugates with 25, 50 and 100 mol% grafting were synthesized and comprehensively characterized. The structural change of the various polymers depending on the degree of polymerization was investigated by ^{1}H-NMR and ATR-FT-IR. Here especially the proportional decrease of the OH peaks with increasing degree of substation was shown. Moreover, the degree of grafting could be calculated by the comparison of the integrals of methylene and methine groups of the poly(glycerol adipate) backbone. This method was verified afterwards by UV spectroscopy. In this way, very high levels of drug loading (35.6 – 54.1 % (w/w)) were demonstrated which are all promising candidates for application in nano- and microscale dosage forms. The thermal properties of the new polymers were investigated by means of DSC. In this case, a shift of the glass transition from -23.7 °C (PGA backbone) to 51°C (PGA-IDMC 100 %) due to the space keeping branches, and no melting peaks for indomethacin could be observed. The backbone polymer as well as the three conjugates are amorphous, whereas the pure substance indomethacin is crystalline, as shown by X-ray diffraction measurements. The molecular weight distribution of these polymers was characterized in detail by GPC. All polymers showed a narrow molecular weight distribution with a PDI between 2.2 and 3.2 which is typical for brached polymers and a general increase of molecular weigth with increasing degree of grafting. In connection with this, a development from almost Newtonian fluid (PGA) to more and more viscoelastic polymers could be observed. These aspects of macroviscosity were mapped

by oscillatory rheology. Furthermore, the new polymers were first formulated as preformed implants. They were pressed into small cylinders with a specifically developed heating press. Subsequently, first release investigations, in phosphate buffer pH 7.4, acetate buffer pH 4.75 and 0.9 % aqueous sodium chloride solution contain lipase from *Pseudomonas* spez., were carried out. In comparison, physical mixtures of PGA and indomethacin were prepared and exposed to phosphate buffer pH 7.4. After 30 days, the conjugates released just about 0.7 % of indomethacin. However, under acidic conditions (16 % after 30 days) or in the presence of enzyme (40 % after 30 days) the release rate was clearly accelerated due to the cleavage of the ester bonds. In comparison, the physical mixtures behaved completely differently. The total amount of indomethacin was already released after 15 days in phosphate buffer pH 7.4. The release behavior is further confirming that indomethacin is covalently bound. The release data are very promising, as there are slightly acidic pH values and enzymes, especially in inflamed tissue, and the polymers provide for a controlled release over a long period of time.

In the second part of this thesis, it was examined whether nanoscale drug delivery systems can be produced from the new material. It was possible to prepare nanoparticles using all three conjugates via an optimized solvent displacement method. Just small amounts of stabilizer (below or equal 0.5 % PVA or Poloxamer188) were necessary. The particle size of all systems was characterized in detail by dynamic light scattering as well as nanoparticle tracking analysis. Most nanoparticle formulations could be prepared in in the size range of 160-220 nm and narrow particles size distribution (PDI below 0.2). Moreover, selected formulations could be freeze dried, stored for 4 weeks (fridge) and redispersed, with just slight changes of the particle size. Additionally, the appearance was investigated by TEM, showing spherical particles. Release experiments were also carried out *in vitro* for these drug delivery systems. A new release cell was developed. The centerpiece is a porous aluminum membrane with a pore size of 20 nm, which makes it possible to separate the released drug from the drug delivery system. The sampling was carried out under reduced pressure and the substitution of the sample volume was fast and easy. The developed release cell is original and universally applicable for various nanoscale drug delivery systems. Using this release cell, the release from PGA-IDMC NPs stabilized with 0.5 % Poloxamer was monitored over 15 days in phosphate buffer pH 7.4. During this period, a controlled and almost linear release rate was achieved. At the end of the experiment 13 % for PGA-IDMC 25 %, 10 % for PGA-IDMC 50 % and 2 % for PGA-IDMC 100 % were released. These values are much higher than those of the preformed implants, which can be attributed to the

enlarged surface. Again, the release rate was different between the various polymers, probably due to the decreasing wettability with increasing degree of grafting. Preparatory for the *in vivo* tolerability and distribution studies, hemolytic and cytotoxic activities were investigated for selected formulations. The toxicity was tested with three different cell lines. Two human cell lines (A549, HeLa) and one animal cell line (LLC-PK1). The cell culture experiments assessed the tolerance of the cells against PGA-IDMC NPs independent from the degree of grafting. The behavior towards red blood cells was more complex. The hemolytic activity decreased with increasing amounts of drug, due to the reduced number of free hydroxyl groups associated with decreasing amphiphilic character. PGA-NPs showed about 10 %, PGA-IDMC 25 %-NPs 5 %, PGA-IDMC 50 %-NPs about 2 % and PGA-IDMC 100 % NPs almost no hemolytic activity. Accordingly, the latter were selected for further characterization *in vivo*.

In an explorative *in vivo* experiment, the distribution and tolerability of PGA-IDMC 100 % NPs was investigated. For this purpose, the lipophilic fluorescent dye DiR was incorporated into the nanoparticle formulation. Distribution of nanoparticles was monitored over three days in five mice (two male, three female) via noninvasive fluorescence imaging. The images prove that the formulations were eliminated by the liver. In a second group, consisting of two animals (male and female), the behavior of PGA-IDMC 100 % NPs was examined which were previously covalently labeled with the fluorescent dye DY-782 via a cleavable ester bond like indomethacin is coupled. After 24 h, clear signals in kidneys, lungs, liver as well in lymph glands were detected. This may be due, to the rapid cleavage of the ester bond and the elimination of the fluorescent dye. However, one mouse of each group and sex was eventual autopsied and the accumulation in the organs was examined in detail *ex vivo*. For the DiR labeled particles, the most intense signals were found in the liver and in the ovaries. The latter confirms previous reports on the accumulation of nanocarriers [82,83]. DY-782 marked NPs accumulated in kidneys, lungs, spleen as well as in the uterus. Accumulation in the ovaries could not be observed, which may be due to the autopsy after 24h. Maybe the accumulation in the ovaries needs more time. The time-dependent accumulation of nanocarriers is an intriguing approach for further research. In conclusion, it can be stated that the tested formulations were well tolerated by all animals, which was evaluated using a developed score sheet.

The dominating field of application for polymer therapeutics are nanoscale DDSs. However, especially for the treatment of inflammations such as osteoarthritis DDSs with

larger particles are highly desirable. Therefore, the possibility to produce microparticles was examined in a third section. For example, during the therapy of osteoarthritis the formulation is injected direct in the synovial joint. The use of microparticles is therefore preferred to prevent mass phagocytosis. Within this work microparticles were prepared using an oil-in-water solvent evaporation techniques from PGA-IDMC 50 % and 100 %. The obtained microparticles were freeze dried and particle sizes between 87 (PGA-IDMC 100 % MP) and 140 μm (PGA-IDMC 50 % MP) were determined by static light scattering. Both particle species had broad particle size distributions. Therefore, the production needs further optimization. The round shape as well as the particle size was confirmed by light microscopy. To get an impression from the detailed structure from particle surface and core, electron scan micrographs were prepared. All particles showed a highly porous structure which gives the impression that the microparticles consist of nanoparticles. The high amount of stabilizer (5 % (w/w) Poloxamer188) is known as porogen. Furthermore, the small particle fractions from the static light scattering measurements could be confirmed by ESEM. In fact, they are actually polymer microparticles and not unbound indomethacin crystals. Finally, release studies in three different media were also carried out for these formulations. After three months just 3 % of indomethacin was released from both particle species in phosphate buffer pH 7.4, the release rate is therefore slower than for nanoparticles which may be due to the larger surface. The release rate could be accelerated by adding enzymes from *Pseudomonas* spez., so 30-40 % could be released after three months. Even under acidic conditions, similar behavior to that of preformed implants could be observed (13-20 % after three months).

Within this work, the first PGA-drug conjugate was successfully synthesized and comprehensively characterized. There are many possibilities for producing innovative drug delivery systems from this new polymer. First preliminary tests showed the successful formulation as *in situ* forming implant, which should be subject of further research. Furthermore, the promising first animal experiments provide space for the treatment of inflammatory diseases such as pancreatitis. The development of suitable animal models would be the next step in preclinical research. On the chemical side, there are almost limitless possibilities. To name only a few, there would be the possibility to introduce diverse linkers and to couple active ingedients via other bonds than esters in order to control the drug release. Furthermore, the grafting of fatty acids and active ingredients to the same backbone could have interesting effects on release and polymer properties.

6   <u>REFERENCES</u>

[1]   L.J. Scott, Glatiramer acetate: a review of its use in patients with relapsing-remitting multiple sclerosis and in delaying the onset of clinically definite multiple sclerosis, CNS Drugs 27 (11) (2013) 971–988.

[2]   L.C. Powell, A. Sowedan, S. Khan, C.J. Wright, K. Hawkins, E. Onsøyen, R. Myrvold, K.E. Hill, D.W. Thomas, The effect of alginate oligosaccharides on the mechanical properties of Gram-negative biofilms, Biofouling 29 (4) (2013) 413–421.

[3]   L.C. Powell, M.F. Pritchard, C. Emanuel, E. Onsøyen, P.D. Rye, C.J. Wright, K.E. Hill, D.W. Thomas, A nanoscale characterization of the interaction of a novel alginate oligomer with the cell surface and motility of Pseudomonas aeruginosa, Am. J. Respir. Cell Mol. Biol. 50 (3) (2014) 483–492.

[4]   F. Canal, J. Sanchis, M.J. Vicent, Polymer--drug conjugates as nano-sized medicines, Curr. Opin. Biotechnol. 22 (6) (2011) 894–900.

[5]   J. Kopeček, Polymer-drug conjugates: origins, progress to date and future directions, Adv. Drug Deliv. Rev. 65 (1) (2013) 49–59.

[6]   G. Pasut, Polymers for Protein Conjugation, Polymers 6 (1) (2014) 160–178.

[7]   E.M. Pelegri-O'Day, E.-W. Lin, H.D. Maynard, Therapeutic protein-polymer conjugates: advancing beyond PEGylation, J. Am. Chem. Soc. 136 (41) (2014) 14323–14332.

[8]   D.C. González-Toro, S. Thayumanavan, Advances in Polymer and Polymeric Nanostructures for Protein Conjugation, Eur. Polyme. J. 49 (10) (2013) 2906–2918.

[9]   Y. Yang, D. Pan, K. Luo, L. Li, Z. Gu, Biodegradable and amphiphilic block copolymer-doxorubicin conjugate as polymeric nanoscale drug delivery vehicle for breast cancer therapy, Biomaterials 34 (33) (2013) 8430–8443.

[10]   N. Li, N. Li, Q. Yi, K. Luo, C. Guo, D. Pan, Z. Gu, Amphiphilic peptide dendritic copolymer-doxorubicin nanoscale conjugate self-assembled to enzyme-responsive anti-cancer agent, Biomaterials 35 (35) (2014) 9529–9545.

[11]   Y. Matsumura, K. Kataoka, Preclinical and clinical studies of anticancer agent-incorporating polymer micelles, Cancer Sci. 100 (4) (2009) 572–579.

[12]   O.M. Merkel, T. Kissel, Quo vadis polyplex? J. Control. Release 190 (2014) 415–423.

[13]   K. Osada, Development of functional polyplex micelles for systemic gene therapy, Polym J 46 (8) (2014) 469–475.

[14]   A. Tschiche, S. Malhotra, R. Haag, Nonviral gene delivery with dendritic self-assembling architectures, Nanomedicine (Lond) 9 (5) (2014) 667–693.

[15]   F. Sheikhi Mehrabadi, W. Fischer, R. Haag, Dendritic and lipid-based carriers for gene/siRNA delivery (a review), Curr. Opin. Solid St. M. 16 (6) (2012) 310–322.

[16]   C. de Duve, T. de Barsy, B. Poole, A. Trouet, P. Tulkens, F. van Hoof, Lysosomotropic agents, Biochem. Pharmacol. 23 (18) (1974) 2495–2531.

[17]   H. Ringsdorf, Structure and properties of pharmacologically active polymers, J. polym. sci., C Polym. symp. 51 (1) (1975) 135–153.

[18]   L. Gros, H. Ringsdorf, H. Schupp, Polymeric Antitumor Agents on a Molecular and on a Cellular Level? Angew. Chem. Int. Ed. Engl. 20 (4) (1981) 305–325.

[19]   A. Abuchowski, J.R. McCoy, N.C. Palczuk, T. van Es, F.F. Davis, Effect of covalent attachment of polyethylene glycol on immunogenicity and circulating life of bovine liver catalase, J. Biol. Chem. 252 (11) (1977) 3582–3586.

[20]   F.F. Davis, The origin of pegnology, Adv. Drug Deliv. Rev. 54 (4) (2002) 457–458.

[21]   G. Pasut, F.M. Veronese, State of the art in PEGylation: the great versatility achieved after forty years of research, J. Control. Release 161 (2) (2012) 461–472.

[22]   A.D. Keefe, S. Pai, A. Ellington, Aptamers as therapeutics, Nat. Rev. Drug Discov. 9 (7) (2010) 537–550.

[23]   C. Duve, Exploring cells with a centrifuge, Science 189 (4198) (1975) 186–194.

[24]   R. Duncan, Polymer therapeutics as nanomedicines: new perspectives, Curr. Opin. Biotechnol. 22 (4) (2011) 492–501.

[25]   R. Duncan, Development of HPMA copolymer-anticancer conjugates: clinical experience and lessons learnt, Adv. Drug Deliv. Rev. 61 (13) (2009) 1131–1148.

[26]   H.-J. Cantow, G. Dall'Asta, K. Dušek, J.D. Ferry, H. Fujita, M. Gordon, G. Henrici-Olivé, J.P. Kennedy, W. Kern, S. Okamura, S. Olivé, C.G. Overberger, T. Saegusa, G.V. Schulz, W.P. Slichter, J.K. Stille (Eds.), Polymers in Medicine, Springer Berlin Heidelberg, Berlin, Heidelberg, 1984.

[27]   R. Duncan, Drug-polymer conjugates: potential for improved chemotherapy, Anticancer. Drugs 3 (3) (1992) 175–210.

[28]   R. Duncan, L.W. Seymour, K.B. O'Hare, P.A. Flanagan, S. Wedge, I.C. Hume, K. Ulbrich, J. Strohalm, V. Subr, F. Spreafico, M. Grandi, M. Ripamonti, M. Farao, A. Suarato, Preclinical evaluation of polymer-bound doxorubicin, J. Control. Release 19 (1-3) (1992) 331–346.

[29]   Y. Matsumura, K. Kataoka, Preclinical and clinical studies of anticancer agent-incorporating polymer micelles, Cancer Sci. 100 (4) (2009) 572–579.

[30]   H. Varkony, V. Weinstein, E. Klinger, J. Sterling, H. Cooperman, T. Komlosh, D. Ladkani, R. Schwartz, The glatiramoid class of immunomodulator drugs, Expert Opin. Pharmacother. 10 (4) (2009) 657–668.

[31]   I. McGowan, K. Gomez, K. Bruder, I. Febo, B.A. Chen, B.A. Richardson, M. Husnik, E. Livant, C. Price, C. Jacobson, Phase 1 randomized trial of the vaginal safety and acceptability of SPL7013 gel (VivaGel) in sexually active young women (MTN-004), AIDS 25 (8) (2011) 1057–1064.

[32]   P.K. Dhal, S.C. Polomoscanik, L.Z. Avila, S.R. Holmes-Farley, R.J. Miller, Functional polymers as therapeutic agents: concept to market place, Adv. Drug Deliv. Rev. 61 (13) (2009) 1121–1130.

[33]   J. Sanchis, F. Canal, R. Lucas, M.J. Vicent, Polymer-drug conjugates for novel molecular targets, Nanomedicine (Lond) 5 (6) (2010) 915–935.

[34]   M. Barz, R. Luxenhofer, R. Zentel, M.J. Vicent, Overcoming the PEG-addiction: Well-defined alternatives to PEG, from structure–property relationships to better defined therapeutics, Polym. Chem. 2 (9) (2011) 1900.

[35]   F.M. Veronese, PEGylated protein drugs: basic science and clinical applications, Birkhäuser, Basel [u.a.], 2009.

[36]   A. Borchers, T. Pieler, Programming pluripotent precursor cells derived from Xenopus embryos to generate specific tissues and organs, Genes (Basel) 1 (3) (2010) 413–426.

[37]   A. V. Yurkovetskiy, R. J. Fram, XMT-1001, A Novel Biodegradable Polyacetal Polymer Conjugate of Camptothecin in Clinical Development, CBC 7 (1) (2011) 15–20.

[38]   J. Hardwicke, R. Moseley, P. Stephens, K. Harding, R. Duncan, D.W. Thomas, Bioresponsive dextrin-rhEGF conjugates: in vitro evaluation in models relevant to its proposed use as a treatment for chronic wounds, Mol. Pharm. 7 (3) (2010) 699–707.

[39]   A. Perner, N. Haase, J. Wetterslev, A. Aneman, J. Tenhunen, A.B. Guttormsen, G. Klemenzson, F. Pott, K.D. Bødker, P.M. Bådstøløkken, A. Bendtsen, P. Søe-Jensen, H. Tousi, M. Bestle, M. Pawlowicz, R. Winding, H.-H. Bülow, C. Kancir, M. Steensen, J. Nielsen, B. Fogh, K.R. Madsen, N.H. Larsen, M. Carlsson, J. Wiis, J.A. Petersen, S. Iversen, O. Schøidt, S. Leivdal, P. Berezowicz, V. Pettilä, E. Ruokonen, P. Klepstad, S. Karlsson, M. Kaukonen, J. Rutanen, S. Karason, A.L. Kjældgaard, L.B. Holst, J. Wernerman, Comparing the effect of hydroxyethyl starch 130/0.4 with balanced crystalloid solution on mortality and kidney failure in patients with severe sepsis (6S--Scandinavian Starch for Severe Sepsis/Septic Shock trial): study protocol, design and rationale for a double-blinded, randomised clinical trial, Trials 12 (2011) 24.

[40]   W. Zhu, J. Ling, Z. Shen, Synthesis and Characterization of Amphiphilic Star-Shaped Polymers With Calix[6]arene Cores, Macromol. Chem. Phys. 207 (9) (2006) 844–849.

[41]   F. Wang, T.K. Bronich, A.V. Kabanov, R.D. Rauh, J. Roovers, Synthesis and evaluation of a star amphiphilic block copolymer from poly(epsilon-caprolactone) and poly(ethylene glycol) as a potential drug delivery carrier, Bioconjug. Chem. 16 (2) (2005) 397–405.

[42]   F. Wang, T.K. Bronich, A.V. Kabanov, R.D. Rauh, J. Roovers, Synthesis and characterization of star poly(epsilon-caprolactone)-b-poly(ethylene glycol) and poly(L-lactide)-b-poly(ethylene glycol) copolymers: evaluation as drug delivery carriers, Bioconjug. Chem. 19 (7) (2008) 1423–1429.

[43]   M. Jelínková, J. Strohalm, T. Etrych, K. Ulbrich, B. Říhová, Starlike vs. Classic Macromolecular Prodrugs: Two Different Antibody-Targeted HPMA Copolymers of Doxorubicin Studied in Vitro and in Vivo as Potential Anticancer Drugs, Pharm. Res. 20 (10) (2003) 1558–1564.

[44] T. Etrych, J. Strohalm, P. Chytil, P. Černoch, L. Starovoytova, M. Pechar, K. Ulbrich, Biodegradable star HPMA polymer conjugates of doxorubicin for passive tumor targeting, Eur. J. Pharm. Sci. 42 (5) (2011) 527–539.

[45] W. Cao, J. Zhou, Y. Wang, L. Zhu, Synthesis and in vitro cancer cell targeting of folate-functionalized biodegradable amphiphilic dendrimer-like star polymers, Biomacromolecules 11 (12) (2010) 3680–3687.

[46] J. Liu, W. Huang, Y. Pang, X. Zhu, Y. Zhou, D. Yan, Hyperbranched polyphosphates for drug delivery application: design, synthesis, and in vitro evaluation, Biomacromolecules 11 (6) (2010) 1564–1570.

[47] L. Ye, K. Letchford, M. Heller, R. Liggins, D. Guan, J.N. Kizhakkedathu, D.E. Brooks, J.K. Jackson, H.M. Burt, Synthesis and characterization of carboxylic acid conjugated, hydrophobically derivatized, hyperbranched polyglycerols as nanoparticulate drug carriers for cisplatin, Biomacromolecules 12 (1) (2011) 145–155.

[48] S. Lee, K. Saito, H.-R. Lee, M.J. Lee, Y. Shibasaki, Y. Oishi, B.-S. Kim, Hyperbranched double hydrophilic block copolymer micelles of poly(ethylene oxide) and polyglycerol for pH-responsive drug delivery, Biomacromolecules 13 (4) (2012) 1190–1196.

[49] F. Hudecz, J.A. Clegg, J. Kajtar, M.J. Embleton, M. Szekerke, R.W. Baldwin, Synthesis, conformation, biodistribution and in vitro cytotoxicity of daunomycin-branched polypeptide conjugates, Bioconjugate Chem. 3 (1) (2002) 49–57.

[50] T. Etrych, P. Chytil, T. Mrkvan, M. Sírová, B. Ríhová, K. Ulbrich, Conjugates of doxorubicin with graft HPMA copolymers for passive tumor targeting, J. Control. Release 132 (3) (2008) 184–192.

[51] X. Bao, W. Wang, C. Wang, Y. Wang, J. Zhou, Y. Ding, X. Wang, Y. Jin, A chitosan-graft-PEI-candesartan conjugate for targeted co-delivery of drug and gene in anti-angiogenesis cancer therapy, Biomaterials 35 (29) (2014) 8450–8466.

[52] D.A. Tomalia, H.I. Baker, J. Dewald, M. Hall, G. Kallos, S. Martin, J. Roeck, J. Ryder, P. Smith, A New Class of Polymers: Starburst-Dendritic Macromolecules, Polymer journal 17 (1) (1985) 117–132.

[53] G. Newkome, Z. Yao, G. Baker, V. Gupta, Micelles. Part 1. Cascade molecules: a new approach to micelles. A [27]-arborol, J. Org. Chem. 50 (11) (1985) 2003–2004.

[54] M.A. Carnahan, M.W. Grinstaff, Synthesis of Generational Polyester Dendrimers Derived from Glycerol and Succinic or Adipic Acid, Macromolecules 39 (2) (2006)

[55] H. Ihre, A. Hult, E. Söderlind, Synthesis, Characterization, and 1 H NMR Self-Diffusion Studies of Dendritic Aliphatic Polyesters Based on 2,2-Bis(hydroxymethyl)propionic Acid and 1,1,1-Tris(hydroxyphenyl)ethane, J. Am. Chem. Soc. 118 (27) (1996) 6388–6395.

[56] D.A. Tomalia, Birth of a new macromolecular architecture: Dendrimers as quantized building blocks for nanoscale synthetic polymer chemistry, Prog. Polym. Sci. 30 (3-4) (2005) 294–324.

[57]   S. Zhu, M. Hong, L. Zhang, G. Tang, Y. Jiang, Y. Pei, PEGylated PAMAM dendrimer-doxorubicin conjugates: in vitro evaluation and in vivo tumor accumulation, Pharm. Res. 27 (1) (2010) 161–174.

[58]   X. Bi, X. Shi, I.J. Majoros, R. Shukla, J.R. Baker, Multifunctional Poly(amidoamine) Dendrimer-Taxol Conjugates: Synthesis, Characterization and Stability, Jnl of Comp & Theo Nano 4 (6) (2007) 1179–1187.

[59]   S. Gurdag, J. Khandare, S. Stapels, L.H. Matherly, R.M. Kannan, Activity of dendrimer-methotrexate conjugates on methotrexate-sensitive and -resistant cell lines, Bioconjug. Chem. 17 (2) (2006) 275–283.

[60]   D. Wang, S. Miller, M. Sima, P. Kopecková, J. Kopecek, Synthesis and evaluation of water-soluble polymeric bone-targeted drug delivery systems, Bioconjug. Chem. 14 (5) (2003) 853–859.

[61]   D. Wang, S.C. Miller, M. Sima, D. Parker, H. Buswell, K.C. Goodrich, P. Kopecková, J. Kopeček, The Arthrotropism of Macromolecules in Adjuvant-Induced Arthritis Rat Model: A Preliminary Study, Pharm Res 21 (10) (2004) 1741–1749.

[62]   D. Wang, S.C. Miller, L.S. Shlyakhtenko, A.M. Portillo, X.-M. Liu, K. Papangkorn, P. Kopecková, Y. Lyubchenko, W.I. Higuchi, J. Kopecek, Osteotropic Peptide that differentiates functional domains of the skeleton, Bioconjug. Chem. 18 (5) (2007) 1375–1378.

[63]   X.-M. Liu, S.C. Miller, D. Wang, Beyond oncology--application of HPMA copolymers in non-cancerous diseases, Adv. Drug Deliv. Rev. 62 (2) (2010) 258–271.

[64]   F. Yuan, L.-d. Quan, L. Cui, S.R. Goldring, D. Wang, Development of macromolecular prodrug for rheumatoid arthritis, Adv. Drug Deliv. Rev. 64 (12) (2012) 1205–1219.

[65]   A. Nan, N.P.D. Nanayakkara, L.A. Walker, V. Yardley, S.L. Croft, H. Ghandehari, N-(2-hydroxypropyl)methacrylamide (HPMA) copolymers for targeted delivery of 8-aminoquinoline antileishmanial drugs, J. Control. Release 77 (3) (2001) 233–243.

[66]   A. Nan, S.L. Croft, V. Yardley, H. Ghandehari, Targetable water-soluble polymer-drug conjugates for the treatment of visceral leishmaniasis, J. Control. Release 94 (1) (2004) 115–127.

[67]   B.J. Kline, E.J. Beckman, A.J. Russell, One-Step Biocatalytic Synthesis of Linear Polyesters with Pendant Hydroxyl Groups, J. Am. Chem. Soc. 120 (37) (1998) 9475–9480.

[68]   J. Uppenberg, M.T. Hansen, S. Patkar, T.A. Jones, The sequence, crystal structure determination and refinement of two crystal forms of lipase B from Candida antarctica, Structure 2 (4) (1994) 293–308.

[69]   S. Kobayashi, Lipase-catalyzed polyester synthesis – A green polymer chemistry, Proc. Jpn. Acad., Ser. B 86 (4) (2010) 338–365.

[70]   V. Taresco, R.G. Creasey, J. Kennon, G. Mantovani, C. Alexander, J.C. Burley, M.C. Garnett, Variation in structure and properties of poly(glycerol adipate) via control of chain branching during enzymatic synthesis, Polymer 89 (2016) 41–49.

[71]   H. Frey, R. Haag, Dendritic polyglycerol: A new versatile biocompatible material, Reviews in Molecular Biotechnology 90 (3-4) (2002) 257–267.

[72]   P. Kallinteri, S. Higgins, G.A. Hutcheon, St Pourçain, Christopher B, M.C. Garnett, Novel functionalized biodegradable polymers for nanoparticle drug delivery systems, Biomacromolecules 6 (4) (2005) 1885–1894.

[73]   S. Puri, P. Kallinteri, S. Higgins, G.A. Hutcheon, M.C. Garnett, Drug incorporation and release of water soluble drugs from novel functionalized poly(glycerol adipate) nanoparticles, J. Control. Release 125 (1) (2008) 59–67.

[74]   C. Korupp, R. Weberskirch, J.J. Müller, A. Liese, L. Hilterhaus, Scaleup of Lipase-Catalyzed Polyester Synthesis, Org. Process Res. Dev. 14 (5) (2010) 1118–1124.

[75]   H. Orafai, P. Kallinteri, M.C. Garnett, Huggins, S., Hutcheon, G., C. Pourcain, Novel Poly (glycerol-adipate) Polymers Used for Nanoparticle Making: A Study of Surface Free Energy, Iran. J. Pharm. Res. 7 (1) (2008) 11–19.

[76]   V.M. Weiss, T. Naolou, G. Hause, J. Kuntsche, J. Kressler, K. Mäder, Poly(glycerol adipate)-fatty acid esters as versatile nanocarriers: From nanocubes over ellipsoids to nanospheres, J. Control. Release 158 (1) (2012) 156–164.

[77]   V.M. Weiss, T. Naolou, E. Amado, K. Busse, K. Mäder, J. Kressler, Formation of structured polygonal nanoparticles by phase-separated comb-like polymers, Macromol. Rapid Commun. 33 (1) (2012) 35–40.

[78]   V.M. Weiss, T. Naolou, T. Groth, J. Kressler, K. Mäder, In vitro toxicity of Stearoyl-poly(glycerol adipate) nanoparticles, J. Appl. Biomater. Funct. Mater. 10 (3) (2012) 163–169.

[79]   A. Wahab, M.E. Favretto, N.D. Onyeagor, G.M. Khan, D. Douroumis, M.A. Casely-Hayford, P. Kallinteri, Development of poly(glycerol adipate) nanoparticles loaded with non-steroidal anti-inflammatory drugs, J. Microencapsul. 29 (5) (2012) 497–504.

[80]   D. Pfefferkorn, M. Pulst, T. Naolou, K. Busse, J. Balko, J. Kressler, Crystallization and melting of poly(glycerol adipate)-based graft copolymers with single and double crystallizable side chains, J. Polym. Sci. Part B: Polym. Phys. 74 (2013)

[81]   T. Naolou, K. Busse, B.-D. Lechner, J. Kressler, The behavior of poly(ε-caprolactone) and poly(ethylene oxide)-b-poly(ε-caprolactone) grafted to a poly(glycerol adipate) backbone at the air/water interface, Colloid Polym Sci 292 (5) (2014) 1199–1208.

[82]   V.M. Weiss, H. Lucas, T. Mueller, P. Chytil, T. Etrych, T. Naolou, J. Kressler, K. Mäder, Intended and Unintended Targeting of Polymeric Nanocarriers: The Case of Modified Poly(glycerol adipate) Nanoparticles, Macromol. Biosci. 18 (1) (2018).

[83]   A. Schädlich, S. Hoffmann, T. Mueller, H. Caysa, C. Rose, A. Göpferich, J. Li, J. Kuntsche, K. Mäder, Accumulation of nanocarriers in the ovary: a neglected toxicity risk? J. Control. Release 160 (1) (2012) 105–112.

[84]   K. Mäder, V.M. Weiss, J. Kressler, T. Naolou (Martin-Luther-Universität Halle-Wittenberg) US2017/0151334A1, 2017.

[85]   L. Xu, S. Liu, M. Guan, Y. Xue, Comparison of Prednisolone, Etoricoxib, and Indomethacin in Treatment of Acute Gouty Arthritis: An Open-Label, Randomized, Controlled Trial, Med Sci Monit 22 (2016) 810–817.

[86]   W.E. Benitz, Treatment of persistent patent ductus arteriosus in preterm infants: time to accept the null hypothesis? J. Perinatol. 30 (4) (2010) 241–252.

[87]   M. Hollingworth, T.M. Young, Melatonin responsive hemicrania continua in which indomethacin was associated with contralateral headache, Headache 54 (5) (2014) 916–919.

[88]   M. Imazio, R. Belli, A. Brucato, R. Cemin, S. Ferrua, F. Beqaraj, D. Demarie, S. Ferro, D. Forno, S. Maestroni, D. Cumetti, F. Varbella, R. Trinchero, D.H. Spodick, Y. Adler, Efficacy and safety of colchicine for treatment of multiple recurrences of pericarditis (CORP-2): A multicentre, double-blind, placebo-controlled, randomised trial, The Lancet 383 (9936) (2014) 2232–2237.

[89]   J. Marjoribanks, M. Proctor, C. Farquhar, R.S. Derks, Nonsteroidal anti-inflammatory drugs for dysmenorrhoea, Cochrane Database Syst. Rev. (1) (2010) CD001751.

[90]   P. Quartier, Current treatments for juvenile idiopathic arthritis, Joint Bone Spine 77 (6) (2010) 511–516.

[91]   N. Butoescu, O. Jordan, E. Doelker, Intra-articular drug delivery systems for the treatment of rheumatic diseases: a review of the factors influencing their performance, Eur. J. Pharm. Biopharm. 73 (2) (2009) 205–218.

[92]   N. Nagai, C. Yoshioka, Y. Ito, Topical therapies for rheumatoid arthritis by gel ointments containing indomethacin nanoparticles in adjuvant-induced arthritis rat, J. Oleo Sci. 64 (3) (2015) 337–346.

[93]   M. Weber, L. Kodjikian, F.E. Kruse, Z. Zagorski, C.M. Allaire, Efficacy and safety of indomethacin 0.1% eye drops compared with ketorolac 0.5% eye drops in the management of ocular inflammation after cataract surgery, Acta Ophthalmol. 91 (1) (2013) e15-21.

[94]   N. Nagai, Y. Ito, N. Okamoto, Y. Shimomura, A nanoparticle formulation reduces the corneal toxicity of indomethacin eye drops and enhances its corneal permeability, Toxicology 319 (2014) 53–62.

[95]   S.F. Rodrigues, L.A. Fiel, A.L. Shimada, N.R. Pereira, S.S. Guterres, A.R. Pohlmann, S.H. Farsky, Lipid-Core Nanocapsules Act as a Drug Shuttle Through the Blood Brain Barrier and Reduce Glioblastoma After Intravenous or Oral Administration, J. Biomed. Nanotechnol. 12 (5) (2016) 986–1000.

[96]   A. Bernardi, E. Braganhol, E. Jäger, F. Figueiró, M.I. Edelweiss, A.R. Pohlmann, S.S. Guterres, A.M.O. Battastini, Indomethacin-loaded nanocapsules treatment reduces in vivo glioblastoma growth in a rat glioma model, Cancer Lett. 281 (1) (2009) 53–63.

[97]   M. O'Brien, J. McCauley, E. Cohen, Indomethacin, in: Klaus Florey (Ed.), Analytical Profile of Drug Substances: Indomethacin, Elsevier, 1984, pp. 211–238.

[98]   A. Nokhodchi, Y. Javadzadeh, M.R. Siahi-Shadbad, M. Barzegar-Jalali, The effect of type and concentration of vehicles on the dissolution rate of a poorly soluble drug (indomethacin) from liquisolid compacts, J. Pharm. Pharm. Sci. 8 (1) (2005) 18–25.

[99]   H. Yamamoto, M. Nakao, A. Kobayashi, 1-Acylindoles. IV. Novel Syntheses of 1-Benzoylindole-3-aliphatic Acids, Chem. Pharm. Bull. 16 (4) (1968) 647–653.

[100] M. de Geus, van der Meulen, Inge, B. Goderis, K. van Hecke, M. Dorschu, van der Werff, Harm, C.E. Koning, A. Heise, Performance polymers from renewable monomers: high molecular weight poly(pentadecalactone) for fiber applications, Polym. Chem. 1 (4) (2010) 525.

[101] B. Neises, W. Steglich, Simple Method for the Esterification of Carboxylic Acids, Angew. Chem. Int. Ed. Engl. 17 (7) (1978) 522–524.

[102] M. Bilal, M. Prehm, A. Njau, M. Samiullah, A. Meister, J. Kressler, Enzymatic Synthesis and Characterization of Hydrophilic Sugar Based Polyesters and Their Modification with Stearic Acid, Polymers 8 (3) (2016) 80.

[103] H. Fessi, F. Puisieux, J.P. Devissaguet, N. Ammoury, S. Benita, Nanocapsule formation by interfacial polymer deposition following solvent displacement, International Journal of Pharmaceutics 55 (1) (1989) R1-R4.

[104] M.C. Garnett, P. Kallinteri, Nanomedicines and nanotoxicology: some physiological principles, Occup. Med. (Lond) 56 (5) (2006) 307–311.

[105] P. Hole, K. Sillence, C. Hannell, C.M. Maguire, M. Roesslein, G. Suarez, S. Capracotta, Z. Magdolenova, L. Horev-Azaria, A. Dybowska, L. Cooke, A. Haase, S. Contal, S. Mano, A. Vennemann, J.-J. Sauvain, K.C. Staunton, S. Anguissola, A. Luch, M. Dusinska, R. Korenstein, A.C. Gutleb, M. Wiemann, A. Prina-Mello, M. Riediker, P. Wick, Interlaboratory comparison of size measurements on nanoparticles using nanoparticle tracking analysis (NTA), J. Nanopart. Res. 15 (2013) 2101.

[106] V. Filipe, A. Hawe, W. Jiskoot, Critical evaluation of Nanoparticle Tracking Analysis (NTA) by NanoSight for the measurement of nanoparticles and protein aggregates, Pharm. Res. 27 (5) (2010) 796–810.

[107] J. Lyklema, Electrokinetics after Smoluchowski, Colloids and Surfaces A: Physicochemical and Engineering Aspects 222 (1-3) (2003) 5–14.

[108] M. Bauer, C. Lautenschlaeger, K. Kempe, L. Tauhardt, U.S. Schubert, D. Fischer, Poly(2-ethyl-2-oxazoline) as alternative for the stealth polymer poly(ethylene glycol): comparison of in vitro cytotoxicity and hemocompatibility, Macromol. Biosci. 12 (7) (2012) 986–998.

[109]   L.R. Beck, D.R. Cowsar, D.H. Lewis, R.J. Cosgrove, C.T. Riddle, S.L. Lowry, T. Epperly, A New Long-Acting Injectable Microcapsule System for the Administration of Progesterone*, Fertil. Steril. 31 (5) (1979) 545–551.

[110]   Q. Fu, W. Sun, Mie theory for light scattering by a spherical particle in an absorbing medium, Appl. Opt. 40 (9) (2001) 1354.

[111]   P. DeLuca, L. Lachman, Lyophilization of Pharmaceuticals I, J. Pharm. Sci. 54 (4) (1965) 617–624.

[112]   R.A. Gross, A. Kumar, B. Kalra, Polymer Synthesis by In Vitro Enzyme Catalysis, Chem. Rev. 101 (7) (2001) 2097–2124.

[113]   S. Kobayashi, Enzymatic polymerization: A new method of polymer synthesis, J. Polym. Sci. A Polym. Chem. 37 (16) (1999) 3041–3056.

[114]   S. Kobayashi (Ed.), New Frontiers in Polymer Synthesis, Springer Berlin Heidelberg, Berlin, Heidelberg, 2008.

[115]   S. Kobayashi, A. Makino, Enzymatic polymer synthesis: an opportunity for green polymer chemistry, Chem. Rev. 109 (11) (2009) 5288–5353.

[116]   S. Kobayashi, H. Ritter, D. Kaplan (Eds.), Enzyme-Catalyzed Synthesis of Polymers, Springer-Verlag, Berlin/Heidelberg, 2006.

[117]   S. Kobayashi, H. Uyama, S. Kimura, Enzymatic Polymerization, Chem. Rev. 101 (12) (2001) 3793–3818.

[118]   S. Kobayashi, H. Uyama, M. Ohmae, Enzymatic Polymerization for Precision Polymer Synthesis, BCSJ 74 (4) (2001) 613–635.

[119]   F. Binns, P. Harffey, S.M. Roberts, A. Taylor, Studies leading to the large scale synthesis of polyesters using enzymes, J. Chem. Soc., Perkin Trans. 1 (19) (1999) 2671–2676.

[120]   Z. Wang, Comprehensive organic name reactions and reagents, John Wiley & Sons, Hoboken, op. 2009.

[121]   D.S. Wishart, B.D. Sykes, F.M. Richards, The chemical shift index: a fast and simple method for the assignment of protein secondary structure through NMR spectroscopy, Biochemistry 31 (6) (1992) 1647–1651.

[122]   G. Rücker, M. Neugebauer, G.G. Willems, Instrumentelle Analytik für Pharmazeuten: Lehrbuch zu spektroskopischen, chromatografischen, elektrochemischen und thermischen Analysenmethoden, 4th ed., Wissenschaftliche Verlagsgesellschaft, Stuttgart, 2008.

[123]   C. Scholz, J. Kressler (Eds.), Tailored Polymer Architectures for Pharmaceutical and Biomedical Applications, J. Am. Chem. Soc., Washington, DC, 2013.

[124]   V.T. Wyatt, G.D. Strahan, Degree of Branching in Hyperbranched Poly(glycerol-co-diacid)s Synthesized in Toluene, Polymers 4 (4) (2012) 396–407.

[125]   L.S. Taylor, G. Zografi, Spectroscopic Characterization of Interactions Between PVP and Indomethacin in Amorphous Molecular Dispersions, Pharm. Res. 14 (12) (1997) 1691–1698.

[126] H.G. Brittain, Spectral methods for the characterization of polymorphs and solvates, J. Pharm. Sci. 86 (4) (1997) 405–412.

[127] P.N. Prasad, J. Swiatkiewicz, G. Eisenhardt, Laser Raman Investigation of Solid State Reactions, Appl. Spectrosc. Rev. 18 (1) (2006) 59–103.

[128] L. Borka, The polymorphism of indomethacine. New modifications, their melting behavior and solubility, Acta Pharm. Suec. 11 (3) (1974) 295–303.

[129] H. Yamamoto, 1-Acyl-indoles. II. A New Syntheses of 1-(p-chlorobenzoyl)-5-methoxy-3-indolylacetic Acid and Its Polymorphism, Chem. Pharm. Bull. 16 (1) (1968) 17–19.

[130] J.C. Moore, Gel permeation chromatography. I. A new method for molecular weight distribution of high polymers, J. Polym. Sci. A Gen. Pap. 2 (2) (1964) 835–843.

[131] M. Gaborieau, P. Castignolles, Size-exclusion chromatography (SEC) of branched polymers and polysaccharides, Anal. Bioanal. Chem. 399 (4) (2011) 1413–1423.

[132] P. Gabbott, Principles and applications of thermal analysis, Blackwell Pub, Oxford, Ames, Iowa, 2008.

[133] J.A. Baird, B. van Eerdenbrugh, L.S. Taylor, A classification system to assess the crystallization tendency of organic molecules from undercooled melts, J. Pharm. Sci. 99 (9) (2010) 3787–3806.

[134] Y. Sun, J. Tao, G.G.Z. Zhang, L. Yu, Solubilities of crystalline drugs in polymers: an improved analytical method and comparison of solubilities of indomethacin and nifedipine in PVP, PVP/VA, and PVAc, J. Pharm. Sci.c 99 (9) (2010) 4023–4031.

[135] N.S. Trasi, S.R. Byrn, Mechanically induced amorphization of drugs: a study of the thermal behavior of cryomilled compounds, AAPS PharmSciTech 13 (3) (2012) 772–784.

[136] M. Otsuka, F. Kato, Y. Matsuda, Determination of indomethacin polymorphic contents by chemometric near-infrared spectroscopy and conventional powder X-ray diffractometry, Analyst 126 (9) (2001) 1578–1582.

[137] M.d.M. Brioude, D.H. Guimarães, R.d.P. Fiúza, Prado, Luis Antônio Sanches de Almeida, J.S. Boaventura, N.M. José, Synthesis and characterization of aliphatic polyesters from glycerol, by-product of biodiesel production, and adipic acid, Mat. Res. 10 (4) (2007) 335–339.

[138] J. Aho, J.P. Boetker, S. Baldursdottir, J. Rantanen, Rheology as a tool for evaluation of melt processability of innovative dosage forms, Int. J. Pharm. 494 (2) (2015) 623–642.

[139] J.D. Ferry, Viscoelastic properties of polymers, 3rd ed., Wiley, New York, 1980.

[140] A. Haddout, G. Villoutreix, Polymer Melt Rheology at High Shear Rates, IPP 15 (3) (2000) 291–296.

[141] H. Takahashi, T. Matsuoka, T. Kurauchi, Rheology of polymer melts in high shear rate, J. Appl. Polym. Sci. 30 (12) (1985) 4669–4684.

[142] T. Naolou, H. Hussain, S. Baleed, K. Busse, B.-D. Lechner, J. Kressler, The behavior of fatty acid modified poly(glycerol adipate) at the air/water interface, Colloids Surf. A 468 (2015) 22–30.

[143]   M.Y. Levy, S. Benita, Drug release from submicronized o/w emulsion: A new in vitro kinetic evaluation model, Int. J. Pharm. 66 (1-3) (1990) 29–37.

[144]   C. Washington, Drug release from microdisperse systems: A critical review, Int. J. Pharm. 58 (1) (1990) 1–12.

[145]   G.L. Amidon, H. Lennernäs, V.P. Shah, J.R. Crison, A Theoretical Basis for a Biopharmaceutic Drug Classification: The Correlation of in Vitro Drug Product Dissolution and in Vivo Bioavailability, Pharm. Res. 12 (3) (1995) 413–420.

[146]   C.J. Thompson, D. Hansford, D.L. Munday, S. Higgins, C. Rostron, G.A. Hutcheon, Synthesis and evaluation of novel polyester-ibuprofen conjugates for modified drug release, Drug Dev. Ind. Pharm. 34 (8) (2008) 877–884.

[147]   A. Göpferich, Mechanisms of polymer degradation and erosion, Biomaterials 17 (2) (1996) 103–114.

[148]   X. Qian, Q. Wu, F. Xu, X. Lin, Lipase-catalyzed synthesis of polymeric prodrugs of nonsteroidal anti-inflammatory drugs, J. Appl. Polym. Sci. 128 (5) (2013) 3271–3279.

[149]   Sykes P., Guidebook to Mechanism in Organic Chemistry (4th edn), London Group Ltd., London, 1975.

[150]   R.J. Coakley, C. Taggart, N.G. McElvaney, S.J. O'Neill, Cytosolic pH and the inflammatory microenvironment modulate cell death in human neutrophils after phagocytosis, Blood 100 (9) (2002) 3383–3391.

[151]   E. Marten, R.-J. Müller, W.-D. Deckwer, Studies on the enzymatic hydrolysis of polyesters I. Low molecular mass model esters and aliphatic polyesters, Polym. Degrad. Stab. 80 (3) (2003) 485–501.

[152]   M.F. Ottaviani, G. Martini, L. Nuti, Nitrogen hyperfine splitting of nitroxide solutions: Differently structured and charged nitroxides as probes of environmental properties, Magn. Reson. Chem. 25 (10) (1987) 897–904.

[153]   A.D. Keith, W. Snipes, R.J. Mehlhorn, T. Gunter, Factors restricting diffusion of water-soluble spin labels, Biophys. J. 19 (3) (1977) 205–218.

[154]   N. Faisant, J. Akiki, F. Siepmann, J.P. Benoit, J. Siepmann, Effects of the type of release medium on drug release from PLGA-based microparticles: experiment and theory, Int. J. Pharm. 314 (2) (2006) 189–197.

[155]   J. Siepmann, N. Faisant, J. Akiki, J. Richard, J.P. Benoit, Effect of the size of biodegradable microparticles on drug release: experiment and theory, J. Control. Release 96 (1) (2004) 123–134.

[156]   D. Klose, F. Siepmann, K. Elkharraz, J. Siepmann, PLGA-based drug delivery systems: importance of the type of drug and device geometry, Int. J. Pharm. 354 (1-2) (2008) 95–103.

[157]   X. Zhang, U.P. Wyss, D. Pichora, M.F.A. Goosen, A. Gonzal, C.L. Marte, Controlled release of testosterone and estradiol-17 β from biodegradable cylinders, J. Control. Release 29 (1-2) (1994) 157–161.

[158]   Y. Barenholz, Doxil®--the first FDA-approved nano-drug: lessons learned, J. Control. Release 160 (2) (2012) 117–134.

[159]   J. Oh, Conjugation of drug to poly(?:?-lactic-co-glycolic acid) for controlled release from biodegradable microspheres, J. Control. Release 57 (3) (1999) 269–280.

[160]   M.G. Rimoli, L. Avallone, P. de Caprariis, A. Galeone, F. Forni, M.A. Vandelli, Synthesis and characterisation of poly(d,l-lactic acid)–idoxuridine conjugate, J. Control. Release 58 (1) (1999) 61–68.

[161]   R. Rosario-Meléndez, W. Yu, K.E. Uhrich, Biodegradable polyesters containing ibuprofen and naproxen as pendant groups, Biomacromol. 14 (10) (2013) 3542–3548.

[162]   J. Griffin, R. Delgado-Rivera, S. Meiners, K.E. Uhrich, Salicylic acid-derived poly(anhydride-ester) electrospun fibers designed for regenerating the peripheral nervous system, J. Biomed. Mater. Res. A 97 (3) (2011) 230–242.

[163]   V. Taresco, J. Suksiriworapong, R. Creasey, J.C. Burley, G. Mantovani, C. Alexander, K. Treacher, J. Booth, M.C. Garnett, Properties of acyl modified poly(glycerol-adipate) comb-like polymers and their self-assembly into nanoparticles, J. Polym. Sci. Part A: Polym. Chem. (54) (2016) 3267–3278.

[164]   V. Taresco, J. Suksiriworapong, I.D. Styliari, R.H. Argent, S.M.E. Swainson, J. Booth, E. Turpin, C.A. Laughton, J.C. Burley, C. Alexander, M.C. Garnett, New N-acyl amino acid-functionalized biodegradable polyesters for pharmaceutical and biomedical applications, RSC Adv. 6 (111) (2016) 109401–109405.

[165]   J. Suksiriworapong, V. Taresco, D.P. Ivanov, I.D. Styliari, K. Sakchaisri, V.B. Junyaprasert, M.C. Garnett, Synthesis and properties of a biodegradable polymer-drug conjugate: Methotrexate-poly(glycerol adipate), Colloids Surf. B Biointerfaces 167 (2018) 115–125.

[166]   T. Wersig, M.C. Hacker, J. Kressler, K. Mäder, Poly(glycerol adipate) - indomethacin drug conjugates - synthesis and in vitro characterization, Int. J. Pharm. 531 (1) (2017) 225–234.

[167]   M.J. Uddin, B.C. Crews, S. Xu, K. Ghebreselasie, C.K. Daniel, P.J. Kingsley, S. Banerjee, L.J. Marnett, Antitumor Activity of Cytotoxic Cyclooxygenase-2 Inhibitors, ACS Chem. Biol. 11 (11) (2016) 3052–3060.

[168]   J.T. DiPiro, Pharmacotherapy: A pathophysiologic approach, 8th ed., McGraw-Hill Medical, New York, 2011.

[169]   M. Durymanov, T. Kamaletdinova, S.E. Lehmann, J. Reineke, Exploiting passive nanomedicine accumulation at sites of enhanced vascular permeability for non-cancerous applications, J. Control. Release 261 (2017) 10–22.

[170]   D.J. Lundy, K.-H. Chen, E.K.-W. Toh, P.C.-H. Hsieh, Distribution of Systemically Administered Nanoparticles Reveals a Size-Dependent Effect Immediately following Cardiac Ischaemia-Reperfusion Injury, Sci. Rep. 6 (2016) 25613.

[171]   A. Watanabe, H. Tanaka, Y. Sakurai, K. Tange, Y. Nakai, T. Ohkawara, H. Takeda, H. Harashima, H. Akita, Effect of particle size on their accumulation in an inflammatory lesion in a dextran sulfate sodium (DSS)-induced colitis model, Int. J. Pharm. 509 (1-2) (2016) 118–122.

[172]   N. Yamakawa, S. Suemasu, A. Kimoto, Y. Arai, T. Ishihara, K. Yokomizo, Y. Okamoto, M. Otsuka, K.-i. Tanaka, T. Mizushima, Low Direct Cytotoxicity of Loxoprofen on Gastric Mucosal Cells, Biol. Pharm. Bull. 33 (3) (2010) 398–403.

[173]   A. Mante, M. Heider, C. Zlomke, K. Mäder, PLGA nanoparticles for peroral delivery: How important is pancreatic digestion and can we control it? Eur. J. Pharm. Biopharm. 108 (2016) 32–40.

[174]   A. Bonaccorso, T. Musumeci, C. Carbone, L. Vicari, M.R. Lauro, G. Puglisi, Revisiting the role of sucrose in PLGA-PEG nanocarrier for potential intranasal delivery, Pharm. Dev. Technol. 23 (3) (2018) 265–274.

[175]   W. Abdelwahed, G. Degobert, S. Stainmesse, H. Fessi, Freeze-drying of nanoparticles: Formulation, process and storage considerations, Adv. Drug Deliv. Rev. 58 (15) (2006) 1688–1713.

[176]   K. Makino, H. Ohshima, T. Kondo, Transfer of protons from bulk solution to the surface of poly(L-lactide) microcapsules, J. Microencapsul. 3 (3) (1986) 195–202.

[177]   M. Zambaux, Influence of experimental parameters on the characteristics of poly(lactic acid) nanoparticles prepared by a double emulsion method, J. Control. Release 50 (1-3) (1998) 31–40.

[178]   S.K. Sahoo, J. Panyam, S. Prabha, V. Labhasetwar, Residual polyvinyl alcohol associated with poly (d,l-lactide-co-glycolide) nanoparticles affects their physical properties and cellular uptake, J. Control. Release 82 (1) (2002) 105–114.

[179]   F. Boury, T. Ivanova, I. Panaïotov, J.E. Proust, A. Bois, J. Richou, Dynamic Properties of Poly(DL-lactide) and Polyvinyl Alcohol Monolayers at the Air/Water and Dichloromethane/Water Interfaces, J. Colloid Interface Sci. 169 (2) (1995) 380–392.

[180]   S. de Carlo, J.R. Harris, Negative staining and cryo-negative staining of macromolecules and viruses for TEM, Micron 42 (2) (2011) 117–131.

[181]   M. Ohi, Y. Li, Y. Cheng, T. Walz, Negative Staining and Image Classification - Powerful Tools in Modern Electron Microscopy, Biol. Proced. Online 6 (2004) 23–34.

[182]   A. Meister, A. Blume, (Cryo)Transmission Electron Microscopy of Phospholipid Model Membranes Interacting with Amphiphilic and Polyphilic Molecules, Polymers 9 (10) (2017) 521.

[183]   E.V. Orlova, H.R. Saibil, Structural analysis of macromolecular assemblies by electron microscopy, Chem. Rev. 111 (12) (2011) 7710–7748.

[184]   J. Robin Harris, R.W. Horne, Negative staining: A brief assessment of current technical benefits, limitations and future possibilities, Micron 25 (1) (1994) 5–13.

[185]   P. Decuzzi, R. Pasqualini, W. Arap, M. Ferrari, Intravascular delivery of particulate systems: does geometry really matter? Pharm. Res. 26 (1) (2009) 235–243.

[186]   ASTM F756, "Standrad Practicle for Assessment of Hemolytic Properties of Materials", Annual Book of ASTM Standards 2000 (Vol. 13. 01) (Philadelphia 2008).

[187]   R. Hamid, Y. Rotshteyn, L. Rabadi, R. Parikh, P. Bullock, Comparison of alamar blue and MTT assays for high through-put screening, Toxicol. In Vitro 18 (5) (2004) 703–710.

[188]   A. Bernardi, R.L. Frozza, E. Jäger, F. Figueiró, L. Bavaresco, C. Salbego, A.R. Pohlmann, S.S. Guterres, A.M.O. Battastini, Selective cytotoxicity of indomethacin and indomethacin ethyl ester-loaded nanocapsules against glioma cell lines: an in vitro study, Eur. J. Pharmacol. 586 (1-3) (2008) 24–34.

[189]   K.L. Klein, W.J. Scott, K.E. Clark, J.G. Wilson, Indomethacin—Placental transfer, cytotoxicity, and teratology in the rat, Am. J. Obstet. Gynecol. 141 (4) (1981) 448–452.

[190]   B. Magenheim, M.Y. Levy, S. Benita, A new in vitro technique for the evaluation of drug release profile from colloidal carriers - ultrafiltration technique at low pressure, Int. J. Pharm. 94 (1-3) (1993) 115–123.

[191]   K.M. Rosenblatt, D. Douroumis, H. Bunjes, Drug release from differently structured monoolein/poloxamer nanodispersions studied with differential pulse polarography and ultrafiltration at low pressure, J. Pharm. Sci. 96 (6) (2007) 1564–1575.

[192]   D.L. Teagarden, B.D. Anderson, W.J. Petre, Determination of the pH-Dependent Phase Distribution of Prostglandin E1 in a Lipid Emulsion by Ultrafiltration, Pharm. Res. 05 (8) (1988) 482–487.

[193]   M. Riehl, M. Harms, H. Lucas, T. Ebensen, C.A. Guzmán, K. Mäder, Dual dye in-vivo imaging of differentially charged PLGA carriers reveals antigen-depot effect, leading to improved immune responses in preclinical models, Eur. J. Pharm. Sci. 117 (2018) 88–97.

[194]   J. Kreuter, U. Täuber, V. Illi, Distribution and Elimination of Poly(methyl-2-14C-methacrylate) Nanoparticle Radioactivity after Injection in Rats and Mice, J. Pharm. Sci. 68 (11) (1979) 1443–1447.

[195]   D. Leu, B. Manthey, J. Kreuter, P. Speiser, P.P. Delucax, Distribution and Elimination of Coated Polymethyl [2-14C]Methacrylate Nanoparticles After Intravenous Injection in Rats, J. Pharm. Sci. 73 (10) (1984) 1433–1437.

[196]   S.D. Tröster, J. Kreuter, Influence of the surface properties of low contact angle surfactants on the body distribution of 14C-poly(methyl methacrylate) nanoparticles, J. Microencapsul. 9 (1) (1992) 19–28.

[197]   S. Hoffmann, L. Vystrčilová, K. Ulbrich, T. Etrych, H. Caysa, T. Mueller, K. Mäder, Dual fluorescent HPMA copolymers for passive tumor targeting with pH-sensitive drug release: Synthesis and characterization of distribution and tumor accumulation in mice by noninvasive multispectral optical imaging, Biomacromolecules 13 (3) (2012) 652–663.

[198]   L. Grislain, P. Couvreur, V. Lenaerts, M. Roland, D. Deprez-Decampeneere and P. Speiser, Pharmacokinetics and distribution of a biodegradable drug carrier, Int. J. Pharm. 1983 (15) (1983) 335–345.

[199]   G. Thurston, J.W. McLean, M. Rizen, P. Baluk, A. Haskell, T.J. Murphy, D. Hanahan, D.M. McDonald, Cationic liposomes target angiogenic endothelial cells in tumors and chronic inflammation in mice, J. Clin. Invest. 101 (7) (1998) 1401–1413.

[200]   A.-C. Faure, S. Dufort, V. Josserand, P. Perriat, J.-L. Coll, S. Roux, O. Tillement, Control of the in vivo biodistribution of hybrid nanoparticles with different poly(ethylene glycol) coatings, Small 5 (22) (2009) 2565–2575.

[201]   M. Goutayer, S. Dufort, V. Josserand, A. Royère, E. Heinrich, F. Vinet, J. Bibette, J.-L. Coll, I. Texier, Tumor targeting of functionalized lipid nanoparticles: Assessment by in vivo fluorescence imaging, Eur. J. Pharm. Biopharm. 75 (2) (2010) 137–147.

[202]   V. Simon, C. Devaux, A. Darmon, T. Donnet, E. Thiénot, M. Germain, J. Honnorat, A. Duval, A. Pottier, E. Borghi, L. Levy, J. Marill, Pp IX silica nanoparticles demonstrate differential interactions with in vitro tumor cell lines and in vivo mouse models of human cancers, Photochem. Photobiol. 86 (1) (2010) 213–222.

[203]   T. Lammers, R. Kühnlein, M. Kissel, V. Subr, T. Etrych, R. Pola, M. Pechar, K. Ulbrich, G. Storm, P. Huber, P. Peschke, Effect of physicochemical modification on the biodistribution and tumor accumulation of HPMA copolymers, J. Control. Release 110 (1) (2005) 103–118.

[204]   T. Lammers, V. Subr, K. Ulbrich, P. Peschke, P.E. Huber, W.E. Hennink, G. Storm, Simultaneous delivery of doxorubicin and gemcitabine to tumors in vivo using prototypic polymeric drug carriers, Biomaterials 30 (20) (2009) 3466–3475.

[205]   T. Lammers, V. Subr, K. Ulbrich, W.E. Hennink, G. Storm, F. Kiessling, Polymeric nanomedicines for image-guided drug delivery and tumor-targeted combination therapy, Nano Today 5 (3) (2010) 197–212.

[206]   M.P. Borgman, T. Coleman, R.B. Kolhatkar, S. Geyser-Stoops, B.R. Line, H. Ghandehari, Tumor-targeted HPMA copolymer-(RGDfK)-(CHX-A''-DTPA) conjugates show increased kidney accumulation, J. Control. Release 132 (3) (2008) 193–199.

[207]   A. Mitra, A. Nan, H. Ghandehari, E. McNeil, J. Mulholland, B.R. Line, Technetium-99m-Labeled N-(2-Hydroxypropyl) Methacrylamide Copolymers: Synthesis, Characterization, and in Vivo Biodistribution, Pharm Res 21 (7) (2004) 1153–1159.

[208]   E.M. Gipps, R. Arshady, J. Kreuter, P. Groscurth, P.P. Speiser, Distribution of Polyhexyl Cyanoacrylate Nanoparticles in Nude Mice Bearing Human Osteosarcoma, J. Pharm. Sci. 75 (3) (1986) 256–258.

[209]   M.J. Vicent, L. Cascales, R.J. Carbajo, N. Cortés, A. Messeguer, E. Pérez Payá, Nanoconjugates as intracorporeal neutralizers of bacterial endotoxins, J. Control. Release 142 (2) (2010) 277–285.

[210] B. Santamaría, A. Benito-Martin, A.C. Ucero, L.S. Aroeira, A. Reyero, M.J. Vicent, M. Orzáez, A. Celdrán, J. Esteban, R. Selgas, M. Ruíz-Ortega, M.L. Cabrera, J. Egido, E. Pérez-Payá, A. Ortiz, A nanoconjugate Apaf-1 inhibitor protects mesothelial cells from cytokine-induced injury, PLoS ONE 4 (8) (2009) e6634.

[211] X.-M. Liu, L.-d. Quan, J. Tian, F.C. Laquer, P. Ciborowski, D. Wang, Syntheses of click PEG-dexamethasone conjugates for the treatment of rheumatoid arthritis, Biomacromolecules 11 (10) (2010) 2621–2628.

[212] J. Kuntsche, K. Klaus, F. Steiniger, Size Determinations of Colloidal Fat Emulsions: A Comparative Study, j biomed nanotechnol 5 (4) (2009) 384–395.

[213] F.M. Etzler, R. Deanne, Particle size analysis: A comparison of various methods ii, Part. Part. Syst. Charact. 14 (6) (1997) 278–282.

[214] N.E. Ceschan, V. Bucalá, M.V. Ramírez-Rigo, Polymeric microparticles containing indomethacin for inhalatory administration, Powder Technology 285 (2015) 51–61.

[215] H.V. Maulding, T.R. Tice, D.R. Cowsar, J.W. Fong, J.E. Pearson, J.P. Nazareno, Biodegradable microcapsules: Acceleration of polymeric excipient hydrolytic rate by incorporation of a basic medicament, Journal of Controlled Release 3 (1-4) (1986) 103–117.

[216] D.T. Birnbaum, J.D. Kosmala, D.B. Henthorn, L. Brannon-Peppas, Controlled release of β-estradiol from PLAGA microparticles, J. Control. Release 65 (3) (2000) 375–387.

[217] J.K. Lalla, K. Sapna, Biodegradable microspheres of poly(DL-lactic acid) containing piroxicam as a model drug for controlled release via the parenteral route, J. Microencapsul. 10 (4) (1993) 449–460.

[218] H.K. Kim, H.J. Chung, T.G. Park, Biodegradable polymeric microspheres with "open/closed" pores for sustained release of human growth hormone, J. Control. Release 112 (2) (2006) 167–174.

<u>APPENDICES</u>

A   SUPPLEMENTARY DATA

Table 1. *Zeta potential of Poloxamer 188 stabilized poly(glycerol adipate)-indomethacin 25 % based nanoparticle measured in different diluents at 25 °C. The equilibration time was 6 h. Measurements were carried out in triplicate.*

Sample	Emulsifier	Diluent	Zeta potential [mV]
PGA-IDMC 25 %	0.1 % Poloxamer 188	Sodium chloride 5 mM	1.1 ± 0.6
		Sodium chloride 10 mM	-5.1 ± 0.5
		Sodium citrate 5 mM	-24.3 ± 0.6
		Sodium citrate 10 mM	-19.7 ± 1.1
		1:10 Sörensen buffer pH 4.9	7.2 ± 0.5
		1:10 Sörensen buffer pH 6.8	-22.8 ± 2.5
PGA-IDMC 25 %	0.2 % Poloxamer 188	Sodium chloride 5 mM	-1.5 ± 0.3
		Sodium chloride 10 mM	-2.1 ± 0.1
		Sodium citrate 5 mM	-2.3 ± 0.5
		Sodium citrate 10 mM	-2.2 ± 0.4
		1:10 Sörensen buffer pH 4.9	0.7 ± 0.1
		1:10 Sörensen buffer pH 6.8	-3.2 ± 0.5
PGA-IDMC 25 %	0.3 % Poloxamer 188	Sodium chloride 5 mM	3.4 ± 0.3
		Sodium chloride 10 mM	-2.0 ± 0.4
		Sodium citrate 5 mM	-22 ± 5.0
		Sodium citrate 10 mM	-25.6 ± 0.7
		1:10 Sörensen buffer pH 4.9	14.9 ± 0
		1:10 Sörensen buffer pH 6.8	-16.2 ± 0.6
PGA-IDMC 25 %	0.4 % Poloxamer 188	Sodium chloride 5 mM	6.3 ± 0.6
		Sodium chloride 10 mM	0.0 ± 0.6
		Sodium citrate 5 mM	-43.0 ± 2.0
		Sodium citrate 10 mM	-42.2 ± 1.4
		1:10 Sörensen buffer pH 4.9	22.5 ± 0.4
		1:10 Sörensen buffer pH 6.8	-24.8 ± 0.8
PGA-IDMC 25 %	0.5 % Poloxamer 188	Sodium chloride 5 mM	-8.8 ±5.6
		Sodium chloride 10 mM	-10.7 ± 1.2
		Sodium citrate 5 mM	-38.3 ± 0.3
		Sodium citrate 10 mM	-32.3 ± 1.5
		1:10 Sörensen buffer pH 4.9	3.8 ± 1.4
		1:10 Sörensen buffer pH 6.8	-24.3 ± 0.7

Table 2. *Zeta potential of poly(vinyl alcohol) stabilized poly(glycerol adipate)-indomethacin 25% based nanoparticle measured in different diluents at 25 °C. The equilibration time was 6 h. Measurements were carried out in triplicate.*

Sample	Emulsifier	Diluent	Zeta potential [mV]
PGA-IDMC 25 %	0.1 % PVA	Sodium chloride 5 mM	-1.7 ± 0.2
		Sodium chloride 10 mM	-3.3 ± 0.3
		Sodium citrate 5 mM	-3.3 ± 0.2
		Sodium citrate 10 mM	-3.3 ± 0.3
		1:10 Sörensen buffer pH 4.9	-0.5 ± 0.2
		1:10 Sörensen buffer pH 6.8	-3.3 ± 0.5
PGA-IDMC 25 %	0.2 % PVA	Sodium chloride 5 mM	0.7 ± 0.2
		Sodium chloride 10 mM	-2.2 ± 0.4
		Sodium citrate 5 mM	-1.5 ± 0.0
		Sodium citrate 10 mM	-2.8 ± 0.1
		1:10 Sörensen buffer pH 4.9	-0.2 ± 0.1
		1:10 Sörensen buffer pH 6.8	-2.7 ± 0.3
PGA-IDMC 25 %	0.3 % PVA	Sodium chloride 5 mM	-0.9 ± 0.1
		Sodium chloride 10 mM	-2.2 ± 0.5
		Sodium citrate 5 mM	-1.0 ± 0.1
		Sodium citrate 10 mM	-1.9 ± 0.1
		1:10 Sörensen buffer pH 4.9	-0.5 ± 0.2
		1:10 Sörensen buffer pH 6.8	-2.4 ± 0.4
PGA-IDMC 25 %	0.4 % PVA	Sodium chloride 5 mM	-0.8 ± 0.2
		Sodium chloride 10 mM	-1.7 ± 0.5
		Sodium citrate 5 mM	-1.2 ± 0.2
		Sodium citrate 10 mM	-1.6 ± 0.4
		1:10 Sörensen buffer pH 4.9	-0.4 ± 0.2
		1:10 Sörensen buffer pH 6.8	-2.1 ± 0.10
PGA-IDMC 25 %	0.5 % PVA	Sodium chloride 5 mM	-0.5 ± 0.1
		Sodium chloride 10 mM	-1.5 ± 0.1
		Sodium citrate 5 mM	-0.3 ± 0.2
		Sodium citrate 10 mM	-1.6 ± 0.2
		1:10 Sörensen buffer pH 4.9	-0.1 ± 0.2
		1:10 Sörensen buffer pH 6.8	-1.9 ± 0.4

Table 3. *Zeta potential of Poloxamer 188 stabilized poly(glycerol adipate)-indomethacin 50 % based nanoparticle measured in different diluents at 25 °C. The equilibration time was 6 h. Measurements were carried out in triplicate.*

Sample	Emulsifier	Diluent	Zeta potential [mV]
PGA-IDMC 50 %	0.1 % Poloxamer 188	Sodium chloride 5 mM	-1.4 ± 0.6
		Sodium chloride 10 mM	-1.8 ± 0.2
		Sodium citrate 5 mM	-3.2 ± 0.4
		Sodium citrate 10 mM	-1.8 ± 0.0
		1:10 Sörensen buffer pH 4.9	-0.7 ± 0.4
		1:10 Sörensen buffer pH 6.8	-6.5 ± 1.1
PGA-IDMC 50 %	0. 2 % Poloxamer 188	Sodium chloride 5 mM	-1.7 ± 0.2
		Sodium chloride 10 mM	-1.5 ± 0.2
		Sodium citrate 5 mM	-10.3 ± 1.9
		Sodium citrate 10 mM	-4.6 ± 0.6
		1:10 Sörensen buffer pH 4.9	-0.5 ± 0.1
		1:10 Sörensen buffer pH 6.8	-1.0 ± 0.2
PGA-IDMC 50 %	0.3 % Poloxamer 188	Sodium chloride 5 mM	-45.7 ± 1.1
		Sodium chloride 10 mM	-46.6 ± 0.8
		Sodium citrate 5 mM	-54.8 ± 0.8
		Sodium citrate 10 mM	-50.8 ± 1.9
		1:10 Sörensen buffer pH 4.9	-46.5 ± 0.8
		1:10 Sörensen buffer pH 6.8	-55.3 ± 0.6
PGA-IDMC 50 %	0.4 % Poloxamer 188	Sodium chloride 5 mM	-9.6 ± 0.7
		Sodium chloride 10 mM	-6.0 ± 0.5
		Sodium citrate 5 mM	-12.7 ± 0.9
		Sodium citrate 10 mM	-9.9 ± 1.2
		1:10 Sörensen buffer pH 4.9	-8.2 ± 0.9
		1:10 Sörensen buffer pH 6.8	-14.2 ± 1.5
PGA-IDMC 50 %	0.5 % Poloxamer 188	Sodium chloride 5 mM	-2.7 ± 0.4
		Sodium chloride 10 mM	-7.0 ± 1.7
		Sodium citrate 5 mM	-10.3 ± 1.7
		Sodium citrate 10 mM	-3.3 ± 0.7
		1:10 Sörensen buffer pH 4.9	-6.1 ± 1.3
		1:10 Sörensen buffer pH 6.8	-2.3 ± 0.3

Table 4. *Zeta potential of poly(vinyl alcohol) stabilized poly(glycerol adipate)-indomethacin 50 % based nanoparticle measured in different diluents at 25 °C. The equilibration time was 6 h. Measurements were carried out in triplicate.*

Sample	Emulsifier	Diluent	Zeta potential [mV]
PGA-IDMC 50 %	0.1 % PVA	Sodium chloride 5 mM	0.8 ± 0.2
		Sodium chloride 10 mM	-1.5 ± 0.3
		Sodium citrate 5 mM	-2.2 ± 0.0
		Sodium citrate 10 mM	-1.2 ± 0.8
		1:10 Sörensen buffer pH 4.9	-0.5 ± 0.2
		1:10 Sörensen buffer pH 6.8	-1.7 ± 0.1
PGA-IDMC 50 %	0.2 % PVA	Sodium chloride 5 mM	-1.5 ± 0.1
		Sodium chloride 10 mM	-0.7 ± 0.2
		Sodium citrate 5 mM	-0.5 ± 0.2
		Sodium citrate 10 mM	-0.8 ± 0.2
		1:10 Sörensen buffer pH 4.9	-0.5 ± 0.2
		1:10 Sörensen buffer pH 6.8	-0.4 ± 0.1
PGA-IDMC 50 %	0.3 % PVA	Sodium chloride 5 mM	-0.8 ± 0.2
		Sodium chloride 10 mM	-1.6 ± 0.2
		Sodium citrate 5 mM	-0.5 ± 0.2
		Sodium citrate 10 mM	-0.2 ± 0.1
		1:10 Sörensen buffer pH 4.9	-1.2 ± 0.3
		1:10 Sörensen buffer pH 6.8	-0.9 ± 0.2
PGA-IDMC 50 %	0.4 % PVA	Sodium chloride 5 mM	-0.6 ± 0.1
		Sodium chloride 10 mM	-0.6 ± 0.1
		Sodium citrate 5 mM	-1.4 ± 0.1
		Sodium citrate 10 mM	-1.2 ± 0.2
		1:10 Sörensen buffer pH 4.9	-0.4 ± 0.1
		1:10 Sörensen buffer pH 6.8	-0.3 ± 0.1
PGA-IDMC 50 %	0.5 % PVA	Sodium chloride 5 mM	-1.7 ± 0.1
		Sodium chloride 10 mM	-1.2 ± 0.2
		Sodium citrate 5 mM	-0.2 ± 0.0
		Sodium citrate 10 mM	-0.0 ± 0.0
		1:10 Sörensen buffer pH 4.9	-0.3 ± 0.0
		1:10 Sörensen buffer pH 6.8	-1.2 ± 0.1

Table 5. *Zeta potential of Poloxamer 188 stabilized poly(glycerol adipate)-indomethacin 100 % based nanoparticle measured in different diluents at 25 °C. The equilibration time was 6 h. Measurements were carried out in triplicate.*

Sample	Emulsifier	Diluent	Zeta potential [mV]
PGA-IDMC 100 %	0.1 % Poloxamer 188	Sodium chloride 5 mM	6.3 ± 1.9
		Sodium chloride 10 mM	5.0 ± 0.4
		Sodium citrate 5 mM	-7.0 ± 0.4
		Sodium citrate 10 mM	-4.1 ± 0.5
		1:10 Sörensen buffer pH 4.9	6.3 ± 0.4
		1:10 Sörensen buffer pH 6.8	0.8 ± 0.2
PGA-IDMC 100 %	0.2 % Poloxamer 188	Sodium chloride 5 mM	5.6 ± 0.5
		Sodium chloride 10 mM	-1.6 ± 0.1
		Sodium citrate 5 mM	-4.1 ± 0.6
		Sodium citrate 10 mM	-1.9 ± 0.2
		1:10 Sörensen buffer pH 4.9	6.8 ± 0.6
		1:10 Sörensen buffer pH 6.8	-2.1 ± 0.1
PGA-IDMC 100 %	0.3 % Poloxamer 188	Sodium chloride 5 mM	6.0 ± 0.2
		Sodium chloride 10 mM	3.6 ± 0.1
		Sodium citrate 5 mM	-5.5 ± 0.4
		Sodium citrate 10 mM	-2.6 ± 0.4
		1:10 Sörensen buffer pH 4.9	-4.3 ± 0.3
		1:10 Sörensen buffer pH 6.8	-1.1 ± 0.3
PGA-IDMC 100 %	0.4 % Poloxamer 188	Sodium chloride 5 mM	4.5 ± 0.2
		Sodium chloride 10 mM	2.6 ± 0.5
		Sodium citrate 5 mM	-1.6 ± 0.2
		Sodium citrate 10 mM	-0.5 ± 0.2
		1:10 Sörensen buffer pH 4.9	7.9 ± 0.3
		1:10 Sörensen buffer pH 6.8	-0.2 ± 0.0
PGA-IDMC 100 %	0.5 % Poloxamer 188	Sodium chloride 5 mM	6.6 ± 0.5
		Sodium chloride 10 mM	3.2 ± 0.1
		Sodium citrate 5 mM	-4.5 ± 0.3
		Sodium citrate 10 mM	-0.9 ± 0.2
		1:10 Sörensen buffer pH 4.9	7.4 ± 0.6
		1:10 Sörensen buffer pH 6.8	0.9 ± 0.2

Table 6. *Zeta potential of poly(vinyl alcohol) stabilized poly(glycerol adipate)-indomethacin 100 % based nanoparticle measured in different diluents at 25 °C. The equilibration time was 6 h. Measurements were carried out in triplicate.*

Sample	Emulsifier	Diluent	Zeta potential [mV]
PGA-IDMC 100 %	0.1 % PVA	Sodium chloride 5 mM	-2.6 ± 0.2
		Sodium chloride 10 mM	-1.5 ± 0.3
		Sodium citrate 5 mM	-2.5 ± 0.0
		Sodium citrate 10 mM	-2.3 ± 0.8
		1:10 Sörensen buffer pH 4.9	-0.8 ± 0.2
		1:10 Sörensen buffer pH 6.8	-1.0 ± 0.1
PGA-IDMC 100 %	0.2 % PVA	Sodium chloride 5 mM	-4.6 ± 0.60
		Sodium chloride 10 mM	-0.7 ± 0.2
		Sodium citrate 5 mM	-1.0 ± 0.1
		Sodium citrate 10 mM	-2.9 ± 0.5
		1:10 Sörensen buffer pH 4.9	-1.4 ± 0.3
		1:10 Sörensen buffer pH 6.8	-0.6 ± 0.1
PGA-IDMC 100 %	0.3 % PVA	Sodium chloride 5 mM	-0.8 ± 0.2
		Sodium chloride 10 mM	-2.6 ± 0.1
		Sodium citrate 5 mM	-2.8 ± 0.3
		Sodium citrate 10 mM	-0.8 ± 0.1
		1:10 Sörensen buffer pH 4.9	-0.4 ± 0.1
		1:10 Sörensen buffer pH 6.8	-2.9 ± 0.2
PGA-IDMC 100 %	0.4 % PVA	Sodium chloride 5 mM	-2.9 ± 0.3
		Sodium chloride 10 mM	-2.5 ± 0.2
		Sodium citrate 5 mM	-0.6 ± 0.1
		Sodium citrate 10 mM	-1.4 ± 0.4
		1:10 Sörensen buffer pH 4.9	-0.9 ± 0.0
		1:10 Sörensen buffer pH 6.8	-2.8 ± 0.3
PGA-IDMC 100 %	0.5 % PVA	Sodium chloride 5 mM	-0.4 ± 0.3
		Sodium chloride 10 mM	-1.0 ± 0.1
		Sodium citrate 5 mM	-2.9 ± 0.3
		Sodium citrate 10 mM	-2.7 ± 0.4
		1:10 Sörensen buffer pH 4.9	-0.2 ± 0.0
		1:10 Sörensen buffer pH 6.8	-0.8 ± 0.1

B   DEUTSCHE ZUSAMMENFASSUNG

Das Interesse an Polymer-Wirkstoffkonjugaten als neuartige Plattform für innovative Drug-Delivery-Systeme nimmt stetig zu. Im Rahmen dieser Arbeit wurde das Potenzial von Poly (glycerol-adipat) als Grundlage für die Entwicklung von Wirkstoffkonjugaten untersucht. Aufgrund seiner hohen therapeutischen Relevanz für eine Vielzahl von Erkrankungen wurde Indomethacin als geeigneter Kandidat für die Synthese von Wirkstoff-modifiziertem PGA ausgewählt.

Der lineare Polyester PGA wurde über eine enzymatische Polytranskondensation unter Verwendung von Lipase aus *Candida antarctica* (CALB) aus Glycerol und Divinyladipat synthetisiert. Diese Veresterung ist selektiv für primäre Hydroxylgruppen. Unter Verwendung der anhängenden sekundären OH-Gruppen von PGA können weitere Modifikationen durchgeführt werden. In einem zweiten Syntheseschritt wurde eine einfache, einstufige Reaktion (Steglich Veresterung) zur kovalenten Kupplung von Indomethacin angewendet. Hierbei wurde weder ein komplexer Linker, noch eine vorherige Modifikation des Arzneistoffes oder des Polymers notwendig.

Im Rahmen dieser Arbeit wurden Indomethacin-PGA-Konjugate mit 25, 50 und 100 mol% synthetisiert und umfassend charakterisiert. Die Strukturänderung der verschiedenen Polymere in Abhängigkeit vom Polymerisationsgrad wurde mittels ^{1}H-NMR und ATR-FT-IR untersucht. Gerade hier war die proportionale Abnahme der OH-Peaks mit steigendem Modifikationsgrad auffällig. Darüber hinaus konnte der Substitutionsgrad durch den Vergleich der Integrale von Methylen- und Methingruppen des PGA-Rückgrats berechnet werden. Diese Methode wurde anschließend durch UV-Spektroskopie verifiziert. Auf diese Weise wurden sehr hohe Arzneimittelbeladungen (35,6 - 54,1 % (m/ m)) nachgewiesen, die vor allem für die Anwendung in nano- und mikroskaligen Arzneiformen vielversprechend sind. Die thermischen Eigenschaften der neuen Polymere wurden mittels DSC untersucht. In diesem Fall konnte eine Verschiebung des Glasübergangs von -23,7 °C (PGA-Rückgrat) auf 51 °C (PGA-IDMC 100 %) aufgrund der raumgreifenden Aromaten, und keine Schmelzpeaks für Indomethacin beobachtet werden. Das Hauptkettenpolymer sowie die drei Konjugate sind amorph, wohingegen die Reinsubstanz Indomethacin kristallin ist, wie Röntgenbeugungsmessungen zeigten. Die Molekulargewichtsverteilung dieser Polymere wurde im Detail durch GPC charakterisiert. Alle Polymere zeigten eine enge Molekulargewichtsverteilung mit einem PDI zwischen 2,2 und 3,2; was für verzweigte

Polymere typisch ist, und eine allgemeine Zunahme des Molekulargewichts mit zunehmendem Substitutionsgrad. In diesem Zusammenhang konnte eine Entwicklung von fast Newtonschen Fluiden (PGA) zu mehr und mehr viskoelastischen Polymeren beobachtet werden. Diese Aspekte der Makroviskosität wurden durch oszillierende Rheologie nachgewiesen.

Darüber hinaus wurden die neuen Polymere zuerst als vorgeformte Implantate formuliert. Sie wurden mit einer speziell entwickelten Heizpresse in kleine Zylinder gepresst. Anschließend wurden erste Freisetzungsuntersuchungen in Phosphatpuffer pH 7,4, Acetatpuffer pH 4,75 und 0,9 %-iger wässriger Kochsalzlösung, welche mit Lipase aus *Pseudomonas* spez. enthielt, durchgeführt. Im Vergleich dazu wurden physikalische Mischungen von PGA und Indomethacin hergestellt und Phosphatpuffer pH 7,4 freigesetzt. Nach 30 Tagen setzten die Konjugate nur etwa 0,7 % Indomethacin frei. Unter sauren Bedingungen (max. 16 % nach 30 Tagen) oder in Gegenwart von Enzym (max. 40 % nach 30 Tagen) war die Freisetzungsrate aufgrund der Spaltung der Esterbindungen jedoch deutlich beschleunigt. Im Vergleich dazu verhielten sich die physikalischen Mischungen völlig anders. Die Gesamtmenge an Indomethacin wurde bereits nach 15 Tagen in Phosphatpuffer pH 7,4 freigesetzt. Das Freisetzungsverhalten ist eine weitere Bestätigung, dass Indomethacin tatsächlich kovalent gebunden wurde. Die Freisetzungsdaten sind sehr vielversprechend, da es insbesondere in entzündetem Gewebe leicht saure pH-Werte und Enzyme gibt und die Polymere eine kontrollierte Freisetzung über einen langen Zeitraum ermöglichen.

Im zweiten Teil dieser Arbeit wurde untersucht, ob aus dem neuartigen Material nanoskalige Arzneiformen hergestellt werden können. Es war möglich, Nanopartikel unter Verwendung aller drei Konjugate über eine optimierte Lösungsmittelextraktions-Methode herzustellen. Geringe Mengen an Stabilisator (≤ 0,5 % PVA oder Poloxamer188) waren notwendig. Die Partikelgröße aller Systeme wurde detailliert durch dynamische Lichtstreuung und Nanopartikel-Tracking-Analyse charakterisiert. Die meisten Nanopartikelformulierungen waren im Größenbereich von 160-220 nm und einer engen Partikelgrößenverteilung (PDI ≤ 0,2) herstellbar. Darüber hinaus konnten ausgewählte Formulierungen gefriergetrocknet, für 4 Wochen gelagert (Kühlschrank) sowie redispergiert werden, mit leichten Änderungen der Partikelgröße. Zusätzlich wurde die Partikelform mittels TEM untersucht, wobei sphärische Partikel nachgewiesen wurden.

Für diese Arzneistoffträgersysteme wurden auch Freisetzungsuntersuchungen *in vitro* durchgeführt. Zuvor wurde eine neuartige Freisetzungszelle entwickelt. Das Herzstück ist eine poröse Aluminiummembran mit einer Porengröße von 20 nm, die es ermöglicht, den freigesetzten Wirkstoff vom Wirkstoffträgersystem zu trennen. Die Probenahme wurde unter vermindertem Druck durchgeführt. Dabei zeichnete sich die Substitution des Probenvolumens durch seine einfache Handhabbarkeit aus. Die entwickelte Freisetzungszelle ist neu und universell für verschiedene nanoskalige Arzneisträgersysteme anwendbar. Unter Verwendung dieser Freisetzungszelle wurde die Freisetzung von mit 0,5 % Poloxamer stabilisierten PGA-IDMC-NP über 15 Tage in Phosphatpuffer pH 7,4 durchgeführt. Innerhalb dieser Beobachtungszeitkonnte wurden nahezu lineare, kontrollierte Freisetzung beobachtet werden. Am Ende des Experiments wurden 13 % Wirkstoff aus PGA-IDMC 25 %, 10 % aus PGA-IDMC 50 % und 2 % aus PGA-IDMC 100 % freigesetzt. Diese Werte sind viel höher als die der vorgeformten Implatate, was auf eine vergrößerte Oberfläche zurückzuführen ist. Wiederum war die Freisetzungsrate zwischen den verschiedenen Polymeren unterschiedlich, wahrscheinlich aufgrund der abnehmenden Benetzbarkeit mit zunehmendem Substitutionsgrad. Vorbereitend für die *in vivo* Verträglichkeits- und Verteilungsstudien wurde die hämolytische und cytotoxische Aktivität für ausgewählte Formulierungen untersucht. Die Toxizität wurde mit drei verschiedenen Zelllinien getestet, zwei humane Zelllinien (A549, HeLa) und eine tierische Zelllinie (LLC-PK1). In den Zellkulturversuchen wurde die Verträglichkeit der Zellen gegen PGA-IDMC NP unabhängig vom Derivatiserungsgrad nachgewiesen. Die hämolytische Aktivität dagegen nahm mit zunehmender Wirkstoffmenge ab, und zwar aufgrund der reduzierten Anzahl freier Hydroxylgruppen, die mit abnehmendem amphiphilen Charakter verbunden ist. PGA-NP zeigten etwa 10 %, PGA-IDMC 25 % NP 5 %, PGA-IDMC 50 % NP etwa 2 % und PGA-IDMC 100 % NP nahezu keine hämolytische Aktivität. Dementsprechend wurden die letzteren zur weiteren Charakterisierung *in vivo* ausgewählt.

In einem explorativem *in vivo* Experiment wurden die Verteilung und Verträglichkeit von PGA-IDMC 100 % NP untersucht. Zu diesem Zweck wurde der lipophile Fluoreszenzfarbstoff DiR in die Nanopartikelformulierung eingearbeitet. Die Verteilung der Nanopartikel wurde über drei Tage in fünf Mäusen (zwei männlich, drei weiblich) mittels nichtinvasiver Fluoreszenzbildgebung untersucht. Die Ergebnisse zeigen, dass die Elimination vor allem über die Leber erfolgt. In einer zweiten Gruppe, bestehend aus zwei Tieren (männlich und weiblich), wurde das Verhalten von PGA-IDMC 100 % NP untersucht, die zuvor kovalent mit dem Fluoreszenzfarbstoff DY-782 über eine spaltbare

Esterbindung (analog zur Indomethacinkopplung) wurden. Nach 24 h konnten deutliche Signale in Nieren, Lunge, Leber sowie in den Lymphknoten nachgewiesen werden. Dies ist auf die schnelle Spaltung der Esterbindung und die Eliminierung des Fluoreszenzfarbstoffs zurückzuführen. Abschließend wurde eine Maus jeder Gruppe und jedes Geschlechts autopsiert und die Akkumulation in den Organen *ex vivo* detailliert untersucht. Für die DiR-markierten Partikel wurden die intensivsten Signale in der Leber und in den Ovarien gefunden. Letzteres bestätigt die bisherigen Berichte über die Akkumulation von Nanoträgern [81, 82]. DY-782 markierte NPs, akkumulierten in den Nieren, Lungen, der Milz sowie im Uterus. Eine Ansammlung in den Eierstöcken konnte nicht beobachtet werden, was aufgrund der Autopsie nach 24 Stunden zeitliche Ursachen haben könnte. Möglicherweise benötigt die Ansammlung in den Eierstöcken mehr Zeit. Die zeitabhängige Akkumulation von Nanotransportern ist ein anhaltender Ansatz für weitere Forschungen. Zusammenfassend kann festgestellt werden, dass die getesteten Formulierungen von allen Tieren gut vertragen wurden, was anhand eines entwickelten Bewertungsbogens festgestellt wurde.

Polymertherapeutika finden meist als nanoskalige Arzneistoffträgersysteme Verwendung. Insbesondere für die Behandlung von Entzündungen wie Osteoarthritis sind DDS mit größeren Partikeln jedoch sehr wünschenswert, da hier der Abbau durch, zum Beispiel durch Phagozytose, reduziert werden kann. Daher wurde in einem dritten Abschnitt die Möglichkeit zur Herstellung von Mikropartikeln untersucht. Zum Beispiel wird während der Therapie von Osteoarthritis die Formulierung direkt in das Synovialgelenk injiziert. Die Verwendung von Mikropartikeln ist bevorzugt, um eine gesteigerte Phygozytose zu verhindern. Im Rahmen dieser Arbeit konnten Mikroteilchen unter Verwendung eines Öl-in-Wasser-Lösungsmittelverdampfungsverfahrens aus PGA-IDMC 50 % und 100 % hergestellt werden. Die erhaltenen Mikropartikel wurden gefriergetrocknet und die Partikelgröße zwischen 87 (PGA-IDMC 100 % MP) und 140 µm (PGA-IDMC 50 % MP) wurde durch statische Lichtstreuung bestimmt. Beide Partikelarten hatten eine breite Partikelgrößenverteilung. Daher muss die Produktion weiter optimiert werden. Die runde Form sowie die Teilchengröße wurden durch Lichtmikroskopie bestätigt. Um einen Eindruck von der detaillierten Struktur von der Partikeloberfläche und dem Kern zu erhalten, wurden Elektronenmikroskopaufnahmen angefertigt. Alle Partikel zeigten eine hochporöse Struktur, die den Eindruck erweckt, dass die Mikropartikel aus Nanopartikeln bestehen. Die hohe Menge an Stabilisator (5 % Poloxamer188) ist als porogen bekannt. Darüber hinaus konnten die kleinen Partikelfraktionen aus den statischen Streulichtmessungen durch ESEM bestätigt

werden. Tatsächlich handelt es sich um Polymer-Mikropartikel und nicht um ungebundene Indomethacinkristalle. Schließlich wurden für diese Formulierungen auch Freisetzungsstudien in drei verschiedenen Medien durchgeführt. Nach drei Monaten wurden nur 3 % Indomethacin aus beiden Partikelspezies, in Phosphatpuffer pH 7,4, freigesetzt, die Freisetzungsgeschwindigkeit ist daher langsamer als für Nanopartikel, was auf die größere Oberfläche dieser zurückzuführen sein kann. Die Freisetzungsrate konnte durch Zugabe von Enzymen aus *Pseudomonas* spez. beschleunigt werden, so dass 30-40 % nach drei Monaten freigesetzt wurden. Ebenso unter sauren Bedingungen, konnte ein ähnliches Verhalten wie bei vorgeformten Implantaten beobachtet werden (13-20 % nach drei Monaten).

Im Rahmen dieser Arbeit wurde das erste PGA-Wirkstoffkonjugat erfolgreich synthetisiert und umfassend charakterisiert. Erste Vorversuche zeigten die erfolgreiche Formulierung als *in situ* bildendes Implantat, was Gegenstand weiterer Untersuchungen sein sollte. Darüber hinaus bieten die vielversprechenden ersten Tierversuche, Raum für die Behandlung von entzündlichen Erkrankungen wie Pankreatitis. Die Entwicklung von geeigneten-Tiermodellen wäre der nächste Schritt in der präklinischen Forschung. Auf der chemischen Seite gibt es fast unbegrenzte Möglichkeiten. Um nur einige zu nennen, die Möglichkeit, verschiedene Linker einzuführen und Wirkstoffe über andere Bindungen als Ester zu koppeln, um die Wirkstofffreisetzung zu kontrollieren. Darüber hinaus könnte die Derivatisierung mit Fettsäuren in Kombination mit aktiven Substanzen auf dasselbe Rückgrat interessante Auswirkungen auf die Freisetzung- als auch auf die Polymereigenschaften haben.

C   ACKNOWLEDGEMENTS

D   ABOUT THE AUTHOR

CURRICULUM VITAE

PERSONAL DETAILS

Name: Tom Wersig

Date of birth: 22. November 1989

Place of birth: Görlitz

EDUCATION AND WORK EXPERIENCE

Since 06/2018   **Head Pharmacist at Main Production**,
                                    Linden Apotheken Group, Görlitz, Germany

01/2015 – 05/2018   **Research and teaching assistant (Doctoral student)**,
                                    Department of Pharmaceutical Technology and
                                    Biopharmaceutics
                                    Group: Prof. Dr. K. Mäder (Pharmaceutical Technology)
                                    Martin- Luther- University, Halle (Saale), Germany

05/2015 – 12/2017   **Pharmacist**
                                    Linden Apotheken Group, Görlitz, Germany

12/2014   **Head Pharmacist**
                                    Apotheke an der Vogelweide, Halle (Saale), Germany

11/2014   Licensure as pharmacist (Approbation)

05/2014 – 10/2014   **Pharmacist in training**
                                    Apotheke an der Vogelweide, Halle (Saale), Germany

11/2013 – 04/2014   **Pharmacist in training**
                          Department of Pharmaceutical Chemistry and Clinical
                          Pharmacy, Martin- Luther- University, Halle (Saale),
                          Germany

10/2009 – 09/2013   **Pharmacy student**
                          Martin- Luther- University, Halle (Saale), Germany
                          12/2014 Third State Examination
                          10/2013 Second State Examination
                          08/2011 First State Examination

08/2008 – 09/2009   Malteser Hilfsdienst gGmbH Görlitz (Civillian service)

07/2008   **German Abitur**,
                          Joliot-Curie-Gymnasium, Görlitz, Germany

The results of this dissertation were prepared in the period from 01.01.2015 - 31.05.2018, at the Martin- Luther- University Halle-Wittenberg, Institute of Pharmacy, Department of Pharmaceutical Technology.

Görlitz, den 01.04.2019

sgd. Tom Wersig

_____

Tom Wersig

PEER REVIEWED ARTICLES

T. Wersig, M. C. Hacker, J. Kressler and K. Mäder

Poly(glycerol adipate) – indomethacin drug conjugates – synthesis and *in vitro* characterization. International Journal of Pharmaceutics 2017; 531(1): pp. 225-234.

T. Wersig, R. Krombholz, C. Janich, A. Meister, J. Kressler and K. Mäder

Indomethacin functionalized poly(glycerol adipate) nanospheres as promising candidates for modified drug release. European Journal of Pharmaceutical Sciences 2018; 123: pp. 350-361.

ABSTRACTS AND POSTERS

K. Mäder, M. Windorf, J. Kutza, V. Weiss, A. Rodrigues, **T. Wersig**, J. Kressler
DIPOs, DIOGs and ISFOGs as novel direct injectable and biodegradable drug delivery systems for parental controlled release; transHAL 2017, Halle (Saale).

T. Wersig, J. Kressler and K. Mäder
Poly(glycerol adipate)-Indomethacin conjugates for modified drug release
22nd annual meeting, Controlled Release Society Local Chapter 2018, Halle (Saale), Germany

T. Wersig, J. Kressler and K. Mäder
In vitro release from Poly(glycerol adipate) – Indomethacin conjugates;
11th World Meeting on Pharmaceutics, Biopharmaceutics and Pharmaceutical Technology 2018; Granada; Spain

D. Gerloff, J. Lützkendorf, **T. Wersig**, K. Mäder, L. Müller, C. Sünderkotter
Tumor derived exosomes alter macrophage function by delivery of microRNAs;
46. ADF-Tagung 2019; Munich; Germany.

E   DECLARATION UNDER OATH

Hiermit erkläre ich an Eides statt, gemäß § 5 der Promotionsordnung der Naturwissenschaftlichen Fakultät I (Biowissenschaften) der Martin-Luther-Universität Halle-Wittenberg, dass ich die vorgelegte Arbeit selbstständig und ohne fremde Hilfe verfasst habe. Die Ergebnisse dieser Arbeit wurden unter Anleitung von Herrn Prof.Dr. rer. nat. habil. Karsten Mäder selbstständig erarbeitet.

Weiterhin habe ich keine anderen als die angegebenen Quellen und Hilfsmittel verwendet und inhaltlich oder wörtlich übernommene Stellen als solche kenntlich gemacht.

Ich habe bisher noch keine Promotionsversuche unternommen und diese Arbeit wurde ausschließlich der Mathematisch-Naturwissenschaftlichen-Fakultät I der Martin-Luther-Universität Halle-Wittenberg vorgelegt und an keiner anderen in- oder ausländischen Fakultät zur Erlangung des Doktorgrades eingereicht.

Görlitz, den 01.04.2019

sgd. Tom Wersig

_____

Tom Wersig